SOME ANALYTICAL APPLICATIONS OF ATOMIC ABSORPTION AND ATOMIC FLUORESCENCE SPECTROSCOPY

by

MICHAEL RONALD GEORGE TAYLOR, B.Sc., A.R.C.S.(Lond.)

A thesis submitted for the Degree of

Doctor of Philosophy

of the University of London

Department of Chemistry,
Imperial College of Science and Technology,
LONDON, S.W.7.

August, 1970

ABSTRACT

The first part of this work was concerned with the atomic absorption and atomic fluorescence spectroscopic determination of traces of low melting elements in nickel base alloys. The elements concerned were extracted into organic solvents to avoid interference from the other elements present and to enhance sensitivity.

Selenium and tellurium were extracted fron concentrated hydrochloric acid solution into methyl isobutyl ketone, and arsenic from such solution into chloroform.

Lead and bismuth were extracted into methyl isobutyl ketone from concentrated iodide solution.

Silver was extracted into methyl isobutyl ketone from concentrated nitric acid solution.

In all cases except arsenic the organic extracts were nebulised into the flame. In view of the hazards associated with the nebulisation of chloroform solutions into flames the arsenic was back extracted into aqueous solution.

The latter part of the work concerns the computer calculations of flame compositions and degrees of atomisation of metals in flames. This was achieved using the method of Free Energy Minimisation.

Many of the flames in use in flame spectroscopic analysis were studied in an attempt to obtain information about the atomisation processes, with particular reference to the stable oxide forming elements aluminium and silicon, and to predict the most useful flames for flame spectroscopic analysis.

Computer generated curves of concentration against flame composition, expressed as the ratio of carbon or hydrogen to oxygen, were plotted for the important flame species . Attempts were made to correlate degrees of metal atomisation with the concentrations of certain flame species.

The Free Energy Minimisation method was also used to study the effect of large excesses of silicon on the atomisation of lithium and magnesium in flames in an attempt to determine the mechanisms of interference in flame spectroscopic analysis.

ACKNOWLEDGEMENTS

The work described in this thesis was carried out in the Department of Chemistry, Imperial College of Science and Technology between October 1967 and June 1970. It is original except where due reference is made and no part has been submitted for any other degree.

I wish to express my thanks to my supervisors, Professor T.S. West and Dr. R.M. Dagnall for their assistance and encouragement throughout this project, and to the other members of the Analytical Department for their helpful suggestions and discussions.

I am indebted to the Ministry of Technology for their financial support of this work.

Finally, I would like to thank my wife, Vivienne, for her assistance with the typing and presentation of this thesis.

CONTENTS

		Page
ATOMIC ABSORPTION AND ATOMIC FLUORESCENCE SPECTROSCOPY		
Introduction		1
PART 1		
DETERMINATION OF LOW MELTING ELEMENTS IN NICKEL BASE ALLOYS BY ATOMIC ABSORPTION AND ATOMIC FLUORESCENCE SPECTROSCOPY		
CHAPTER 1	Determination of Selenium and Tellurium	29
CHAPTER 2	Determination of Arsenic	45
CHAPTER 3	Determination of Lead and Bismuth	52
CHAPTER 4	Determination of Silver	65
PART 2		
COMPUTER CALCULATIONS OF FLAME COMPOSITIONS AND DEGREES OF ATOMISATION BY THE METHOD OF FREE ENERGY MINIMISATION		
Introduction and mathematical derivation		70
CHAPTER 5	Acetylene flames	83
	5.1 Nitrous oxide-acetylene	
	5.2 Air-acetylene	
	5.3 Oxygen-acetylene	

			Page
CHAPTER	6	Some less common analytical flames	115
	6.1	Nitrous oxide-hydrogen	
	6.2	Oxygen-cyanogen	
	6.3	Miscellaneous hydrocarbon flames	
CHAPTER	7	Atomisation of Lithium and Magnesium and the effect of excesses of Silicon in the Nitrous oxide-acetylene and Air-acetylene flames.	138
CHAPTER	8	Conclusions and suggestions for future work	151
References			154
APPENDIX	1	Computer program	162

INTRODUCTION

The use of atomic absorption spectroscopy as an analytical technique was first reported in I955 by Walsh (I) and Alkemade and Milatz (2) although , in the last century, Bunsen (3) and Kirchhoff (4) had demonstrated that the positions of the dark absorption lines in the spectrum (5) of the sun corresponded with lines in the emission spectra of certain elements. The main reason for the delay in the application of the technique to inorganic analysis was the unsuitability of most of the available sources of radiation. If a continuum is used, the integrated absorption over a finite bandwidth must be measured, and to measure absorption line profiles is difficult and imprecise.

Walsh (I) suggested that the absorption coefficient be measured at the wavelength of maximum absorption by using a stable high intensity sharp atomic-line source. The hollow cathode lamp was proposed as such a source since it emitted sharp atomic line spectra of the cathode element and was sufficiently stable for atomic absorption measurements to be made with a high degree of accuracy. These observations are borne out by the widespread use of atomic absorption in trace metal analysis today and by the almost exclusive use of hollow cathode lamps as sources of radiation.

Theory

The theory of flame emission, atomic absorption and atomic fluorescence spectroscopy has been given elsewhere and recently, with particular reference to the shapes of analytical curves, by Zeegers, Smith and Winefordner (6). Only a brief discussion is therefore given here.

In conventional flame emission spectroscopy the integrated intensity of a line, neglecting self absorption and induced emission, is given by :-

$$\int I \, d\nu = C . N_j . f \qquad (I)$$

where N_j is the number of atoms in the excited state involved in the transition giving rise to the emission.

f is the oscillator strength which is a measure of the average number of electrons per atom capable of the transition.

C is a constant dependent on the system concerned.

If the atomic vapour is in thermal equilibrium at an absolute temperature T^oK then N_j the number of atoms in the excited state j of excitation energy E_j is given by :-

$$N_j = N_o . \frac{g_j}{g_o} . \exp(-E_j / kT) \qquad (2)$$

where N_o is the number of atoms in the ground state.

k is the Boltzmann constant.

g_j and g_o are the statistical weights for the excited and ground states respectively.

Thus the population of the excited state and the resulting emission intensity are directly related to temperature and inversely related to the excitation energy which for resonance lines is inversely proportional to wavelength. From equation (2) at conventional flame temperatures N_o is at least 10^4 times greater than N_j and for elements with resonance lines in the far ultra violet e.g. zinc at 213.9 nm it can be as much as 10^{16} times greater. Also N_o is effectively constant over a wide temperature range while

N_j exhibits an exponential variation with temperature.

Atomic Absorption Spectroscopy

Consider a parallel beam of radiation of frequency and intensity I_o incident on an atomic vapour of thickness I cm. If I_ν is the intensity of the transmitted radiation, then the absorption coefficient of the atomic vapour at frequency ν is defined by the relation

$$I_\nu = I_o . \exp(-K.I) \qquad (3)$$

From classical dispersion theory the integrated absorption and concentration are linked by the relation :-

$$\int K \, d\nu = \frac{\pi e^2}{m c} . N_\nu . f \qquad (4)$$

where e is the electronic charge

m is the electronic mass

c is the velocity of light

N is the number of atoms per cm^3 capable of absorption of radiation in the range ν to $\nu + d\nu$.

This assumes a refractive index of unity over the breadth of the absorption line and is not applicable to strong absorption lines. For a resonance line due to a transition from the ground state well separated from the lowest excited state N_ν may be considered equal to N the total number of atoms per cm^3.

Expressing equation (4) in terms of transition probabilities :-

$$\int K \, d\nu = \frac{\lambda^2 g_j}{8\pi g_i} . N . A_{ji} . (I - g_i N_j / g_j N_\nu) \qquad (5)$$

where λ is the wavelength at the centre of the absorption line.

g_i and g_j are the statistical weights.

A_{ji} is the Einstein coefficient for spontaneous emission for the j - i transition.

In the general case where $N_\nu \gg N_j$ equation (5) reduces to :-

$$\int K \, d\nu = \frac{\lambda^2 g_j}{8\pi g_i} . N . A_{ji} \qquad (6)$$

For resonance lines N_ν is equal to N and, if the j - i transition is the only one possible (as in the case of resonance lines) $A_{ji} = I/T$ where T is the average lifetime of an atom in the excited state j .

The main problem is the measurement of the integrated absorption. In conventional flames of temperatures between 2000°K and 3500°K the absorption line width is of the order of 0.002 nm. The width of the line depends on a number of factors :-

i) the natural line width due to the finite time that the atom is in the excited state.

ii) Doppler broadening due to the random thermal motions of the atoms.

III) Lorentz broadening due to collisions between atoms and foreign flame atoms and molecules.

iv) Holtzmark broadening due to collisions between atoms.

v) Stark broadening due to electric fields which may be internal (ions or electrons) or external.

In addition to the causes of line broadening lines may also have hyperfine structure as a result of the presence of several isotopes absorbing radiation at slightly different wavelengths. The natural linewidth is of the order of 10^{-5} nm and may be neglected relative to the other factors. At low partial pressures of the atomic vapour in flames Doppler broadening probably predominates.

Doppler broadening produces an absorption width of the order of 0.001 nm at 2000°K and this width is given by :-

$$D_\lambda = 1.67. \frac{\lambda}{c} . (2RT/M)^{\frac{1}{2}} \qquad (7)$$

where λ is the wavelength, M the atomic weight and R the Gas constant.

The same factors affect the emission line width from the source. Thus for maximum sensitivity the source must be operated at as low a temperature as possible. Also the path of the light through non-emitting regions of the source should be a minimum to minimise self absorption which also affects the line width.

If, as in the method suggested by Walsh (1), the source line width is small compared to the absorption line width and if the shape of the absorption line is governed solely by Doppler broadening, the absorption coefficient K_{max} is given by :-

$$K_{max} = \frac{2\lambda^2}{D_\lambda} . (\ln 2/\pi)^{\frac{1}{2}} . \frac{e^2}{mc^2} . N . f \qquad (8)$$

The Doppler broadening is proportional to the square root of temperature (equation (7)) and therefore the absorption coefficient is independent of quite large variations in temperature. Equation (8) shows K_{max} to exhibit a linear relationship with N but in practice this is only true at low atomic concentrations because at higher atomic concentrations. the other broadening factors compete with Doppler broadening for determination of the line width.

In flames Lorentz broadening will occur due to the presence of high concentrations of gases other than the

atomic vapour. This is constant and independent of the sample concentration so that it causes a constant reduction in K_{max} reducing sensitivity but not affecting the linearity between absorption coefficient and concentration. At high atomic concentrations Holtzmark broadening causes a lowering of the absorbance which is not linear with respect to the concentration of atomic vapour and destroys the linearity between K_{max} and N causing curves of absorbance vs. concentration to bend towards the concentration axis.

The maximum sensitivity of measurement will be obtained at the strongest resonance lines of the element concerned and these should clearly lie in a region of the spectrum in which absorption measurements may conveniently be made. Most elements have their principal resonance lines within the range I90 - 900 nm at which wavelengths measurements are easily made. Only the inert gases, the halogens, carbon, hydrogen, oxygen, nitrogen, phosphorus and sulphur are excluded since their main resonance lines lie well below I90 nm.

Apparatus for measurement

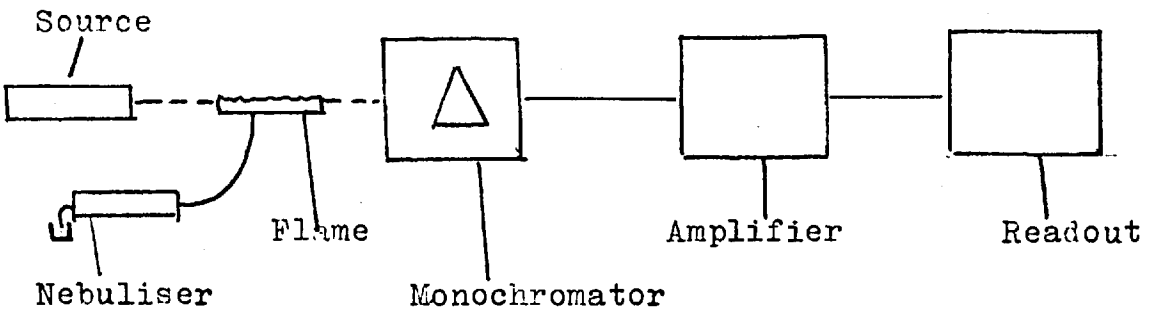

Fig. I Basic experimental arrangement for atomic absorption

Hollow cathode lamps (7,8) are by far the most widely used sources in atomic absorption spectroscopy. These consist of a gas discharge tube in which the cathode is hollow, cylindrical and open at one or both ends. The pressure of the gas is such that the negative glow at the cathode is restricted almost entirely to the inside of the cathode. The potential gradient is then a maximum near the surface of the cathode. Positive ions from the filler gas are accelerated through this field and bombard the cathode causing sputtering of the cathode element. The resulting atoms of the cathode element are then excited by further collisions and so the glow within the cathode is made up of the spectra of the carrier gas and of the cathode element. This carrier gas is normally argon since the element spectrum is made up mainly of atomic lines whereas ionic lines feature largely in the spectrum when helium is used.

The emission lines obtained from hollow cathode lamps are narrow since the pressure is small (I-2 mm Hg) and pressure broadening is minimal. The potential gradient in the negative glow is small and Stark broadening is therefore negligible. The cathode metal becomes quite hot, and Doppler broadening is important, but the source temperature is always lower than that of the flame and the source line is therefore always narrower than the absorption line. To obviate interference from thermal emission in the flame hollow cathode lamps may be modulated and a tuned amplifier used so that only the signal at the modulation frequency is amplified.

Other sources have been used in atomic absorption spectroscopy including discharge lamps (9) (obtainable for only the most volatile elements), plasmas (IO), continua (II), xenon arcs (II) and electrodeless discharge tubes(I2-I4). These latter are of greater importance in atomic fluorescence spectroscopy in view of their high intensity and will be discussed more fully in this connection. The use of the continuum as a source is somewhat limited because it is only suitable for use in conjunction with a high resolution monochromator and the energy within the 0.00I nm of the absorption line is small.

The flame is also a source of atomic line spectra but is unsuitable as a source for atomic absorption spectroscopy since the lines are subject to substantial broadening in view of the high operating temperatures and pressures. Moreover the stability of the emission,which can vary with slight temperature fluctuations,is insufficient for the flame to be a suitable source.

Nebulisation and atomisation of sample

The analyte element must be present as an atomic vapour and this is achieved by introducing the sample into the flame as a fine mist via a nebuliser and spray chamber. In the flame the remaining solvent is evaporated and the resulting solid melts, boils and vaporises. The mist is carried to the flame by a jet of gas which is normally the support gas of the flame.

Nebulisation converts the solution to fine droplets which reach the flame directly as in the total consumption burner or indirectly via a spray chamber. In this chamber

the larger droplets separate since they are too large to be carried into the flame or are broken up into smaller droplets. Solvent evaporation commences in the spray chamber and is completed in the flame.

Various losses occur in the nebulisation process . In the spray chamber the larger drops separate and therefore do not reach the flame. In the total consumption burner these drops reach the flame but are too large to give complete vaporisation. As a result thegreater part of the sample fails to reach the flame in the required form and this reduces the sensitivity of the method.

The amount of sample reaching the flame is governed by the drop size, and the rate of sample uptake is dependent solely on the viscosity of the solution and the flow rate of the nebulising gas. The liquid having passed through capillary of the nebuliser forms spherical drops due to the forces of surface tension. The drop size may be reduced by collisions with the walls or by being broken up by the gas stream. A dynamic pressure of wV^2 is set up(where w is the gas density in g/cm^3 and V the velocity of the gas relative to the drop) due to the friction of the gas. These forces are in opposition to the forces of viscosity and surface tension which keep the drop together. At high gas velocities viscosity is negligible and the drop breaks up when the dynamic pressure exceeds the surface tension pressure by a factor of three. The critical drop radius is then given by :-

$$wV^2 = 3.\ (\ 2S/r\ ) = 6S/r \qquad (9)$$

and the maximum droplet diameter 2r may be calculated and is of the order of 10μ. The size of the droplets depends

almost entirely on the surface tension, the density of the liquid and the gas velocity. Recombination of the drops can occur as well as the breaking up of larger drops and this can affect the average drop size.

Evaporation of the sample clearly affects the drop size distribution in the flame and this effect may be estimated by consideration of the loss by evaporation in unit time from a stationary drop in still dry air. The Langmuir equation based on the assumption that the free path of air molecules is small compared to the drop diameter applies :-

$$-\frac{dm}{dt} = 4\pi M D \frac{P_s r}{RT} \qquad (IO)$$

where m is the mass of the drop

t is the time

M is the molecular weight of vapour

D is the diffusion coefficient of the vapour with air

R is the gas constant

T is the absolute temperature

P_s is the vapour pressure of saturation

r is the drop radius

Thus the rate of surface loss is given by :-

$$-\frac{dF}{dt} = 8\pi M D \frac{P_s}{\rho RT} \quad (II) \text{ since } F = 4\pi r^2$$

where ρ is the density of the liquid.

Thus at constant temperature the rate of surface contraction $-\frac{dF}{dt}$ is approximately constant. For water droplets at room temperature it is approximately IO^{-4} cm^2/sec so that a drop of diameter 50μ evaporates completely in one

second, about the time a drop spends in the spray chamber. Thus drops of diameter less than 50μ have lost all the solvent before reaching the flame.

The nebuliser efficiency of an indirect nebuliser is expressed as the percentage sample reaching the flame and is between I and I0% for aqueous solutions but may be as high as 20% for organic solvents. The nebulisation of the sample element in organic solvents is an important method of increasing the sensitivity of atomic absorption spectroscopy (I5,I6) and can lead to up to five-fold enhancements in sensitivity. If the velocity of the support gas is kept constant the use of the organic solvent can decrease the surface tension and the density so that a finer mist results. Thus more sample reaches the flame and the sensitivity is improved.

An ultrasonic nebuliser has been used (I7) and enables far more sample solution to reach the flame. Its disadvantage is that it requires a large volume of solution.

The flame is almost invariably used as the atom reservoir but other systems have been used including the L'vov crucible (I8), long heated tubes (I9), carbon filaments (20) and plasmas (I0).

On reaching the flame the aerosol loses the solvent and the resulting solid particle melts, boils and vaporises. The gaseous molecules dissociate and the atomic vapour is formed. The atomic population may then be reduced in three ways :-

i) some atoms may be raised to excited states if the flame temperature is sufficiently high;

ii) high flame temperatures may lead to ionisation of atoms;

iii) the atoms may react with molecules or radicals in the

flame with the formation of stable molecular species via reactions of the type :-

$$M + O = MO$$

$$M + OH = MOH$$

The lifetime of solution droplets in the flame depends on the speed of the passage of the flame gases through the laminar flame and the height at which complete atomisation will occur for a given drop size may be calculated. For an air-acetylene flame at I0 m/sec droplets of initial diameter Iμ will be completely atomised within 0.05 mm and those of initial diameter I0μ within 3 mm. At the normal height of measurement in the flame viz. I-2 cm almost all drops will be atomised in the laminar flame. This is not the case in the turbulent flames on total consumption burners and measurements must be made at greater heights to avoid scatter by water droplets.

If absorbance is plotted against height of measurement then the maximum normally corresponds to the hottest portion of the flame but a substantial population of ground state atoms persists in the cooler regions unless stable compounds are formed with flame gas molecules or radicals. For elements that are relatively easily atomised (e.g. the alkaline earths) the use of high temperature flames may result in a considerable depletion of the atomic population due to ionisation. This may normally be overcome however by the addition of a more easily ionisable element to the sample solution e.g. potassium. The ionisation of potassium $K = K^+ + e^-$ tends to push the equilibrium of the reaction of ionisation of calcium $Ca = Ca^+ + e^-$ to the left.

The air-acetylene and air-propane flames are capable of atomising most elements but are unsuitable for the determination of elements that tend to form stable oxide species or for the determination of other elements in their presence. Interference and the selection of suitable flames for determinations are discussed more fully in Chapters 5 - 8.

The dimensions of the burner also affect the sensitivity of the method. The long path laminar flow burners in common use give large absorbance values but absorbance is not directly proportional to burner length as in the Lambert-Beer law . This is because an increase in burner length causes a decrease in the number of atoms / unit path length. The maximum burner length in common use is approximately IO cm. To increase path length multipass systems (2I) have been used.

Detection and measurement of signals

The use of sharp atomic line sources removes the need for high resolution monochromators. This is particularly marked in the case of elements with simple spectra in which the lines are widely separated(e.g. zinc). Walsh (22) proposed the use of another hollow cathode lamp as a monochromator and a practical system has been developed by Sullivan and Walsh (23). The use of modulated sources and tuned detector systems has also facilitated the use of monochromators of low resolution.

The detector and amplifier system is required to measure small differences between two relatively large signals of the incident and transmitted radiation (i.e. log (I_0/ I)). This is achieved in conjunction with conventional photomultipliers and amplifiers tuned to the source modulation frequency the signal differences being displayed on a galvanometer or a chart recorder.

Atomic Fluorescence Spectroscopy

Atomic fluorescence in flames was first observed by Nichol and Howes (24) in I923 but the analytical potentialities were not realised until I962 (25). The technique was first used as a means of trace metal analysis by Winefordner et al. (26-29).

Atomic fluorescence measurements are made by focussing intense radiation on a flame cell containing the atomic vapour of the analyte element. The fluorescence radiation is observed at right angles to the incident radiation so that the detector does not detect the source radiation. The wavelength of the fluorescence is characteristic of the analyte element and its intensity is a measure of the analyte element concentration. The basic experimental arrangement is shown in Fig. 2.

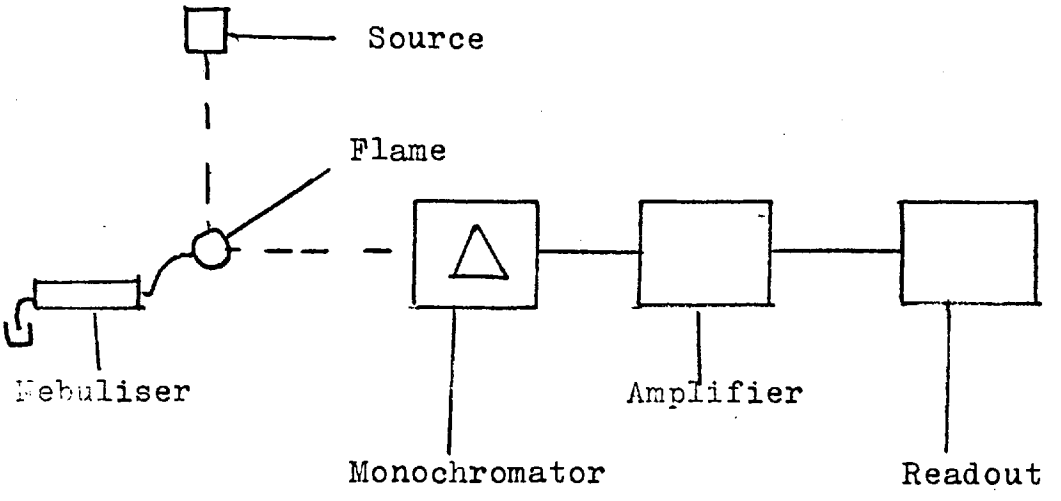

Fig. 2 Basic experimental arrangement for Atomic Fluorescence

The atoms of the analyte element are raised to excited states by absorption of the incident radiation and are then

deactivated by collisional quenching with flame gas molecules and by the emission of the fluorescence radiation which may be at the same wavelength as the incident radiation or at a longer wavelength. (In some rare cases radiation of a shorter wavelength may be emitted.)

There are five main types of atomic fluorescence :-

i) resonance fluorescence which occurs when the atom emits radiation of the same wavelength as the exciting radiation.

ii) direct-line fluorescence which occurs when the atom emits radiation of longer wavelength than the exciting radiation. Both the exciting and emitting lines originate from the same excited state and after the fluorescence the atom is in a metastable state above the ground state.

iii) stepwise fluorescence which is observed when the atom emits resonance radiation after excitation to a higher energy state than the first resonance state and then undergoes radiationless deactivation to the first excited state. An example of this is the emission of the bismuth 306.8 nm line resulting from excitation at 206.2 nm.

iv) sensitised fluorescence which takes place when an atom emits radiation after collisional excitation by a foreign atom which has been excited by the absorption of resonance radiation. For example, in a high pressure of mercury and thallium vapour the mercury atoms having been excited by absorption of the 253.7 nm line, the following reactions take place :-

$$Hg^{*} + Tl = Hg + Tl^{*}$$

$$Tl^{*} = Tl + h\nu$$

resulting in thallium emission at 377.6 nm and 535.0 nm. This type of fluorescence has never been observed in flames presumably because of the low partial pressures of atomic vapour and low fluorescence intensities involved.

v) thermally assisted fluorescence which involves the excitation of the atom both by absorption of radiation and thermally, and can occur in three ways :-

a) thermally assisted direct-line fluorescence

This was first observed by Dagnall, Thompson and West (I3) in the fluorescence of bismuth at 293.8 nm after excitation at 206.2 nm. The atom is raised to an excited state by absorption of resonance radiation and is then excited thermally to a slightly higher excited state. Fluorescence emission occurs from this state to either the ground state or to a metastable state above the ground state.

b) thermally assisted resonance fluorescence

This involves thermal excitation of the atom above the ground state and subsequent absorption and fluorescence at the same wavelength the atom returning to this state above the ground state. This type of fluorescence was first observed by Omenetto and Rossi (30) for gallium at 403.3 nm and indium at 4I0.2 nm.

c) thermally assisted anti-Stokes fluorescence

This type of fluorescence is similar to thermally assisted resonance fluorescence but the fluorescence emission is of shorter wavelength than the exciting radiation and was observed by Omenetto and Rossi (30)

in the fluorescence of gallium at 403.3 nm after excitation at 4I7.2 nm.

Relationship between Fluorescence Intensity and Concentration

Since the atomic fluorescence studies in this thesis concern only resonance and direct-line fluorescence only the intensities for these types of fluorescence will be considered. The relationship has been derived elsewhere(26,3I,32) and only a brief discussion is therefore given :-

The integrated atomic fluorescence intensity for an isolated spectral line is given by (3I) :-

$$I_F = I_A \cdot \frac{\phi_T}{4\pi} \cdot f_z \quad W/cm^2 - \text{steradian} \qquad (I2)$$

where I_A is the intensity absorbed by the resonance line (W/cm^2)

f_z is a dimensionless factor to account for the decrease in fluorescence intensity due to absorbing atoms

ϕ_T is the total power efficiency for fluorescence(33)

The power efficiency is the ratio of the power emitted to the power absorbed and is given by :-

$$\phi_T = \frac{V_f}{V_a} \cdot \phi \qquad (I3)$$

where ϕ is the quantum efficiency

V_f and V_a are the frequencies (sec^{-I}) of the fluorescence (f) and absorbed (a) photons respectively.

The intensity absorbed by a spectral line I_A is given by :-

$$I_A = I_o \cdot f_x \cdot \Omega_a \cdot A_T \quad W/cm^2 \qquad (I4)$$

where f_x is a dimensionless factor to take account of the decrease in the intensity of the incident radiation by atoms in the flame unseen by the detector

Ω_a is the solid angle of incident radiation used for excitation of the atomic vapour

I_o is the incident intensity of the exciting radiation from a continuous source (W-sec/ cm^2-steradian). This is the radiant power per unit source area per unit solid angle per frequency interval.

If the exciting radiation is a narrow line I_o becomes :-

$$I_o = I_L \cdot \frac{2\sqrt{\ln 2}}{\sqrt{\pi}\,\Delta\nu_L} \qquad (I5)$$

where I_L is the intensity of the source line (W/cm^2 - steradian)

$\Delta\nu_L$ is the source line half width in sec^{-I} for a Gaussian contour. The factor $\frac{2\sqrt{\ln 2}}{\sqrt{\pi}}$ is required to convert to triangular half widths simplifying the calculation ofline areas.

A_T is the total absorption factor (sec^{-I}) and represents the fraction of incident radiation absorbed within the solid angle over which excitation occurs and emission is measured. It is given by (33) :-

$$A_T = \int_o^\infty \frac{I_{\nu_o} - I_{\nu_t}}{I_{\nu_o}}\, d\nu = \int_o^\infty (I - \exp(-k_\nu L))d\nu \ sec^{-I} \qquad (I6)$$

where I_{ν_o} is the intensity of the exciting radiation as a function of frequency (W-sec / cm^2-steradian)

I_{V_t} is the intensity transmitted through the flame of average width L at frequency V

k_v is the atomic absorption coefficient in cm^{-I} as a function of the frequency V.

L is the average path length over which absorption occurs and fluorescence is measured.

The factors f_x and f_z are related to the distances over which absorption occurs and to the atomic absorption coefficient averaged over all frequencies and all atoms. They approach unity as the solid angles over which excitation occurs and fluorescence is measured approach the entire flame cell.

For resonance fluorescence at an isolated atomic resonance line the fluorescence intensity is given by combining equations (I2) and (I4) :-

$$I_F = I_o . f_x . \frac{\Omega a}{4\pi} . A_T . \phi_T . f_z \qquad (I7)$$

For direct-line fluorescence (3I,34) the intensity may be similarly obtained but all the absorption lines (other than resonance absorption) which can excite the energy level concerned must be considered as must the re-absorption of the fluorescence radiation by like atoms within the region of measurement in the flame. The intensity is therefore given by (assuming j routes of excitation) :-

$$I_F = \frac{\Omega a}{4\pi} . f_z . f_y . \sum_{i=I}^{j} I_{o_i} . f_{x_i} . A_{T_i} \qquad (I8)$$

where f_y accounts for re-absorption of fluorescence radiation by non-resonance absorption within the area of excitation and measurement in the flame. For resonance fluorescence re-absorption is

inherently considered in the A_T term and f_y is unity. If there is no thermal population of the metastable state of the direct-line fluorescence transition then both f_z and f_y will be unity since the ground state is not involved in the fluorescence transition.

All terms in the summation concern the absorption line which produces the fluorescing line i.e. I_{o_i} is the intensity of the exciting radiation at the ith absorption line.so that :-

A_{T_i} is the total absorption for the absorption line i.

ϕ_T is the total power efficiency for the fluorescence line (33)

Thus assuming constant source intensity and that ϕ_T is independent of the concentration of the analyte element in the flame (which at conventional analytical concentrations is a good approximation) then for a given set of flame conditions for resonance fluorescence :-

$$I_F \propto f_x . f_z . A_T \qquad (19)$$

and for direct-line fluorescence :-

$$I_F \propto f_z . f_y . \sum_{i=I}^{j} f_{x_i} . A_{T_i} \qquad (20)$$

for j absorption lines.

At low concentrations f_x, f_y and f_z are effectively constant and equal to unity. The fluorescence intensity I_F is therefore directly proportional to the A_T factor or the sum of such factors.

Evaluation of the A_T factor

This factor depends on the line width of the absorption

line relative to the line width of the exciting radiation and on the product of the number of ground state atoms per cm^3 (N) and the absorption path length of the region in which excitation occurs and fluorescence is measured (L).

Continuum source (line half width $\gg$ absorption line half width)

i) Low value of NL product.

Under these conditions A_T is approximately given by (34) :-

$$A_T = \int_0^\infty (I - \exp(-k_\nu L)) \, dV = \int_0^\infty k_\nu L \, dV \ (\sec^{-I}) \quad (2I)$$

$$= \frac{\pi e^2 . N . f . L}{m . c}$$

Thus at low concentrations A_T and therefore I_F (Equation (20)) increase linearly with N.

ii) High value of NL product

A_T is given by the equation (3I) :-

$$A_T = \left[\frac{k_o L \Delta V_D^2 a \pi^{\frac{1}{2}}}{\ln 2} \right]^{\frac{1}{2}} = \left[\frac{2\pi e^2 f N L \Delta V_D a}{mc (\ln 2)^{\frac{1}{2}}} \right]^{\frac{1}{2}} \quad (22)$$

since $k_o = \frac{(4\pi \ln 2)^{\frac{1}{2}} e^2 N f .}{m c \Delta V_D}$

Thus A_T and therefore I_F increase liearly with $N^{\frac{1}{2}}$.

Sharp line source (line half width $\ll$ absorption line half width)

i) Low value of NL product

A_T is given by :-

$$A_T = \int_0^{\frac{\Delta V_L}{2} \cdot \left(\frac{\pi}{\ln 2} \right)^{\frac{1}{2}}} (I - \exp(-k_\nu L)) \, dV = \int_0^{\frac{\Delta V_L}{2} \cdot \left(\frac{\pi}{\ln 2} \right)^{\frac{1}{2}}} k_\nu L \, dV \quad (23)$$

$$= \frac{k'_o \, L \, \Delta\nu_L}{2} \cdot \left(\frac{\pi}{\ln 2} \right)^{\frac{1}{2}}$$

where k'_o is the peak atomic absorption coefficient at the centre of the line. The limits of integration are the source line half width (triangular distribution). At low values of the product NL $k'_o = K. k_o$ where k_o is the maximum absorption coefficient when only Doppler broadening occurs, and K is a constant.

Since $I_F \propto I_o . A_T$ (this expression is used instead of A_T as I_o for a line source depends on the source line half width and the use of $I_o . A_T$ yields a simpler expression) then from equation (I6) :-

$$I_o = \frac{2I_L}{\Delta\nu_L} \cdot \left(\frac{\pi}{\ln 2} \right)^{-\frac{1}{2}} \qquad (24)$$

and therefore from equation (23) :-

$$I_o . A_T = K \, k_o \, L \, I_L = \frac{K \, (\, 4\pi \ln 2 \,)^{\frac{1}{2}} \, e^2 \, N \, L \, f \, I_L}{m \, c \, \Delta\nu_D} \qquad (25)$$

Thus I_F will increase linearly with N .

ii) <u>High values of NL product</u>

Under these conditions A_T may be found by assuming that complete absorption of the source line occurs (i.e. $\exp(-k_\nu L) = 0$) and therefore :-

$$A_T = \int_0^{\frac{\Delta\nu_L}{2} \cdot \left(\frac{\pi}{\ln 2} \right)^{\frac{1}{2}}} (\, I \, - \exp(-k_\nu L) \,) \, d\nu = \int_0^{\frac{\Delta\nu_L}{2} \cdot \left(\frac{\pi}{\ln 2} \right)^{\frac{1}{2}}} d\nu \qquad (26)$$

$$= \frac{\Delta \nu_L}{2} \cdot \left(\frac{\pi}{\ln 2}\right)^{\frac{1}{2}}$$

Hence $I_o \cdot A_T = I_L$ and $I_F \propto I_L$.

Thus I_F is independent of N and depends only on I_L . Essentially complete absorption occurs over the entire source line profile and further absorption can only occur if the source line half width increases or the intensity increases (i.e. I_F is constant as N increases).

It is seen therefore that at low values of the product NL the atomic fluorescence intensity I_F should vary linearly with the concentration of the atomic vapour using either a continuum or sharp line source and these conditions are made use of in atomic fluorescence analysis. At high values of NL the intensity is independent of NL for a sharp line source and is proportional to $(NL)^{\frac{1}{2}}$ for a continuum source. At very high values of NL the factors f_x and f_z may fall to considerably below unity and the curves of intensity vs. concentration bend back towards the concentration axis. A maximum fluorescence intensity is achieved and the intensity then decreases with increasing concentration.

In general it has been found that , for elements with their most sensitive lines below ca. 300. nm , atomic fluorescence spectroscopy is I-2 orders of magnitude more sensitive than atomic absorption spectroscopy (I2-I4). It is seen that the magnitude of the fluorescence signal is dependent on the source intensity and therefore an increase in this intensity will lead to greater sensitivity. In the

case of atomic absorption however the absorbance signal is a ratio (log (I/I_0)) and any increase in I_0 is associated with a corresponding increase in I and the absorbance remains unaltered.

Atomic absorption normally occurs only at resonance lines whereas atomic fluorescence need not. Thus there are more fluorescence lines than absorption lines and there is therefore greater scope in wavelength of measurement.

Apparatus for measurement

Sources

Many types of sharp line source have been used in atomic fluorescence spectroscopic analysis. The conventional hollow cathode lamps in use in atomic absorption spectroscopy are unsuitable since they are of insufficient intensity. Higher intensity hollow cathode lamps have been manufactured for several elements and atomic fluorescence measurements have been using these as sources (35-37). Vapour discharge lamps have also been used (27-29,38,39) but they are available for only the most volatile lements.

Microwave excited electrodeless discharge tubes (I2-I4, 28,29,40) have been prepared for many elements and are in most cases sufficiently intense to effect sensitive atomic fluorescence measurements. They are prepared by sealing small amounts of the element or, if the element is not sufficiently volatile, the element and iodine,the element being in excess,in a thin (ca. Icm diameter) quartz tube at a pressure of about 3 torr. The filler gas is usually argon and the bulb length about 5-7 cm. Excitation of the

tubes (40) is achieved using a "Microtron 200" high frequency generator (Electro-Medical Supplies) and either a $\frac{1}{4}$ wave or $\frac{3}{4}$ wave discharge cavity. The tubes are especially advantageous for volatile elements such as selenium for which the preparation of even low intensity hollow cathode lamps is extremely difficult. To prevent interference from thermal emission in the flame the tubes may be modulated (4I) and tuned amplifiers used.

The xenon-arc lamp may be used as a source for atomic fluorescence spectroscopy (42,43) since it emits a continuum from the infra red to approximately 200 nm. However the intensity falls off rapidly below 250 nm and its use is therefore restricted to those elements with lines of longer wavelength than 250 nm.

Flame and Nebulisation Systems

The atomisation processes are identical to those in atomic absorption the only difference being the burner dimensions. In atomic fluorescence spectroscopy it is desirable to use a small circular flame so that the solid angles of the excitation and emission measurement include as much of the flame as possible.

Nebulisation must be efficient since unevaporated solvent droplets can cause scatter of the exciting radiation. This is particularly noticeable in the use of total consumption burners.

It is desirable to use a flame of low radiative background provided that such a flame is an efficient atom reservoir for the element concerned. For elements that are easily

atomised hydrogen flames are preferable to flames of carbon containing fuels since there is less quenching in the hydrogen flames.

Detection Systems

The main difference in the detector system lies in the type of signal to be measured. In atomic absorption the detector system is required to detect small differences between two relatively large signals. In atomic fluorescence spectroscopy small signals must be detected over a low background and the magnitude of the recorded signal is dependent on the gain of the instrument. Even with modulated sources it is desirable to use low background flames since large monochromator slitwidths are used and high background radiation can seriously increase noise levels.

Limitations of Atomic Absorption and Atomic Fluorescence Spectroscopy

Both techniques may be applied to the determination of traces of many metals in pure solution. Problems arise however in the determination of refractory elements and of other elements in their presence. Solid particles may result in the flame from incomplete atomisation of the refractory elements and these particles may occlude the analyte element and may scatter the incident radiation. This may be avoided by using high temperature flames such as nitrous oxide-acetylene (44) but such flames have a high radiative background.

Large amounts of foreign ions in sample solutions can

affect the viscosity of these solutions and, as a result, the nebulisation processes so that all standards must be of similar composition to the test solutions. Moreover the nebulisation of aqueous acid solutions of metal alloys can lead to corrosive attack on the burner head and neutralisation of the acid merely increases the electrolyte concentration increasing the viscosity and possibly clogging the burner head.

A more satisfactory approach to the problem of trace metal analysis in alloys is to extract and concentrate the trace metals into an organic solvent. Thus the analyte element is separated from the matrix elements and advantage may be taken of the improvement in sensitivity associated with the use of organic solvents previously described.

The purpose of this thesis is partially to determine, by atomic absorption and atomic fluorescence spectroscopy, traces of low melting elements in nickel based alloys containing several metals some of which are refractory in nature. The latter part of the thesis involves the computer calculation of flame compositions and the study of the atomisation processes in the flames in use in atomic absorption and atomic fluorescence spectroscopy. This was achieved using the method of Free Energy Minimisation which is described fully in Part II.

PART I

DETERMINATION OF LOW MELTING ELEMENTS IN NICKEL BASE ALLOYS BY ATOMIC ABSORPTION AND ATOMIC FLUORESCENCE SPECTROSCOPY

Foreword

It is required to determine by atomic absorption and atomic fluorescence spectroscopy traces (down to 5 ppm) of selenium, tellurium, arsenic, lead, bismuth and silver. The nickel alloys consist mainly of nickel (40-60%), chromium (maximum 20%) and cobalt (maximum 20%). A number of other metals may also be present in varying proportions including iron (maximum 10%), molybdenum (maximum 5%) and aluminium (maximum 2%).

In view of the complex nature of the samples it is clearly impossible to determine the test elements directly in aqueous solution because solutions containing sufficient amounts of the analyte elements would be too viscous for efficient nebulisation. Moreover the preparation of complex blank and standard solutions would be required. For the reasons previously described it is better to extract the analyte elements into organic solvents and thus increase the sensitivity of the determination. For these reasons it was decided to devise solvent extraction procedures to separate the test elements from at least the bulk of the matrix elements and to subject the organic extracts to atomic absorption and atomic fluorescence measurements.

CHAPTER I

DETERMINATION OF SELENIUM AND TELLURIUM

I.I Selenium

Introduction

The principal selenium resonance lines (I96.I nm, 204.0 nm etc.) are all in the far ultraviolet and the flame emission spectroscopic determination of selenium is therefore difficult with conventional flames. However, a significant population of ground state selenium atoms is obtained in cool flames such as air-acetylene and air-hydrogen. Rann and Hambly (45) have determined selenium by atomic absorption spectroscopy using a hollow cathode lamp and an electrodeless discharge tube modulated at I5 MHz. A limit of detection of I ppm at I96.I nm was obtained.

Chakrabarti (46) has determined selenium by atomic absorption using a hollow cathode and a triple pass optical system. In the air-acetylene flame the sensitivity at I96.I nm was 0.72 ppm in aqueous solution and 0.30 ppm after extraction into methyl isobutyl ketone as the diethyldithiocarbamate complex. The sensitivities at the I96.I nm, 204.0 nm, 206.3 nm and 207.5 nm lines were in the ratio I : 9 : 60 ; 93 .

A continuous source (47) and a medium quartz spectrograph have also been used for the determination of selenium by atomic absorption spectroscopy. The limit of detection at the 204.0 nm line was 5 ppm.

The atomic fluorescence determination of selenium has been reported by Dagnall, Thompson and West (I2) using a microwave excited electrodeless discharge tube as source. The most sensitive line was at 204.0 nm at which a limit of detection of 0.I5 ppm was obtained. The I96.I nm line is the strongest fluorescence line but the photomultiplier used in the determinations (EMI 960IB) is very insensitive below 200 nm and the 204.0 nm line gave the higher readings.

Selenium may be extracted into a number of organic solvents (e.g. chloroform (48), carbon tetrachloride) with sodium diethyldithiocarbamate from solutions of pH 5-6. The unselectivity of this reagent renders this extraction method inapplicable for the determination of selenium in nickel alloys since the major components also extract in this pH range and must therefore be masked.

Mabuchi and Nakahara (49) have reported the extraction of selenium by dithizone from 6N hydrochloric acid into chloroform. However, Irving and Ramakrishna (50) have shown that the coloured species resulting is an oxidation product of dithizone and that selenium is not extracted.

Thioglycollic acid (5I) has been used to extract selenium into ethyl acetate from I-5 N hydrochloric acid. The optimum acid concentration is I N to prevent extraction of chloride complexes. Even under these conditions molybdenum interferes by such an extraction, and iron (III) consumes the reagent. Ethyl acetate has also been used as a solvent in the extraction of selenium with mercapto benzoic acid (52). The extraction is virtually quantitative in the pH range 0.5-2.5 but nickel and cobalt interfere seriously.

Futekov and Jordanov (53,54) have reported the extraction of selenium fron concentrated hydrochloric acid in the form of a reactive chloro complex which forms selenium compounds with ketones . These compounds are soluble in chloroform and carbon eterachloride and the compound with methyl ethyl ketone is reported to be quantitatively extracted from 7 N hydrochloric acid. It is undesirable to nebulise solutions in chloroform into hydrocarbon flames since one of the products, phosgene $COCl_2$, is toxic.

However it is also possible to extract selenium from concentrated hydrochloric acid into methyl isobutyl ketone (55). Selenium is virtually quantitatively extracted from 8.5 N hydrochloric acid but several other elements extract under these conditions e.g. iron(III), molybdenum (VI) and cobalt (partially). Since iron and molybdenum are not always present in the samples under consideration this extraction would in almost all cases remove the selenium from at least 90 % of the matrix elements. Moreover,if only hydrochloric acid is used in sample dissolution, the iron present will mostly be in the ferrous state.

Experimental

Apparatus

The apparatus consisted of a Hilger and Watts AA-2 atomic absorption conversion to the Uvispek spectrophotometer. The atomic absorption measurements were made using a 10 cm air-propane flame and the source was a selenium microwave excited electrodeless discharge tube containing selenium at a pressure of 8 torr. The hollow cathode lamp mounting was removed and

and the discharge tube placed in the position normally assumed by the cathode of the hollow cathode lamp. The discharge was maintained by a "Microtron 200" magnetron and a 2IOL ¾-wave discharge cavity and was initiated by means of a Tesla coil. The tube was modulated at I00 Hz and the frequency of the tuned amplifier altered to this frequency.

For atomic fluorescence measurements the long path burner housing was removed and a shortened Unicam air-propane emission burner placed as close to the monochromator slit as possible (approximately 5 cm away). To facilitate a linear readout for fluorescence measurements the logariser diode of the instrument was removed and substituted by a 330 ohm ¼ watt high stability carbon resistor.

Air was provided from a compressor and propane from a cylinder.

Reagents

i) Selenium solution (I000 ppm). Sodium selenite (0.4780 g) was dissolved in distilled water and the solution made up to 250 ml.

ii) Simulated sample solution (50,000 ppm). Nickel chloride (30.15 g), cobalt chloride (10.05 g) and chromic chloride (11.20 g) were dissolved in concentrated hydrochloric acid. (250 ml)

iii) Molybdenum solution (30,000 ppm). Ammonium molybdate (97.50 g) was dissolved in distilled water and the solution made up to 250 ml.

iv) Iron(III) solution (50,000 ppm). Ferric ammonium sulphate (107.9 g) was dissolved in distilled water and

the solution made up to 250 ml.

v) Hydrochloric acid (30 %).

vi) Methyl isobutyl ketone.

vii) Amyl acetate.

Optimisation of Experimental Conditions

a) Atomic absorption

The discharge tube was operated without cooling and maximum absorbance was observed at low operating powers. Absorption measurements were made with tube operated at 25 watts.

The effects of the variation of burner height and propane flow rate were investigated and are shown in Figs. I a and b. The air flow rates were 7.0 l/min atomiser air and 2.0 l/min supplementary air.

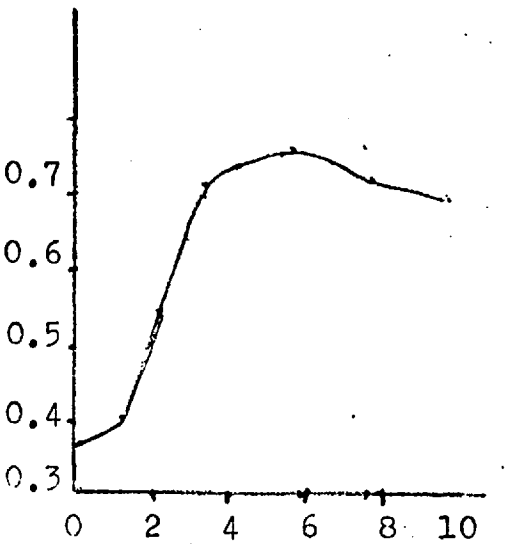

Fig. I a Absorbance vs. burner height (position on scale). 100 ppm Se.

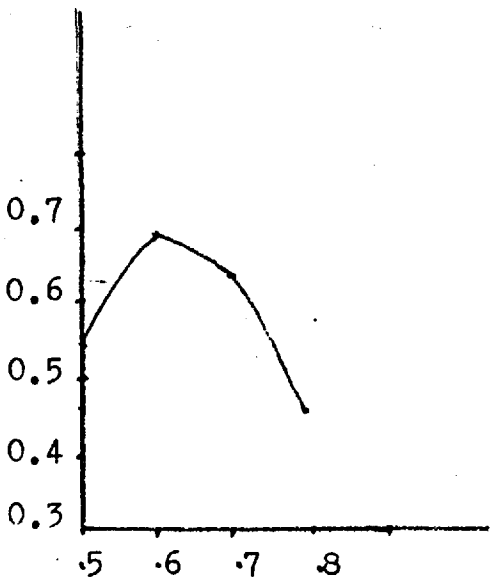

Fig. I b Absorbance vs. propane flow rate (arbitrary units).100 ppm Se.

The absorbance was virtually independent of monchromator slitwidth over the range 0.025 mm - o.I5 mm and a slitwidth

of 0.10 mm was employed to minimise the photomultiplier gain necessary and, as a result, the noise.

The optimum conditions are a propane flow rate of 0.5 (arbitrary units since the only available flowmeter was for acetylene) and burner height 5 . On nebulising methyl isobutyl ketone solutions the flame became very fuel rich and the propane flow rate was reduced to 0.3.

b) Atomic fluorescence

Since the burner system for all the atomic fluorescence studies consisted of improvised apparatus the burner height was optimised but could not be expressed in any units. The oxident and propane flow rates were the same for the emission burner as for the long path burner the optimum fuel flow for all fluorescence studies were the same as for atomic absorption.

The maximum fluorescence signal consistent with discharge tube stability was obtained at an operating power of 45 watts (uncooled). The monochromator slitwidth was 1.0 mm to minimise the photomuliplier gain required for zeroing the instrument and, as a result, the moise.

Wavelength of measurement

The atomic absorption of selenium was studied at the 196.1 nm resonance line in pure solution and a sensitivity (1% absorption) of 0.5 ppm was obtained. The calibration curve was linear up to 80 ppm.

The atomic fluorescence of selenium was measured at the resonance lines at 196.1 nm, 204.0 nm and 206.3 nm. The relative fluorescence intensities are shown in Table I.

Wavelength (nm)	Relative Intensity
I96.I	80
204.0	62
206.3	20

The use of the more ultraviolet sensitive photomultiplier in this study (EMI 6256B) shows that the strongest absorbing line at I96.I nm is the strongest fluorescence line as would be expected. All atomic fluorescence measurements were therefore made at this line and a detection limit (signal : noise = 2) of 0.08 ppm was obtained in aqueous solution in the air-propane flame. The discharge tube was run at 45 watts without cooling.

The calibration curve was linear to at least I0 ppm but, due to the lack of control of the photomultiplier gain required to zero the instrument which is primarily designed for routine atomic absorption determinations, higher concentrations could not be studied.

Separation

The extraction form concentrated hydrochloric acid (55) was selected as the most promising extraction for the separation of selenium. The use of 8 N hydrochloric acid yielded an extraction of more than 90 % but the use of 9 N acid merely resulted in the dissolution of the ketone. To minimise this effect with 8 N acid the ketone was shaken with 8 N acid to saturate it before the extraction. Cobalt and iron (III) both extracted under these conditions but did not affect the selenium absorbance. Molybdenum (VI) extracted and caused a decrease in the selenium absorbance.

The first attempt at the separation of selenium from the other extracting elements was to pre-extract the iron(III), molybdenum(VI) and cobalt from the 8 N hydrochloric acid into amyl acetate. When the extraction was tested by atomic absorption no selenium appeared to have extracted but the more sensitive fluorescence technique showed that small amounts of selenium had passed into the amyl acetate layer.

If instead all the extractable elements are extracted into methyl isobutyl ketone without the prior extraction with amyl acetate, and the ketone layer is washed with distilled water, all elements except selenium pass back into the aqueous phase. This is presumably due to the formation of a selenium compound with the ketone as reported by Futekov and Jordanov (53,54).

Analysis of Simulated Sample Solutions

Standard nickel base alloy samples containing known amounts of selenium were unavailable as were other standards (e.g. steels) and the extraction was therefore tested by the preparation and comparison of calibration curves for the selenium extraction from pure solution and from simulated sample solutions .

The aqueous phase of the pure solution extractions consisted of I6 ml concentrated hydrochloric acid, 2 ml selenium solutions of concentration up to 200 ppm,to produce I0 ml organic extracts containing up to 40 ppm selenium, and 2 ml distilled water. The sample solutions consisted of I6 ml of the simulated sample solution, 2 ml of the selenium solutions as before and 1 ml each of solutions of I5,000 ppm molybdenum(VI) and 50,000 ppm iron(III). This

corresponds to a 0.5 g alloy sample and I0 ml organic solvent were used for each extraction.

The results of the comarisons tested by atomic absorption are shown in Table 2.

Table 2

Extract concentration	40 ppm	30 ppm	20 ppm	I0 ppm	5 ppm
Absorbance in pure solution	0.44	0.36	0.24	0.I3	0.056
Absorbance in sample solution	0.44	0.36	0.23	0.I2	0.052

Similar comparisons were carried out for atomic fluorescence with concentrations of up to 2 ppm in the organic extract. These comparisons are shown in Table 3.

Table 3

Extract concentration(ppm)	2.0	I.5	I.0	0.5
Fluorescence (a.u.) pure solution	74	58	38	I9
Fluorescence (a.u.) sample solution	76	57	40	I9

(a.u.) = arbitrary units.

The sensitivity (I% absorbance) in atomic absorption was 0.2 ppm in the organic solvent and the atomic fluorescence detection limit (signal : noise = 2) was 0.025 ppm. Based on the extraction of the selenium in a 0.5 g sample into I0 mls organic solvent these figures correspond to 4 and 0.5 ppm in the alloy sample respectively.

I.2 Tellurium

As with selenium the main resonance lines of tellurium are in the far ultraviolet and are therefore difficult to excite thermally. However, Dean and Simms (56) have determined tellurium by flame emission using an oxygen-acetylene flame. The tellurium was extracted as the diethyldithiocarbamate complex into carbon tetrachloride and this solution evaporated to dryness. The complex was then redissolved in methyl isobutyl ketone and this solution aspirated into the flame. The detection limit was 2 ppm.

Ground state tellurium atoms are readily formed in cool flames such as air-acetylene and air-propane. Chakrabarti (57) has determined tellurium by atomic absorption spectroscopy with a hollow cathode lamp as source. Using a multipass (5) system the sensitivity at the 214.3 nm line was 0.23 ppm. A two-fold enhancement in sensitivity was achieved by extraction of tellurium as the diethyldithiocarbamate complex into methyl isobutyl ketone. The sensitivities at the 214.3 nm, 225.9 nm and 238.6 nm lines were in the ratio 1 : 9.9 : 187 . A continuous source and medium quartz spectrograph (47) have also been used giving a detection limit of 0.5 ppm at the 214.3 nm line.

Dagnall, Thompson and West (12) have determined tellurium by atomic fluorescence spectroscopy in the air-propane flame using an electrodeless discharge tube as source. The unresolved 238.3 and 238.6 nm lines gave the largest signals but the 214.3 nm line was used since the flame background was much less at this wavelength. This line is the strongest

absorbing line and,with the use of a photomultiplier more sensitive in the ultraviolet than the one used (EMI 960IB), it should give the greatest sensitivity in fluorescence. The limit of detection at this line was 0.05 ppm.

Tellurium (IV) may be extracted into a number of organic solvents with sodium diethyldithiocarbamate in the pH range 8.5-8.8 (58). However, at this pH the extraction is rather unselective. The use of EDTA and cyanide as masking agents is recommended but the amount of masking agents required for the analysis under consideration renders the extraction unsuitable.

Tribenzylamine will extract tellurium (IV) from 6 N hydrochloric acid solutions (59). The solvent recommended was chloroform but this is unsuitable for the reasons previously described. Oxygen containing solvents such as ketones are more convenient in this respect but they extract cobalt, iron(III) and molybdenum(VI) from hydrochloric acid.

Methyl isobutyl ketone has been used (55) to extract tellurium (IV) from concentrated hydrochloric acid. The extraction is virtually quantitative but cobalt, iron(III) and molybdenum(VI) also extract.

Experimental

Apparatus

The apparatus was identical to that used in the selenium determinations except that the tellurium discharge tube was operated in a 2I4L $\frac{1}{4}$-wave discharge cavity. The tube contained tellurium and iodine (tellurium in excess) at a pressure of 0.I torr. The filler gas was argon.

Reagents

i) Tellurium solution (1000 ppm). Sodium tellurite (0.4363 g) was dissolved in distilled water and the solution made up to 250 mls.

ii) Simulated sample solution . As for selenium determinations.

iii) Iron (III) solution. As for selenium determinations.

iv) Molybdenum solution. As for selenium determinations.

v) Hydrochloric acid (30 %)

vi) Sodium diethyldithiocarbamate (1%). Sodium diethyldithiocarbamate (1 g) was dissolved in 100 mls distilled water.

vii) Methyl isobutyl ketone.

Optimisation of Experimental Conditions

a) Atomic absorption

The discharge tube was operated at 20 watts without cooling. The effect of the variation of burner height and propane flow rate was investigated and is shown in Fig. 2a and b. As before the air flow rates were 7.0 l/min and 2.0 l/min .

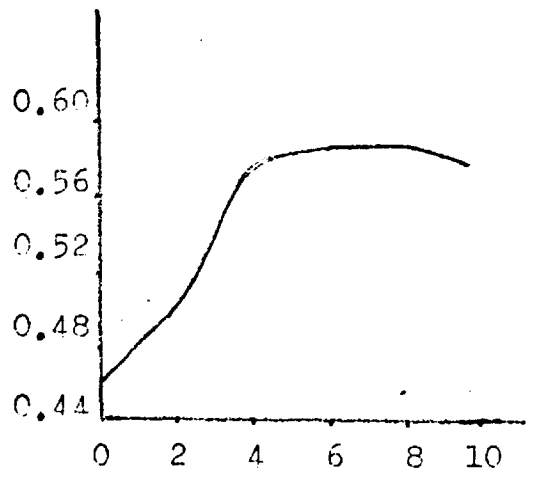

Fig. 2a Absorbance vs. burner height (position on scale) 60 ppm Te.

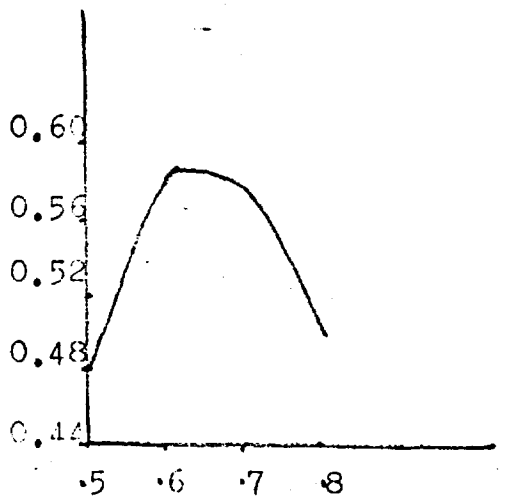

Fig. 2b Absorbance vs. propane flow rate (arbitrary units) 60 ppm Te.

The absorbance was virtually independent of monochromator slitwidth over the range 0.025 - 0.I5 mm and a slitwidth of 0.I mm was used to minimise noise as before.

b) Atomic fluorescence

As before the only parameters that could be measured were the tube operating power and the monochromator slitwidth. The discharge tube was run at 40 watts without cooling and the monochromator slitwidth was I.0 mm.

Wavelength of measurement

All atomic absorption measurements were made at the 2I4.3 nm line. A sensitivity (I% absorption) of 0.5 ppm was obtained in aqueous solution. The calibration curve was linear up to 80 ppm.

Atomic fluorescence measurements were made at the 2I4.3 nm resonance line. The limit of detection (signal : noise = 2) was 0.025 ppm in aqueous solution.

Extraction

The extraction procedure used for the separation of selenium was also employed for tellurium. Tellurium was virtually quantitatively extracted from 8 N hydrochloric acid into methyl isobutyl ketone. The ketone was previously saturated with 8 N acid as before. Cobalt and iron(III) extracted but did not affect the atomic absorption or fluorescence of tellurium. Large amounts of molybdenum interfere.

The shaking of the organic extract with distilled water used in the separation of selenium was attempted but the tellurium passed back into the aqueous phase with the other elements. If cobalt and iron are both absent i.e. only

molybdenum can extract into the methyl isobutyl ketone, the tellurium is easily separated by washing the organic layer with distilled water as before.to bring both elements back into aqueous solution. The pH of the resulting aqueous layer is then adjusted to 8.5 - 8.8 with ammonia and the tellurium may be extracted selectively into methyl isobutyl ketone as its diethyldithiocarbamate complex even in the absence of masking agents.

If cobalt and/or iron are present this extraction may be carried out only after their removal. Preliminary studies indicated that cobalt could be removed by extraction of its pyridine thiocyanate complex ($Co(py)_2(CNS)_2$) into chloroform and both iron(III) and cobalt by extraction of their thiocyanate complexes into methyl isobutyl ketone at pH I . Both these extractions did not appear to extract any tellurium. However, such multiple extractions are time consuming and are therefore unsuitable for routine analysis. Moreover the use of hotter less oxidising flames such as air-acetylene would probably minimise the molybdenum interference without seriously impairing the sensitivity of the tellurium determination.

Analysis of Simulated Sample Solutions

Standard nickel alloy samples containing known amounts of tellurium were not available. The extraction was tested by a similar method to that used in the selenium extraction. In the absence of molybdenum there is good agreement between the extractions of tellurium from pure solution and from the simulated alloy solutions. These solutions were prepared in

a manner similar to those in the selenium determinations except that they contained no molybdenum. The results are listed in Table 4.

Table 4

Extract concentration	20 ppm	I6 ppm	I2 ppm	8 ppm	4 ppm
Absorbance in pure solution	0.58	0.46	0.35	0.25	0.I2
Absorbance in sample solution	0.58	0.47	0.37	0.25	0.I2

If large amounts of molybdenum are present then equal amounts must be present in all standards used in the calibration curves or the molybdenum must be removed by the methods previously described.

The sensitivity (I% absorption) for atomic absorption of tellurium in methyl isobutyl ketone was 0.I5 ppm and the limit of detection for atomic fluorescence was 0.007 ppm. Based on the extraction of the tellurium in a 0.5 g sample into I0 mls organic solvent these figures correspond to 3 ppm and 0.I4 ppm in the sample.

Suggested procedure for Selenium and Tellurium

Dissolve the alloy sample (2.5 g) in concentrated hydrochloric acid and calculate the theoretical amount of acid consumed. Based on this figure make up the solution to 50 mls with the requisite amounts of water and hydrochloric acid to give a final acid concentration of 8 N.

Pipette I0 ml aliquots into 50 ml separating funnels

and extract with IO mls methyl isobutyl ketone previously satureted with 8 N hydrochloric acid. Discard the lower aqueous layer.

For the determination of tellurium the organic solvent may be nebulised directly into the flame. For selenium determinations shake the organic layer with IO mls distilled water when all interfering elements pass back into the aqueous phase leaving selenium alone in the organic phase. Discard the lower aqueous phase and nebulise the upper organic phase into the flame.

Calibration curves should be prepared as previously described using simulated sample solutions of approximately the same composition as the samples to be determined. The addition of the requisite amount of molybdenum , if present in large amounts, in the tellurium determinations is particularly important.

CHAPTER 2

DETERMINATION OF ARSENIC

Introduction

The determination of arsenic by flame emission is difficult because the lowest energy resonance line has an excitation energy of over 6 eV, and this is unattainable with the conventional flames in use in flame spectroscopic analysis. However, arsenic has been determined by measurement of the chemiluminescence in the primary reaction zone of an oxygen-acetylene flame (60) when aspirating solutions in organic solvents. A limit of detection of 2.2 ppm was obtained at the 235.0 nm line. Similar studies have been made by Gilbert (6I) of chemiluminescence resulting from aspirating isopropanol solutions of arsenic into an air-hydrogen flame.

An abundance of ground state arsenic atoms is achieved however in cool flames such as air-acetylene, air-hydrogen and even nitrogen- and argon-hydrogen diffusion flames. Arsenic hollow cathode lamps give a low radiative output at the resonance lines (I89.0 nm, I93.7 nm and I97.2 nm) and are difficult to prepare in view of the volatility of of arsenic. Slavin et al. (62) have determined arsenic by atomic absorption at the I93.7 nm line with a sensitivity of 2 ppm. The strongest absorption was observed at the I89.0 nm resonance line but, in view of the decreased sensitivity of the photomuliplier at this wavelength

less noise was observed at the I93.7 line and this line was therefore used in the measurements.

Dagnall, Thompson and West (I4) have used a microwave excited electrodeless discharge tube for the determination of arsenic by both atomic absorption and atomic fluorescence spectroscopy in a number of flames. They report maximum sensitivity in both techniques in the nitrogen- and argon-hydrogen diffusion flames and this is presumably due to their considerably smaller absorption (relative to air-hydrocarbon flames) at the wavelength of measurement. This in turn is due to the much smaller proportion of oxygen in the diffusion flames. The limits of detection at the I89.0 nm resonance line were 0.2 ppm in the nitrogen-hydrogen diffusion flame and I.0 ppm in the air-acetylene flame.

A common method for the isolation of micro and macro amounts of arsenic is the distillation of arsenic trichloride ($AsCl_3$) from hydrochloric acid solution (63,64). A reducing agent such as hydrazine sulphate is used to reduce arsenic in the quinquevalent state to the trivalent state. Another important method involves the volatilisation of arsenic as arsine (AsH_3) by the action of zinc in hydrochloric or sulphuric acid. This method is not suitable for samples containing large amounts of reducible heavy metals which would be likely to interfere in the production of arsine (65).

After isolation in the trivalent state arsenic may be oxidised to the quinquevalent state and ammonium molybdate to form a heteropolymolybdiarsenate. This is then reduced by a suitable reducing agent such as hydrazine sulphate (66) to a strongly coloured 'molybdenum blue' in which the

molybdenum is present in a lower valency state but whose composition is unknown.

Trivalent arsenic may be extracted from solutions of pH 4.0 - 5.8 using sodium diethyldithiocarbamate into a variety of organic solvents e.g. chloroform (67). A similar but more selective method of extraction is to use a chloroform solution of diethylammonium diethyldithiocarbamate and extract from mineral acid solutions (I - IO N sulphuric acid). The less expensive sodium salt is unsuitable under these conditions since it decomposes rapidly in acid solutions and cannot be used in solution in the organic phase since it is insoluble in organic solvents. Iron (II) and nickel are not extracted under these conditions (68).

Trivalent arsenic may be extracted from concentrated hydrochloric acid solution by chloroform and carbon tetrachloride (69). The only other element extracted by this system is germanium (IV). For reasons previously described it is inconvenient to aspirate solutions in chloroform and carbon tetrachloride into flames. Methyl isobutyl ketone has also been used (55) to extract arsenic from concentrated hydrochloric acid solution but this method is less selective than the extraction into chloroform.

Experimental

Apparatus

The apparatus was identical to that employed in the determination of selenium. The arsenic electrodeless discharge tube which contained arsenic (in excess) and iodine was operated in the 2IOL $\frac{3}{4}$-wave cavity. The tube filler gas was argon and the pressure 3 torr.

Reagents

i) Arsenic solution (I000 ppm). Arsenious oxide (0.330I g) was dissolved in distilled water with addition of the minimum of sodium hydroxide to assist solution and the solution made up to 250 mls.

ii) Interference solutions. As for selenium and tellurium determinations.

iii) Sodium diethyldithiocarbamate (I%) solution. As before.

iv) Methyl isobutyl ketone.

v) Chloroform.

Optimisation of Experimental Conditions

a) Atomic absorption

The electrodeless discharge tube was operated at 30 watts without cooling. The effect on the absorbance of the variation of the burner height and propane flow rate was investigated and is shown in Figs. 3a and b. The air flow rates were 7.0 l/min and 2.0 l/min as before.

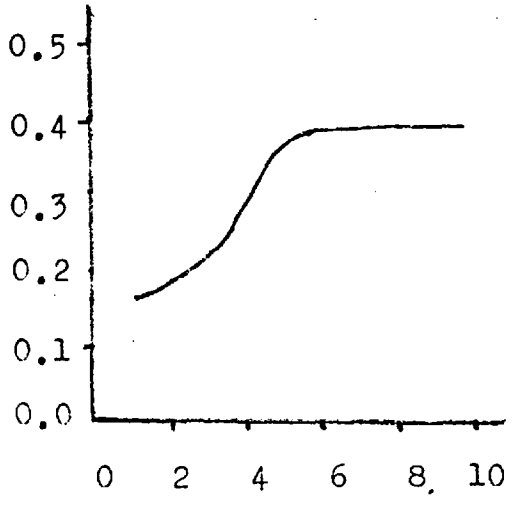

Fig. 3a Absorbance vs burner height (position on scale) 400 ppm As.

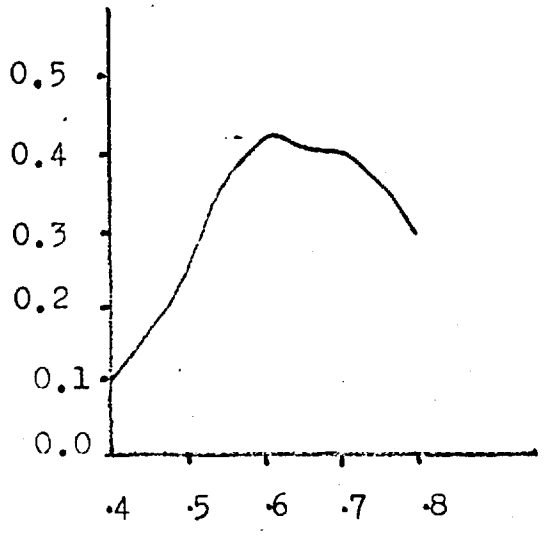

Fig. 3b Absorbance vs propane flow rate (arbitrary units) 400 ppm As.

The absorbance increased with increasing monochromator slitwidth and a slitwidth of 0.3 mm was used throughout.

b) Atomic fluorescence

As before the only two parameters than could be expressed in any units were the tube operating power and the monochromator slitwidth. These were 40 watts (without cooling) and I.0 mm respectively.

Wavelength of measurement

The atomic absorption of arsenic was studied at the three resonance lines at I89.0 nm, I93.7 nm and I97.2 nm. The absorbances of I000 ppm arsenic solutions at these lines are shown in Table 5.

Table 5

Line	Absorbance
I89.0 nm	0.78
I93.7 nm	0.74
I97.2 nm	0.38

The greatest absorbance is observed at the I89.0 nm resonance line but the I93.7 nm line yielded far less noisy signals and was therefore used in all determinations. A sensitivity of 3 ppm (I% absorption) was obtained in aqueous solution in the air-propane flame.

The atomic fluorescence of arsenic at the same three lines was measured and limits of detection of I.5, I.0 and I.5 ppm (signal : noise = 2) were obtained in the air-propane flame. The poor limits of detection in the air-propane

flame are due to the substantial absorption of the exciting radiation by the flame. To improve the sensitivity the nitrogen-hydrogen diffusion flame was used in which the limit of detection was 0.2 ppm in aqueous solution.

Separation

The most convenient method of separation of arsenic appeared to be the extraction into methyl isobutyl ketone (55) from concentrated hydrochloric acid solutions that had been used for selenium and tellurium. However, the 90 % extraction reported could not be achieved under the conditions recommended. Instead the extraction into chlorofrom (69) from hydrochloric acid was investigated. Of the other elements present in the alloy samples none extracted from 8 N hydrochloric acid and over 80 % of the arsenic was extracted using a 2 : I ratio of organic to aqueous phase volumes.

Since it is undesirable to nebulise chlorofrom into flames the chloroform layers were shaken with distilled water when the arsenic passed back into the aqueous phase. The sensitivity of the method may be improved by washing the chloroform layer with small volumes of distilled water or, if necessary, by extracting the arsenic into methyl isobutyl ketone as the diethyldithiocarbamate complex from a solution of pH 5.5 . The extraction is virtually quantitative.

The limit of detection in atomic fluorescence (signal : noise = 2) was 0.07 ppm at the I93.7 nm line in the

nitrogen-hydrogen diffusion flame and the atomic absorption sensitivity (I% absorption) in the air-propane flame was I.0 ppm at the same line both in methyl isobutyl ketone. Chloroform solutions were not studied.

Suggested procedure for Arsenic.

Dissolve the alloy sample (2.5 g) in concentrated hydrochloric acid taking care not to lose arsenic by volatilisation of the trichloride. Calculate the theoretical amount of acid consumed and add the requisite amounts of concentrated hydrochloric acid and water to make the solution up to 50 mls in 8 N acid.

Pipette I0 ml aliquots into 50 ml separating funnels and extract with 20 mls chloroform. Run off the lower chloroform layer and discard the acid layer. Shake the chloroform layer with I0 mls distilled water and discard the lower chloroform phase. The upper aqueous phase may then be subjected to atomic absorption or atomic fluorescence measurements.

Standards should be prepared by the extraction of arsenic from simulated sample solutions of similar composition to the samples for analysis as previously described. The method is only suitable for samples which will dissolve in concentrated hydrochloric acid in the cold or for systems where evolution of volatile arsenic halides may be prevented.

CHAPTER 3

DETERMINATION OF LEAD AND BISMUTH

3.I Lead

Introduction

Lead may be determined by flame emission at the 405.8 nm line and a limit of detection of 0.2 ppm has been reported (70) using the nitrous oxide-acetylene flame. The first atomic absorption measurements were made at the 283.3 nm line (7I) and subsequently Allan (47) used the 2I7.0 nm line and found it to be less sensitive. The use of higher intensity hollow cathode lamps has since shown that the 2I7.0 nm line is approximately twice as sensitive as the 283.3 nm line. Lead is readily atomised in cool flames and has been determined in a variety of samples by atomic absorption spectroscopy.

Browner et al. (72) have determined lead by atomic fluorescence spectroscopy using an electrodeless discharge tube as source. The most intense fluorescence is the 405.8 nm direct-line emission resulting from excitation at the 283.3 nm resonance line. A detection limit of 0.0I ppm was reported in the argon/oxygen/hydrogen flame.

Dagnall and West (73) investigated the effect of I000-fold mole excesses of 25 metals in the air-propane flame. Interference was observed only in the case of Al, Be, Th and Zr presumably due to occlusion.

Lead may be extracted into organic solvents using sodium

or diethylammonium diethyldithiocarbamate under a variety of conditions. The sodium salt has been used (74,75) to extract lead into chloroform from alkaline solutions using citrate and cyanide as masking agents. The diethylammonium salt extracts lead into chloroform from solutions of pH 3-4 (76) and from I.5-2 M hydrochloric acid. Lead is not extracted from 6 M hydrochloric acid and this affords a means of separation from bismuth which extracts under these conditions (77).

Dithizone may be used to extract lead from alkaline solution (65). Cyanide is again used as a masking agent and only bismuth and thallium extract from the alkaline cyanide solution.

Both the above extraction methods require cyanide as a masking agent and are unsuitable for the separation of lead from the other metals in the samples to be analysed. The large amounts of cyanide that would be required to mask the nickel and cobalt in a sample of the order of 0.5 g would render the method inconvenient and unsafe. An extraction that is more selective and therefore does not require large quantities of masking agents is therefore required.

If an excess of potassium iodide is added to a solution of lead in 5% (w/v) hydrochloric acid the complex iodide PbI_4^{2-} is formed and may be extracted into a number of oxygen containing solvents such as ketones (78). A number of other elements are completely or partially extracted e.g. zinc, cadmium, bismuth, copper and arsenic, and oxidising ions such as iron(III) interfere by oxidising the iodide to

iodine.

Many of the interferences may be removed by pre-extraction from acidic thiocyanate solution into similar oxygen containing solvents after which the iodide may be added and the lead extracted. Alternatively iron(III) may be removed by extraction into similar oxygen containing solvents from more concentrated hydrochloric acid. The acid solution is then diluted and iodide added, and the lead extracted as before.

Experimental

Apparatus

The experimental system was identical to that used in the determination of selenium and arsenic. The lead discharge tube containing lead and iodine was operated in the 2IOL discharge cavity without cooling.

Reagents

i) Lead solution (I000 ppm). Lead acetate (0.4580 g) was dissolved in distilled water and the solution made up to 250 mls.

ii) Nickel solution (I00,000 ppm). Nickel chloride ($NiCl_2.6H_2O$) (I00.5 g) was dissolved in 250 mls distilled water.

iii) Cobalt solution (I00,000 ppm). Cobalt chloride ($CoCl_2.6H_2O$) (I00.5 g) was dissolved in 250 mls distilled water.

iv) Chromium solution (I00,000 ppm). Chromic chloride ($CrCl_3.6H_2O$) (II2.0 g) was dissolved in 250 mls distilled water

v) Potassium iodide (60% w/v) solution. Potassium iodide (60 g) was dissolved in I00 mls distilled water.

vi) Hydrochloric acid (30 %). 5% (w/v) solution was prepared by dilution with 5 parts distilled water.

vii) Nitric acid (70 %).

viii) Methyl isobutyl ketone.

Optimisation of Experimental Conditions

a) Atomic absorption

The electrodeless discharge tube was operated at 50 watts uncooled. The absorbance was virtually independent of monochromator slitwidth and a slitwidth of 0.I0 mm was used to minimise noise as before. The effects of the variation of burner height and propane flow rate were investigated and are shown in Figs. 4a and b.

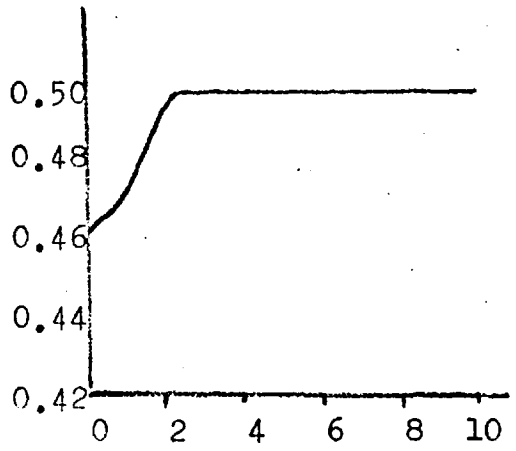

Fig. 4a Absorbance vs. burner height (scale reading) 40 ppm Pb.

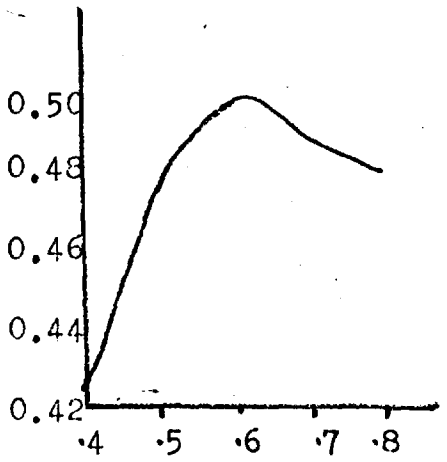

Fig. 4b Absorbance vs. propane flow rate (arbitrary units) 40 ppm Pb.

b) Atomic fluorescence

The optimum values of the only two measurable parameters were a tube operating power of 60 watts (uncooled) and a monochromator slitwidth of I.0 mm.

Wavelength of measurement

Absorbance measurements were made at the two resonance lines at 217.0 nm and 283.3 nm. Sensitivities (I % absorption) of 0.25 and 0.4 ppm were obtained in aqueous solution.

Only the direct-line fluorescence at 405.8 nm resulting from excitation at 283.3 nm was studied since this is the most sensitive emission (72) for lead. A limit of detection (signal : noise = 2) of 0.05 ppm was obtained in aqueous solution.

Separation

The extraction of lead from excess iodide solution (78) is clearly the most suitable for the determination of lead in the nickel alloys under consideration. Interfering elements iron(III) and molybdenum(VI) may be pre-extracted from concentrated hydrochloric acid solution without removing any lead. In view of this only the effect of nickel, cobalt and chromium on the lead was studied.

No interference was observed from 0.2 g nickel, 0.1 g cobalt and 0.1 g chromium (all as chlorides) in the lead extraction. There appeared at first to be an increased extraction in the presence of the foreign ions but this was found to be due to the presence of lead as an impurity in the chlorides used. The lead was removed by pre-extraction with iodide before the addition of lead to the standard solutions.

The atomic absorption sensitivity (1% absorption) in methyl isobutyl ketone was 0.063 ppm and the atomic fluorescence detection limit (signal : noise = 2) 0.015 ppm . Based on a 0.5 g sample and 10 mls organic solvent these figures

correspond to I.3 ppm and 0.3 ppm in the sample respectively.

Analysis of Standard Steels

No nickel base alloy samples containing known amounts of lead were available and the method was therefore tested by the analysis of four standard steels containing between 0.0I and 0.05 % lead. The method adopted for the analyses was similar to that employed by Dagnall, West and Young (79).

The steel samples (0.5 g) were dissolved in hydrochloric acid (30%). Dissolution was aided by warming and the iron oxidised to the ferric state by the addition of nitric acid (70%). The solutions were then cooled and transferred to 50 ml separating funnels and the iron(III) extracted by shaking twice with 25 ml aliquots of methyl isobutyl ketone. The final aqueous layer was evaporated to dryness and the residue dissolved in I0 mls 5% hydrochloric acid. This solution was transferred to 50 ml separating funnels and 5 mls potassium iodide (60%) solution added. The lead was then extracted with I0 mls methyl isobutyl ketone and the upper organic layer subjected to atomic fluorescence measurements. The results of the analyses are shown in Table 6. Each result is the mean of three determinations.

Table 6

Determination of Lead in Standard Steels by A.F.S.

Steel	Lead found (%)	Certificate	Range
BCS 326	0.014_8	0.014	0.014-0.017
BCS 327	0.011_0	0.010	0.009-0.012
BCS 328	0.014_6	0.015	0.012-0.018
BCS 329	0.048_0	0.050	0.042-0.053

3.2 Bismuth

Introduction

The flame emission spectroscopic determination of bismuth is rather difficult because the principal resonance line at 306.8 nm lies in the region of intense hydroxyl emission which tends to obscure the atomic emission. The other bismuth resonance lines are in the far ultraviolet and are therefore difficult to excite thermally.

The problem of intense hydroxyl emission has been overcome by Hobbs et al. (80) using a nitrogen shielded air-acetylene flame. The background level is drastically reduced and bismuth may be determined with quite high sensitivity. The limit of detection in aqueous solution was 2.0 ppm and 0.3 ppm in 50 % ethanolic solution.

Hydroxyl emission does not occur to a great extent in the oxygen-cyanogen flame and bismuth has been determined in this flame with a detection limit of 3 ppm (8I). Dean and Carnes (60) have reported detection limits of 6.4 ppm at the 223.I nm line in the primary reaction zone of an oxygen-acetylene flame and 2.8 ppm at 289.8 nm in an air-hydrogen flame. In both cases organic solvents were nebulised.

The atomic absorption determination of bismuth has been studied by Gatehouse and Willis (7I). They obtained a limit of detection of 2 ppm at the 306.8 nm line. The most sensitive line for atomic absorption of bismuth is at 223.I nm.

Dagnall, Thompson and West (I3) have determined bismuth by atomic fluorescence spectroscopy using an iodine electrodeless discharge tube as source. The exciting radiation from the source is at 206.I63 nm and fluorescence is

observed at the bismuth resonance line at 206.170 nm and direct-line fluorescence at 269.7 nm and 302.5 nm. Since the fluorescence radiation is of different wavelength to the exciting radiation no problems of source scatter were encountered. The limit of detection in the argon-hydrogen diffusion flame was 0.05 ppm at 302.5 nm.

Fluorescence at the 306.8 nm resonance line was observed in this study at about half the sensitivity of the 302.5 nm fluorescence and this line should be the most sensitive for the atomic fluorescence determination of bismuth. Atomic fluorescence at this wavelength using a bismuth discharge tube can result from excitation at 206.170 nm by both bismuth and iodine and by resonance fluorescence at the 306.8 nm line.

Bismuth may be extracted from alkaline solutions of pH 11 - 12 (82) into a number of solvents using sodium diethyldithiocarbamate. Cyanide and EDTA are used as masking agents and may be present in a large excess. However, for the samples under consideration the amount of cyanide required would be inconvenient.

Dithizone will also extract bismuth from alkaline solution into chloroform (83). Cyanide and citrate are used as masking agents which again makes this method unsuitable.

If an excess of iodide ion is added to an acidic solution of bismuth a yellow-orange colour is produced. This is due to the formation of the iodobismuthite ion (probably more than one species is formed). Because they are ionic, the complexes are not extracted into solvents such as benzene and chloroform but are extracted as the acids into oxygen containing solvents such as higher alcohols and esters. A mixture of amyl alcohol and ethyl acetate has been recommended (83). Several other elements extract e.g. copper

cadmium and lead, and oxidising ions such as iron(III) and molybdenum(VI) interfere by oxidation of the iodide to iodine. They must therefore be absent or a reducing agent used. Sulphurous acid or sulphite are often used but must not be present in a large excess if a spectrophotometric finish is employed since sulphite can also give a yellow colour with iodide due to the formation of iodosulphinic acid $I(HSO)_2$. Alternatively iron(III) may be pre-extracted into oxygen containing solvents from more acidic solutions.

Experimental

Apparatus

The apparatus used was identical to that used in the other determinations. The bismuth discharge tube (containing bismuth (in excess) and iodine) was operated in the 210L $\frac{3}{4}$-wave cavity and the iodine discharge tube in the 214L $\frac{1}{2}$-wave cavity. The iodine tube was strongly cooled in view of the volatility of iodine.

Reagents

i) Bismuth solution (1000 ppm). Bismuth metal (0.25 g) was dissolved in 5 mls concentrated (70%) nitric acid and the solution made up to 250 mls with distilled water.

ii) Cobalt, nickel and chromium solutions (100,000 ppm). As in the lead determinations.

iii) Potassium iodide solution (60%). As for the lead determinations.

iv) Methyl isobutyl ketone.

Optimisation of Experimental Conditions

a) Atomic absorption

The bismuth discharge tube was run at 30 watts without

cooling. The effects of the variation of the burner height and propane flow rate on the absorbance were investigated and are shown in Figs. 5a and b.

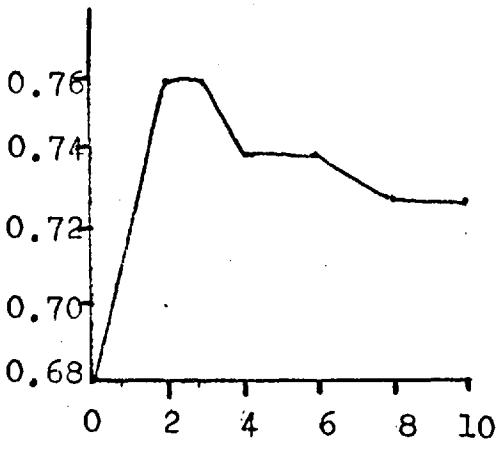

Fig. 5a Absorbance vs. burner height (scale divisions). 200 ppm Bi.

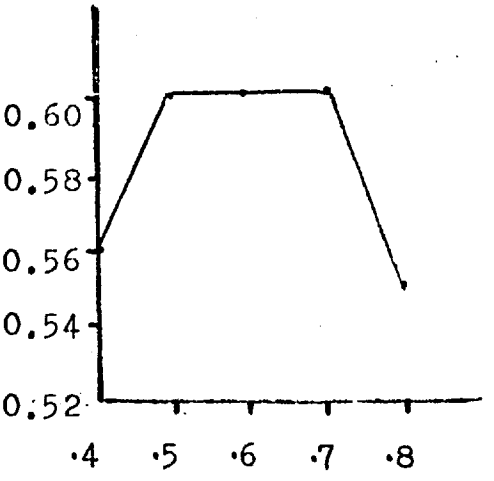

Fig.5b Absorbance vs. propane flow rate (arbitrary units). 200 ppm Bi.

The absorbance appeared to increase with increasing monochromator slitwidth up to 0.2 mm. A slitwidth of 0.2 mm was therefore used in all determinations.

b) Atomic fluorescence

The bismuth discharge tube was run at 45 watts without cooling and the iodine tube at 25 watts with strong cooling. The monochromator slitwidth employed at all wavelengths was 1.0 mm. As before the other parameters could not be expressed in any units.

Wavelength of measurement

Absorbance measurements were made at the bismuth resonance lines at 206.1 nm, 223.1 nm and 306.8 nm. The absorbances of 200 ppm bismuth solutions at these wavelengths are given in Table 7.

Table 7

Line	Absorbance
206.1 nm	0.12
223.1 nm	0.77
306.8 nm	0.38

The bismuth electrodeless discharge tube was used as source in all determinations. The most sensitive line was the 223.1 nm line at which a sensitivity (1 % absorption) of 0.55 ppm was obtained in aqueous solution.

Atomic fluorescence measurements were made in the air-propane flame using both bismuth and iodine discharge tubes at the resonance lines at 206.1 nm, 223.1 nm and 306.8 nm and at 302.5 nm. This latter is direct-line fluorescence resulting from excitation at the 206.1 nm resonance line from both bismuth and iodine as previously described. The relative intensities from 10 ppm bismuth solutions are listed in Table 8.

Table 8

Tube	Line	Intensity (a.u.)
Bi/I_2	206.1 nm	9
Bi/I_2	223.1 nm	28
Bi/I_2	302.5 nm	60
I_2	302.5 nm	40
Bi/I_2	306.8 nm	70

(a.u. - arbitrary units)

The most sensitive line is the 306.8 nm resonance line as would be expected. This having been established, the effect of other flames on the sensitivity was investigated in an attempt to improve the limit of detection by reducing the noise due to the intense hydroxyl emission close to the atomic line. The nitrogen-hydrogen diffusion flame and the argon shielded air-propane flame were investigated and the relative fluorescences in the flames (10 ppm bismuth) are listed in Table 9.

Table 9

Flame	Intensity (a.u.)
Air - propane	50
Argon shielded air-propane	100
Nitrogen-hydrogen	40*

* noise less than in the unshielded air-propane flame so that the detection limits were approximately equal (0.3 ppm)

The optimum conditions are therefore the use of the argon shielded air-propane flame and measurement at the 306.8 nm line. Under these conditions a detection limit (signal : noise = 2) of 0.15 ppm was obtained in aqueous solution.

Separation

Bismuth was separated by extraction of the complex iodo-bismuthous acid into methyl isobutyl ketone from 5 % hydrochloric acid. The extraction takes place under the same conditions as the lead extraction previously described, and this permits their determination in a single extraction.

As in the case of lead the extraction was unaffected by 0.2 g nickel, 0.1 g cobalt and 0.1 g chromium (all present as chlorides). The sensitivity (1 % absorption) for atomic absorption in methyl isobutyl ketone was 0.17 ppm in the air-propane flame. The atomic fluorescence detection limit (signal : noise = 2) was 0.08 ppm in the same flame at the 306.8 nm resonance line.

Suggested analytical procedure for Lead and Bismuth

Dissolve the sample (2.5 g) in concentrated hydrochloric acid warming to aid dissolution and add a few drops of concentrated nitric acid to oxidise any iron and molybdenum present to the trivalent and hexavalent states respectively. Transfer the solution to a 100 ml separating funnel and extract twice with 25 mls methyl isobutyl ketone to remove iron (III) and molybdenum (VI). (If the samples are known not to contain iron and molybdenum these last two steps may of course be omitted).

Discard the organic phases and add the requisite amounts of distilled water and concentrated hydrochloric acid to make the solution up to 50 mls 15 % in hydrochloric acid. These amounts may be calculated from the theoretical amount of acid consumed and the initial volume of acid used in the dissolution. Pipette 10 ml aliquots into 100 ml separating funnels and add 15 mls distilled water and 5 mls 60 % potassium iodide solution. Extract the lead and bismuth by shaking with 10 mls methyl isobutyl ketone and discard the lower aqueous layer. The organic phase may then be subjected to atomic absorption or atomic fluorescence measurements.

CHAPTER 4

DETERMINATION OF SILVER

Introduction

An abundance of silver ground state atoms may be obtained in cool flames such as air-hydrogen and air-propane. Silver hollow cathode lamps are very intense and stable, and , as a result, the sensitive determination of silver by atomic absorption spectroscopy may be performed without difficulty. The resonance lines at 328.1 nm and 338.3 nm both afford sensitive measurements, and Robinson (84) has reported sensitivities of 0.1 and 0,15 ppm respectively at these lines.

The atomic fluorescence determination of silver has been studied using a continuum source (43) and a high intensity hollow cathode lamp. Dagnall, Thompson and West (43) obtained 40% greater sensitivity at the 338.3 nm line but this was presumably due to the greater intensity of the source at this longer wavelength. Using a high intensity hollow cathode lamp West and Williams (85) obtained a detection limit of 0.001 ppm at the 328.1 nm line (which was found to be the more sensitive) in an air-acetylene flame.

Silver electrodeless discharge tubes are on the whole somewhat unsatisfactory and are no more intense than the available silver high intensity hollow cathode lamps. If a tube containing silver and iodine is used there is considerable silver iodide band emission close to the silver atomic lines (86) and this reduces the line : background ratio. Silver chloride

is more satisfactory in this respect but is less volatile. In this study a high intensity hollow cathode lamp was not available and therefore only atomic absorption measurements were made.

Silver may be extracted at pH 11 by sodium diethyldithiocarbamate . EDTA is recommended as a masking agent (58) but for the reasons previously described the use of large amounts of masking agents is to be avoided if possible.

Betteridge and West (87) have extracted the ion association complexes of silver with di-n-butylamine and salicylate and stearate into methyl isobutyl ketone. Certain elements interfere by gel formation with stearate but such interference (except nickel) is removed by the addition of 1.5 M sodium nitrate solution. Several metals interfere in the extraction (copper, cobalt, nickel and iron(III)) but may be masked by anthranilic acid NN-diacetic acid (AADA).

Dithizone extracts silver (65) from acidic solutions up to 6 N mineral acid. Chloride causes incomplete extraction in acid solution but the extraction is complete at pH 5 even in 20 % ammonium chloride.

Experimental

Apparatus

In view of the unsatisfactory nature of silver discharge tubes a silver hollow cathode lamp was used for atomic absorption measurements and fluorescence measurements were not attempted.

Reagents

i) Silver solution (1000 ppm). Silver nitrate (0.3961 g) was dissolved in distilled water and the solution made up to 250 mls.

ii) Nickel solution (100,000 ppm). As for lead determinations.

iii) Nickel nitrate solution (100,000 ppm Ni). Nickel nitrate (123.8g) was dissolved in 250 mls distilled water.

iv) Cobalt solution (100,000 ppm). As for lead determinations.

v) Cobalt nitrate solution (100,000 ppm Co). Cobalt nitrate (121.1g) was dissolved in 250 mls distilled water.

vi) Nitric acid (70%).

vii) Extracting solution A. Salicylic acid (0.8 g) and di-n-butylamine (7.5 mls) were dissolved in 250 mls methyl isobutyl ketone.

viii) Anthranilic acid NN-diacetic acid. (0.5 M). Anthranilic acid NN-diacetic acid (3.166 g) was dissolved with the minimum of sodium carbonate in distilled water and the solution made up to 25 mls with distilled water.

ix) Dithizone (0.1 % in methyl isobutyl ketone). Dithizone (0.1 g) was dissolved in 100 mls methyl isobutyl ketone. and 10 mls of this solution were diluted with 90 mls methyl isobutyl ketone.

Optimisation of Experimental Conditions

The absorbance was virtually independent of lamp current within the range 2-5 milliamps and of the monochromator slitwidth in the range 0.025 mm - 0.15 mm. All measurements were made using a lamp current of 4 milliamps and a monochromator slitwidth of 0.10 mm. The effects of the variation of burner height and propane flow rate are shown in Figs 6a and b.

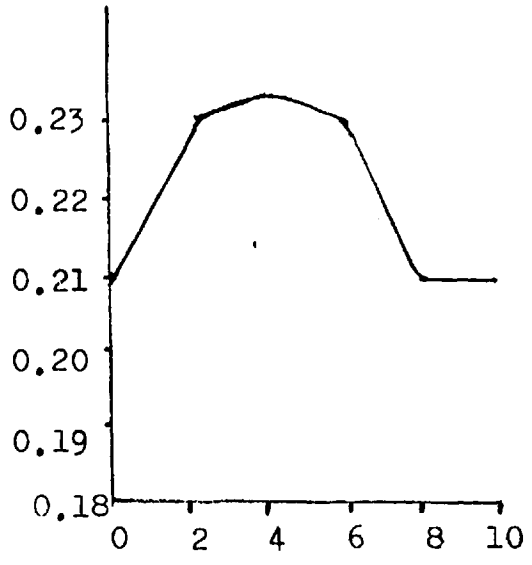

Fig. 6a Absorbance vs. burner height (scale divisions). 10 ppm Ag.

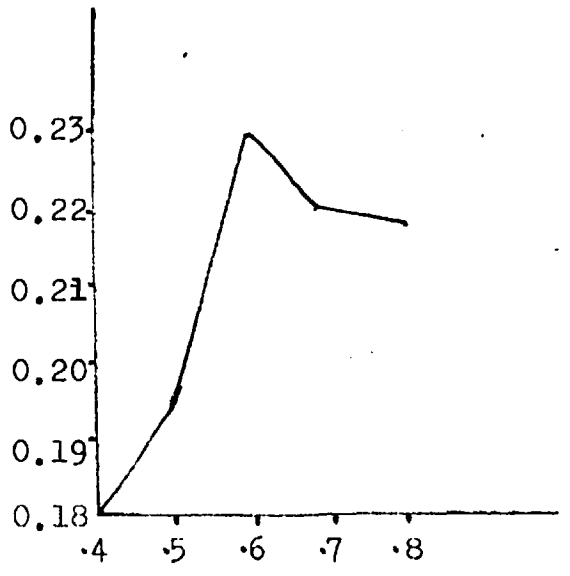

Fig. 6b Absorbance vs. propane flow rate (arbitrary units). 10 ppm Ag.

Wavelength of measurement

Absorbance measurements were made at the 328.1 nm and 338.3 nm resonance lines and sensitivities (1% absorption) in the ratio 1 : 2 were obtained. The sensitivity at the more sensitive 328.1 nm line was 0.15 ppm in aqueous solution.

Separation.

The extraction of silver as the ion association complex with di-n-butylamine and salicylate into methyl isobutyl ketone (Solution A) was investigated but found to be unsuitable. Very large amounts of the masking agent anthranilic acid NN-diacetic acid are required to mask the nickel and cobalt present even in a 0.25 g sample. The largest amount of masking agent used was 7.5 mls of 0.5 M solution and the high cost of this reagent therefore renders the method unsuitable for routine analysis.

As a result the extraction from concentrated mineral acid as the dithizonate into methyl isobutyl ketone was studied. Iron(III) and molybdenum do not form dithizonate complexes

and only the effects of cobalt and nickel on the extraction were investigated since iron may be easily converted to the ferric state merely by sample dissolution in nitric acid. The silver extraction was carried out from 5 N nitric acid solution and was unaffected by 0.1 g nickel and 0.1 g cobalt (both as nitrates).

The sensitivity (1% absorption) for atomic absorption in the organic solvent was 0.04 ppm. Based on the extraction of the silver from a 0.25 g sample into 10 mls organic solvent this figure corresponds to 1.6 ppm in the alloy sample.

Suggested analytical procedure for Silver

Dissolve the sample (1.25 g) in concentrated nitric acid (70%) and calculate the theoretical amount of acid consumed. Based on this figure add the requisite amounts of concentrated nitric acid and water to make the solution up to 50 mls 5 N nitric acid. Pipette 10 ml aliquots of this solution into 50 ml separating funnels and extract with 10 mls 0.1 % dithizone solution in methyl isobutyl ketone. Discard the lower aqueous layer and subject the upper organic layer to atomic absorption measurements.

Calibration curves should be prepared by extracting known amounts of silver from simulated sample solutions of approximately the same composition as the samples to be analysed.

PART II

COMPUTER CALCULATIONS OF FLAME COMPOSITIONS AND DEGREES OF ATOMISATION BY THE METHOD OF FREE ENERGY MINIMISATION

Introduction

The spectral interferences associated with flame emission spectroscopy are substantially reduced in atomic absorption because of the narrow monochromator slitwidths used in this method of analysis. For spectral interference to occur in atomic absorption spectroscopy the line profiles must overlap. This is observed in the case of copper (324.754 nm) and europium (324.753 nm) (88) and of gallium (403.298 nm) and manganese (403.307 nm) (89). In these instances it is possible to observe atomic absorption of one element using a line source of the other. This type of interference can be avoided however by using other lines for measurement e.g. 287.424 nm for gallium and 279.482 nm for manganese (which are in fact the most sensitive lines for the atomic absorption determination of these elements.

Differences in atomiser uptake rates occur due to differences in the viscosity and surface tension of solutions containing large amounts of foreign ions and this leads to apparent interference. This can normally be avoided by the preparation of calibration curves for the analyte element in the presence of the requisite concentrations of the interfering elements. The principal sources of interference are suppression of the atomisation of the analyte element due to occlusion by solid particles and the formation of stable compounds e.g. mixed oxides such as $MgAl_2O_4$. Scatter of the incident radiation in atomic fluorescence spectroscopy by solid particles arising from incomplete atomisation of refractory elements can also occur.

It is relatively simple to determine low boiling elements such as those previously considered by atomic absorption spectroscopy using cool flames such as air-propane. This is not the case however with elements that tend to form stable oxide species such as aluminium and silicon. Significant atomisation of such elements is observed only in hot reducing atmospheres such as the fuel rich nitrous oxide-acetylene (44) and oxygen-acetylene flames (90). For this reason it was not possible to determine the low boiling elements considered in the complex mixture of metals in the samples because some of these metals were refractory in nature (molybdenum, aluminium). It was therefore necessary to design separation procedures to remove the test element from all or at least the bulk of the matrix elements, and such procedures are time consuming for routine analysis.

The purpose of the computer calculations of compositions of both hot reducing flames such as nitrous oxide-acetylene and of cooler flames such as air-acetylene was therefore to study the atomisation processes with varying flame type and composition. Consideration of the variations in concentrations of the metal atoms and certain flame species, and of systems in which critical species are present and absent, yields information about the atomisation process, and facilitates a prediction of the most efficient flame for atomisation of refractory elements and for suppression of chemical interferences by these elements.

For simple systems equilibrium concentrations of the species concerned may be calculated from the equilibrium constant data for the reactions taking place. This is not possible, however, for more complex systems such as the flames previously quoted since insufficient equilibrium constant data is available and the flame reactions are not all

characterised. For this reason the technique of Free Energy Minimisation has been used to calculate the equilibrium compositions of several flames that are in use in analytical flame spectroscopy and the concentrations of free metal atoms therein.

The technique was proposed initially by White, Johnson and Dantzig (91) for vapour phase equilibria and later extended to include condensed phases by Kubert and Stephanou (92). The method has more recently been used via a digital computer program to study the compositions of oxy-acetylene flames (93). A considerably modified version of this program was used in the calculations in this study of nitrous oxide-acetylene and other analytically useful flames.

The fundamental criterion for the application of the method is that in a system in chemical equilibrium the free energy is a minimum. Some basic assumptions must therefore be made :-

i) the rate of chemical reactions must be high compared to the residence time of the species involved,

ii) all gaseous species must exhibit ideal gas behaviour,

iii) all condensed species must be immiscible.

The assumption of equilibrium may strictly speaking be a questionable one, but,in view of the good agreement between experimentally determined flame temperatures (94,95) and maximum theoretical temperatures (96) which are based on equilibrium calculations, it is considered that the flames are sufficiently close to equilibrium for the solutions not to be in serious error as a result of this assumption.

The following steps are involved in the derivation of the calculation :-

i) An expression is developed for the total free energy of the system (at I atmosphere) as a function of the free energies of the individual components for a mixture of an assumed composition.

ii) The equilibrium composition (unknown) is expressed in

terms of the assumed composition and of unknown increments representing the changes required to bring the composition to that at equilibrium. This is achieved by using the first two terms of a Taylor's expansion.

iii) The expanded function is then minimised subject to mass balance constraints using Lagrange multipliers.

iv) As a result, a system of linear simultaneous equations is generated and then solved by the method of Gaussian elimination with maximum pivot to yield a new approximation to the composition corresponding to minimum free energy.

v) The process is repeated until successive solutions agree to the desired accuracy and the solutions are then stored and used as initial guesses for the calculation at the next temperature.

vi) The solutions at all temperatures for each flame are stored and those at the final temperature are used as initial guesses for the first temperature of the next flame.

Mathematical Derivation

The complete mathematical derivation has been given by Oliver et al. (97) and therefore only a summary is given. The total free energy of a mixture of n gaseous and p condensed components is the sum of the free energies of the individual components and may be expressed as :-

$$F = \sum_{i=1}^{n} f_i^g + \sum_{h=1}^{p} f_h^c \qquad (1)$$

The free energy of a gaseous species is given by:

$$f_i^g = x_i^g \cdot (c_i^g + \ln(x_i^g/\bar{x}) + \ln P) \qquad (2)$$

where

$$c_i^g = (F/RT)_i^g \qquad (3)$$

and P is the pressure in atmospheres, $(F/RT)_i^g$ is a dimensionless function obtained by dividing the free energy F by the product RT (which has the dimensions of energy) for the ith species, x_i^g is the mole number of the ith gaseous species and $\bar{x}$ is the sum of the mole numbers of all the gaseous species.

For condensed species the effect of pressure and mixing are neglected so that the free energy expression becomes

$$f_h^c = x_h^c . c_h^c \qquad (4)$$

where $$c_h^c = (F/RT)_h^c \qquad (5)$$

and $(F/RT)_h^c$ is the free energy function (defined above) for the hth condensed species, and x_h^c is the mole number of the hth condensed species.

In the free energy expressions (3) and (5) the function $(F/RT)_i$ is defined thus:

$$(F/RT)_i = \frac{I}{R} . \left[\frac{F - H_{298}}{T}\right]_i + \frac{\Delta H^f_{298}}{RT} \qquad (6)$$

where R is the universal gas constant, T the absolute temperature, ΔH^f_{298} the standard enthalpy of formation at 298°K and $\left[\frac{F - H_{298}}{T}\right]_i$ the free energy function (obtainable from the JANAF thermochemical tables) for the ith species.

To determine the equilibrium composition it is necessary to calculate a non-negative set of mole numbers ($X_I^g, \ldots X_n^g$, $X_I^c, \ldots X_p^c$) which will minimise the total free energy F of the system. However this set of mole numbers must also satisfy the mass balance requirements. Therefore :-

$$\sum_{i=I}^{n} a_{ij} . x_i^g + \sum_{h=I}^{p} a_{hj} . x_h^c = b_j, \quad j=I,..m \qquad (7)$$

where m is the number of elements, b_j the number of gram atoms of the jth element and a_{ij} the number of atoms of the

jth element in the ith species.

Let $Y^g = (y_I^g, \ldots y_n^g)$ be an initial guess for the mole numbers of the gaseous species $(x_I^g, \ldots x_n^g)$ and $Y^c = (y_I^c, \ldots y_n^c)$ similarly be a guess for the mole numbers of the condensed species. Also let $Y = (Y^g, Y^c)$. Y is chosen such that it is a positive set and that it satisfies the mass balance requirements. The free energy for this mixture is given by

$$F(Y) = \sum_{i=I}^{n} y_i^g (c_i^g + \ln(y_i^g/\bar{y}) + \sum_{h=I}^{p} c_h^c . y_h^c \qquad (8)$$

where $\bar{y} = \sum_{i=I}^{n} y_i^g$

An expression Q(X) is obtained as an approximation for F(X), the minimum free energy, by using a Taylor's expansion about the initial guess Y. Using this expansion technique and substituting values of the partial derivatives $\partial F/\partial x_i^g$ and $\partial F/\partial x_h^c$ the following expression may be obtained.

$$Q(X) = F(X) = \sum_{i=I}^{n} (c_i^g + \ln(y_i^g/\bar{y}) \Delta_i^g + \sum_{h=I}^{p} c_h^c \Delta_h^c + \frac{1}{2} \sum_{i=I}^{n} y_i^g \left(\frac{\Delta_i^g}{y_i^g} - \frac{\Delta'}{\bar{y}} \right) \qquad (9)$$

where $\Delta_i^g = x_i^g - y_i^g, \Delta_h^c = x_h^c - y_h^c, \Delta' = \bar{x} - \bar{y}$

To find a better approximation to the equilibrium solution, Q(X) is minimised subject to the mass balance constraints of equation (7). It is required to define a function G(X) so that

$$G(X) = Q(X) + \sum_{j=I}^{m} \pi_j (b_j - \sum_{i=I}^{n} a_{ij} x_i^g - \sum_{h=I}^{p} a_{hj} x_h^c) \qquad (10)$$

where the π_j's are the Lagrange multipliers. Then setting the partial differentials $\partial G(X)/\partial x_i^g$ and $\partial G(X)/\partial x_h^c$ equal to zero the change in free energy with a change in the number of moles of the gaseous species becomes

$$\partial G(X)/\partial x_i^g = \left(c_i^g + \ln(y_i^g/\bar{y}) \right) + \left(x_i^g/y_i^g - \bar{x}/\bar{y} - \sum_{j=I}^{m} \pi_j a_{ij}^g \right) = 0 \qquad (II)$$

and the change in the free energy with a change in the number of moles of condensed species is

$$\partial G(X)/\partial x_h^c = c_h^c - \sum_{j=I}^{m} \pi_j a_{ij}^c = 0 \qquad (I2)$$

Solving equation (II) for x_i^g and summing over all i gives

$$x_i^g = -y_i^g \left(c_i^g + \ln(y_i^g/\bar{y}) \right) + y_i^g(\bar{x}/\bar{y}) + \sum_{j=I}^{m} \pi_j a_{ij}^g y_i^g \qquad (I3)$$

and then

$$\sum_{j=I}^{m} \pi_j \sum_{i=I}^{n} a_{ij}^g y_i^g = \sum_{i=I}^{n} y_i^g \left(c_i^g + \ln(y_i^g/\bar{y}) \right) \qquad (I4)$$

Now let

$$r_{jk} = r_{kj} = \sum_{i=I}^{n} \left(a_{ij}^g a_{ik}^g \right) y_i^g \qquad j,k = I,\ldots..m \qquad (I5)$$

The substitution of equation (I3) into equation(7) gives m equations which together with equations (I2) and (I4) give a system of m+p+I linear equations in the unknowns $\pi_I,\ldots\pi_n$ and $x_I,\ldots x_p^c$ and $\bar{x}/\bar{y}$ thus :-

$$\alpha_I(\bar{x}/\bar{y}) + a_{II}^c x_I^c + a_{2I}^c x_2^c \ldots.+ a_{pI}^c x_p^c + r_{II}\pi_I + r_{I2}\pi_2 \ldots r_{Im}\pi_m = b_I + \sum_{i=I}^{n} a_{iI}^g f_i^g$$

$$\alpha_m(\bar{x}/\bar{y}) + a_{Im}^c x_I^c + a_{2m}^c x_2^c \ldots.+ a_{pm}^c x_p^c + r_{mI}\pi_I + r_{m2}\pi_2 \ldots r_{mm}\pi_m = b_m + \sum_{i=I}^{n} a_{im}^g f_i^g$$

$$\alpha_I\pi_I + \alpha_2\pi_2 \ldots.\alpha_m\pi_m = \sum_{i=I}^{n} f_i^g$$

$$a_{II}^c\pi_I + a_{I2}^c\pi_2 \ldots. \quad a_{Im}^c\pi_m = c_I^c$$

$$a_{mI}{}^{c}\pi_{I} + a_{m2}{}^{c}\pi_{2} + \ldots\ldots\ a_{pm}{}^{c}\pi_{m} = c_{p}{}^{c}$$

where $$\alpha_{j} = \sum_{i=I}^{n} a_{ij}{}^{g}y_{i}{}^{g} \qquad (I6)$$

The solution to this set of equations yields the new approximation to the condensed species $x_{h}{}^{c}$ directly. To find the new values of the gaseous species $x_{i}{}^{g}$ it is necessary to substitute the π_{j}, $\bar{x}/\bar{y}$ and $y_{i}{}^{g}$ values into equation (I3). In this way a new set of $x_{i}{}^{g}$ and $x_{h}{}^{c}$ values are found which represent a new approximation to the desired result. In addition, values of trace species omitted from the system are calculated from the equation :-

$$x_{i}{}^{g} = \bar{x}.\ \exp\left(-c_{i}{}^{g} + \sum_{j=I}^{m} \pi_{j}a_{ij}{}^{g} \right) \qquad (I7)$$

where $$I.0 \times I0^{-5} \geqslant x_{i}{}^{g} \geqslant I.0 \times I0^{-35}$$

and the species are then added to the system. The procedure is repeated using the x_{i} values found as answers for the last calculation as new y_{i} values, until the differences between successive iterations are less than $I.0 \times I0^{-6}$.

The computed part of the new mole numbers $x_{i}{}^{g}$ and $x_{h}{}^{c}$ may contain some negative numbers. If this is the case, the computed set of mole numbers cannot be used directly in the next approximation and, instead, the new set is taken to be an indication of the direction of desired travel and x is permitted to proceed in this direction only so far as it remains a positive set.

This is achieved by setting a value of λ so that

$$y_{i}' = y_{i} + \lambda(x_{i} - y_{i}) \qquad (I8)$$

is positive. The method of setting λ is to compute for

each species where ($x_i - y_i$) is negative a value of λ' such that y_i' is zero

$$\lambda' = -y_i / (x_i - y_i) ,$$

select the smallest value of λ_i' and then set $\lambda = 0.99\ \lambda'$ so that all y_i are positive. The same value of λ is used in adjusting all the mole numbers to satisfy the mass balance constraint in the resulting set.

In each iteration, after the set of mole numbers has been adjusted to a positive set, a test is used to determine if omitted condensed species should be added to the system. If the relationship, for the Hth condensed species, holds

$$\left| (F/RT)_H - \sum_{j=I}^{m} \pi_j a_{hj}{}^c \Big/ (F/RT)_H \right| \geq I.0 \times I0^{-3} \quad (I9)$$

then the species is added to the system with a value of $I.0 \times I0^{-8}$.

To minimise matrix system difficulties, any species (gaseous or condensed) which is less than $I.0 \times I0^{-8}$ is rejected from the calculation and omitted by setting it to zero.

Summary of computer program

The program used in the oxy-acetylene study was simplified, modified and converted to Fortran IV for use with an IBM 7094 computer using a PUFFT (Purdue University Fast Fortran Translator) compiler and a CDC 6600 computer. The modified program consists of a main routine in which the thermodynamic data is read in and the values of F/RT (molar standard free energy function) are calculated. From this a subroutine THERMO is called in which the problem data is read in, the stoichiometry set for the mass balance constraints and the

system of equations generated. This set of equations is solved by calling subroutine GPIVOT (Gauss elimination with maximum pivot). The solutions are tested for convergence and the process repeated until convergence is achieved (difference between successive solutions $< 10^{-6}$). The solutions are then stored in a two dimensional array and used as the initial guesses for the calculation at the next temperature.

Solutions are calculated in moles per mole feed and those of the gaseous species in volume per cent. Solutions for species in moles per mole feed which are less than the reciprocal of the Avogadro number (ca. 1.6×10^{-24}) are clearly meaningless but are retained since they do not affect the concentrations of the major species. Moreover the computers used are able to deal with considerably smaller numbers (IBM 7094 - 10^{-38} and CDC 6600 - 10^{-292}). If a problem fails to converge in 50 iterations a message to this effect is printed out together with the current values of the concentrations and the temperature, and the program is terminated. Finally, a subroutine GLYPHO is called which enables the concentrations of selected species to be plotted with respect to flame composition via the CALCOMP plotter available on the CDC 6600 computer. The flame composition is expressed as the ratio of carbon to oxygen in the flames of carbon containing fuels and the hydrogen to oxygen ratio in the nitrous oxide-hydrogen flame.

Isothermal temperatures were plotted since temperature data for all the flames studied was not available. The complete program is listed in Appendix I .

Summary of data

The data is in two parts. The first is the thermodynamic data which consists of a card with the number of species and the number of temperatures to be considered, followed by sets of cards, one set for each species, punched with the species title (columns 2-7), the absolute temperature (cols. I0-I3), $-((F - H_{298})/T)$ (cols. I8-23) and the enthalpy of formation at 298°K (cols. 27-33). The temperature is in ascending order in increments of I00°K. The last two functions are obtained from the JANAF thermochemical tables (98).

The first card of the problem data is punched with the flame title (e.g. nitrous oxide-acetylene) and this is followed by a card with the number of flames to be studied and the number of metals in the system. The next card contains the numbers of elements, gaseous and condensed species, the initial temperature and the pressure. Two cards then follow with the element titles and their atomic weights. These are always in the order C, H, O, N, Metals. The next card contains the number of the oxidising element (oxygen), (this will be either 2 or 3 depending on the presence or absence of carbon and hydrogen) the initial number of moles of the fuel gas, the increment in the number of moles of fuel (normally 0.05 or 0.I0) and the number of moles of non-fuel components required in the combustion of one mole of fuel in the stoichiometric flame. There then follows a set of cards (one for each gas element (C, H, O, N) containing the number of gram atoms of the element present in one mole of fuel and the number of gram atoms present in the amount

of oxident and water required in the combustion of one mole of fuel. The next card is punched with the parameters for selection of the temperatures for which the curves are to be plotted in the CALCOMP routine. The problem data is completed by a set of cards, one for each species, containing the species title, the initial estimate of the concentration and the numbers of atoms of each element present in the species. The order of the species in this set of cards must be the same as that in the thermodynamic data.

The remaining data necessary for the CALCOMP generation of the concentration composition curves is read in in subroutine GLYPHO. This consists of the symbols and labels for the curves and axes and the number of species for which curves are to be plotted.

Calculation of Stoichiometry

The species concentrations are calculated in moles per mole feed and those of the gaseous species in volume per cent. The numbers of gram atoms of each element in one mole feed are calculated by taking the numbers of gram atoms in the number of moles of oxident and water involved in the combustion of one mole of fuel gas (DIVO) and the number of moles of fuel gas (RED(INDEX)) in the flame concerned and dividing by the total number of moles of feed (DIVO + RED(INDEX)). The amount of water reaching the flames is calculated from flow rates and solution uptake rates observed in practical atomic absorption analyses e.g. ca. 5 l/min flow of nitrous oxide, 5% atomiser efficiency and ca. 5 ml/min uptake of water. Variations in the amount of water will not affect the general trend of the concentration

curves but will affect the carbon to oxygen ratio at a particular degree of fuel richness.

Limitations of the method

In addition to the assumptions made in the derivation of the method there are some further limitations of the technique. No account is taken of air entrainment in the flames since no measurements of this phenomenon are currently available. Thus the systems studied may be considered as approximating to the conditions prevailing in the interconal zone of a flame-shielded premixed flame (99) or to the central regions of a conventional circular premixed flame.

The absence of data for the species C_2H from the available JANAF tables and hence its omission from the system is unlikely to have a great influence on the concentrations of the other species. The effect of omitting minor species was studied and found to be negligible. However, all major flame species must be considered otherwise erroneous results will certainly be obtained. It is also not possible to consider ionic flame species e.g. NO^+ in the flame since data is not available. Moreover it would be impossible to subject the electrons accompanying these ions to the mass balance constraint and another constraint is introduced namely that of charge balance.

For these reasons the absolute values of the concentrations of the flame components are not strictly comparable to observations made in practice on flames of the same fuel : oxident ratio. However, the trends associated with the concentration composition curves are indicative of those that are observed in practice.

CHAPTER 5

ACETYLENE FLAMES

5.I Nitrous oxide-acetylene

The flame reaction is :-

$$2N_2O + C_2H_2 (+ 0.I25\ H_2O) = 2CO + 2N_2 + H_2$$

A range of flames was studied by varying the number of moles of acetylene from I.0 to I.5 in steps of 0.05. Thus DIV0 = 2.I250 and the normalising factor DIV = 2.I250 + RED(INDEX). The numbers of gram atoms of each element B(J) are given by

Carbon B(I) = 2x RED(INDEX) / DIV

and FRAC(I) = 2.0000 ADD(I) = 0.0000

Hydrogen B(2) = (2 x RED(INDEX) + 0.2500) / DIV

and FRAC(2) = 2.0000 ADD(2) = 0.2500

Oxygen B(3) = 2.I250 / DIV

and FRAC(3) = 0.0000 ADD(3) = 2.I250

Nitrogen B(4) = 4.0000 / DIV

and FRAC(4) = 0.0000 ADD(4) = 4.0000

The amounts of oxygen and nitrogen are of course independent of the amount of fuel. All metals were studied at a level of 0.000I gram atom per mole feed and FRAC and ADD data are therefore unnecessary.

The carbon to total oxygen ratio is given by :-

RATIO(INDEX) = 2xRED(INDEX) / 2.I25

and equals 0.94I2 in the stoichiometric flame. It equals unity when RED(INDEX) = 2.I25 / 2 = I.0625 i.e. when the flame is 6.25% fuel rich.(This figure will of course vary

with the amount of water reaching the flame and is only 6.25% in this instance.)

The computer calculations indicate that, as is found in practice, the degrees of atomisation of both aluminium (Fig. I) and silicon (Fig. 2) are markedly dependent on the flame composition. In the case of aluminium there is significant atomisation in the stoichiometric flame but atomisation increases as the flame becomes fuel rich. In the case of silicon there is little atomisation in the stoichiometric flame although the atomisation is substantially increased in the fuel rich flames. The degrees of atomisation of both elements are critically dependent on the ratio of carbon to total oxygen (oxidant + water). When this ratio exceeds unity (in flames more than 6.25% fuel rich) the degrees of atomisation of both elements are a maximum and approximately constant.

In addition the degrees of atomisation of both elements are inversely related to the concentrations of the oxidising species such as atomic oxygen (O) (Fig. 3) and the hydroxyl radical (OH) (Fig. 4). This would be expected from consideration of reactions of the type :-

$$M + O = MO$$

$$M + OH = MO + \tfrac{1}{2}H_2$$

As in the case of the degrees of atomisation of the metals the critical factor is the ratio of carbon to oxygen. At carbon to oxygen ratios of greater than unity the concentrations of the oxidising species are a minimum and approximately constant.

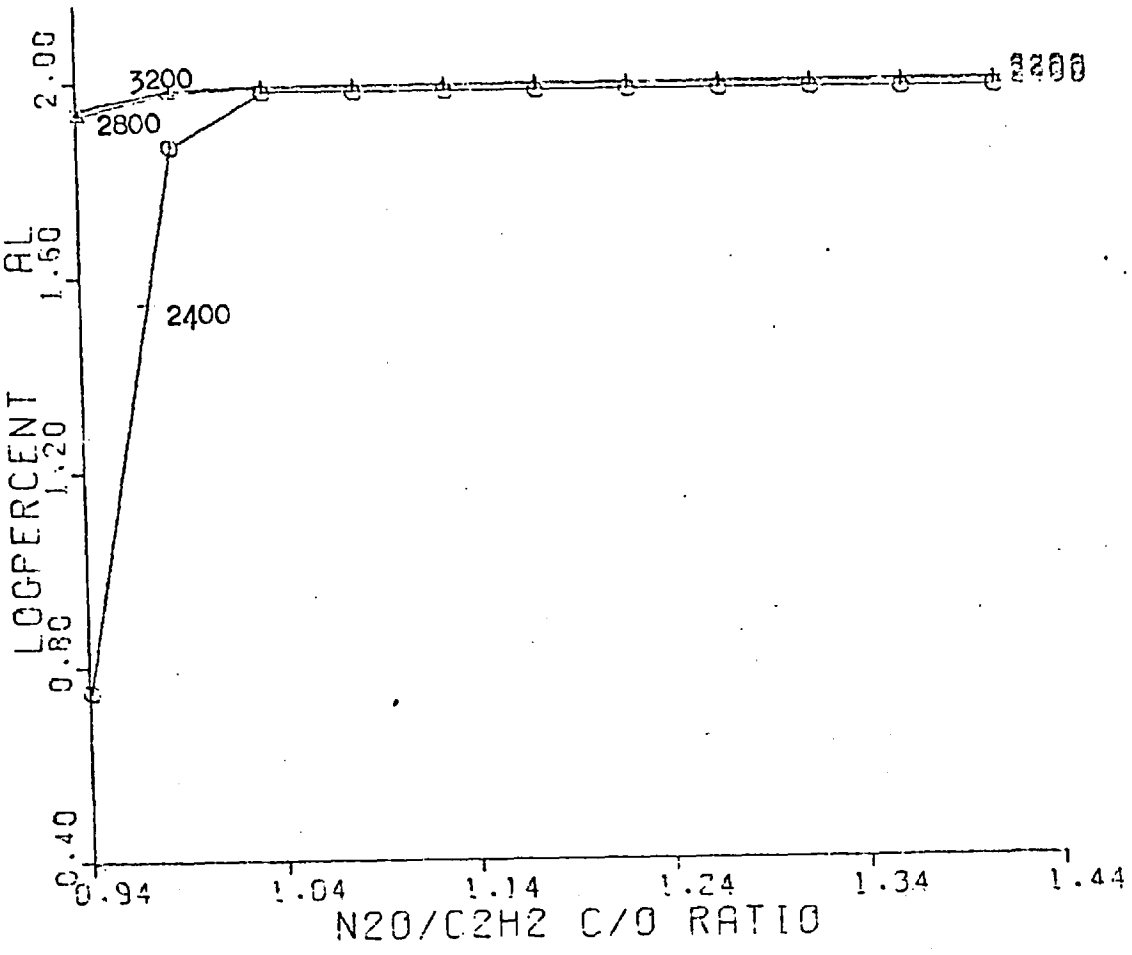

Fig. 1 Log (Per cent atomisation Aluminium) v. C:O ratio.

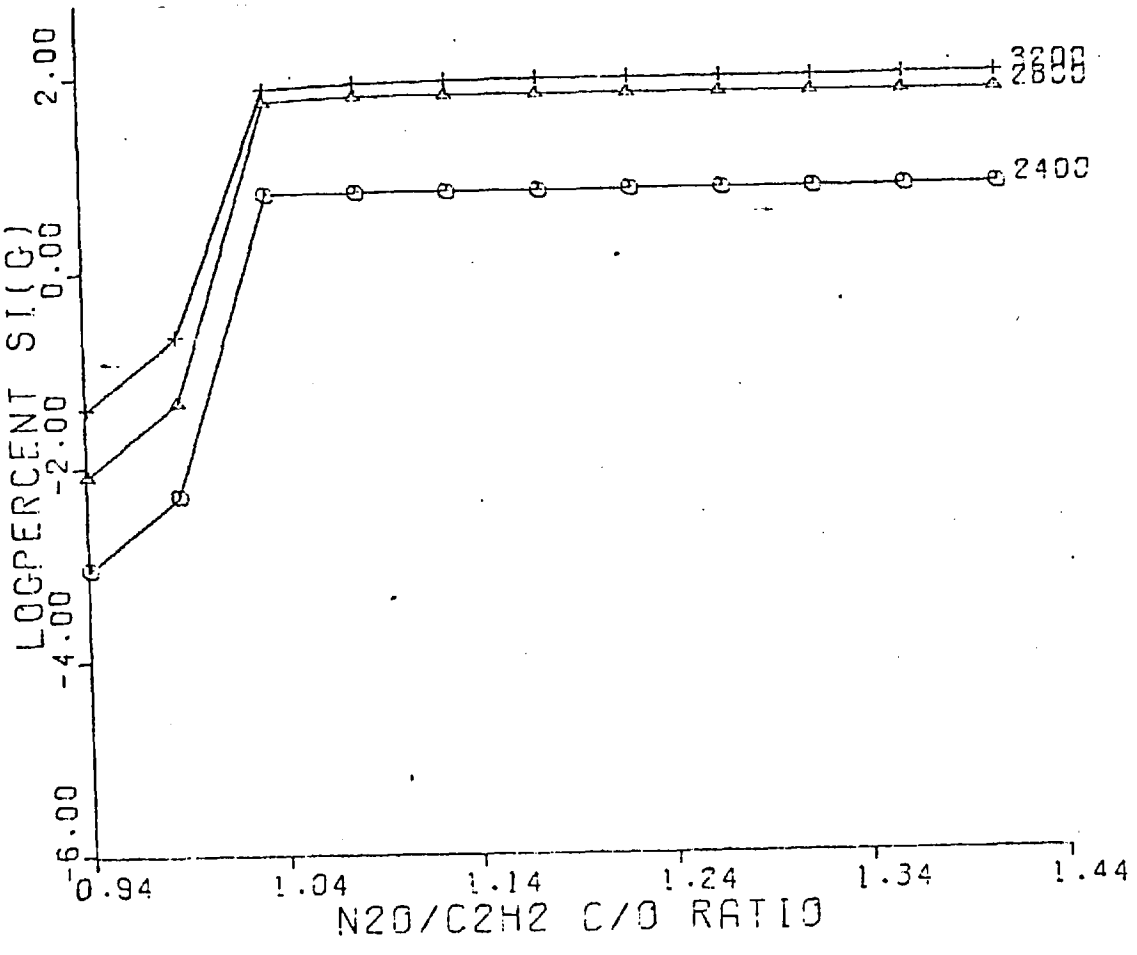

Fig. 2 Log(per cent atomisation Silicon) vs. C:O ratio

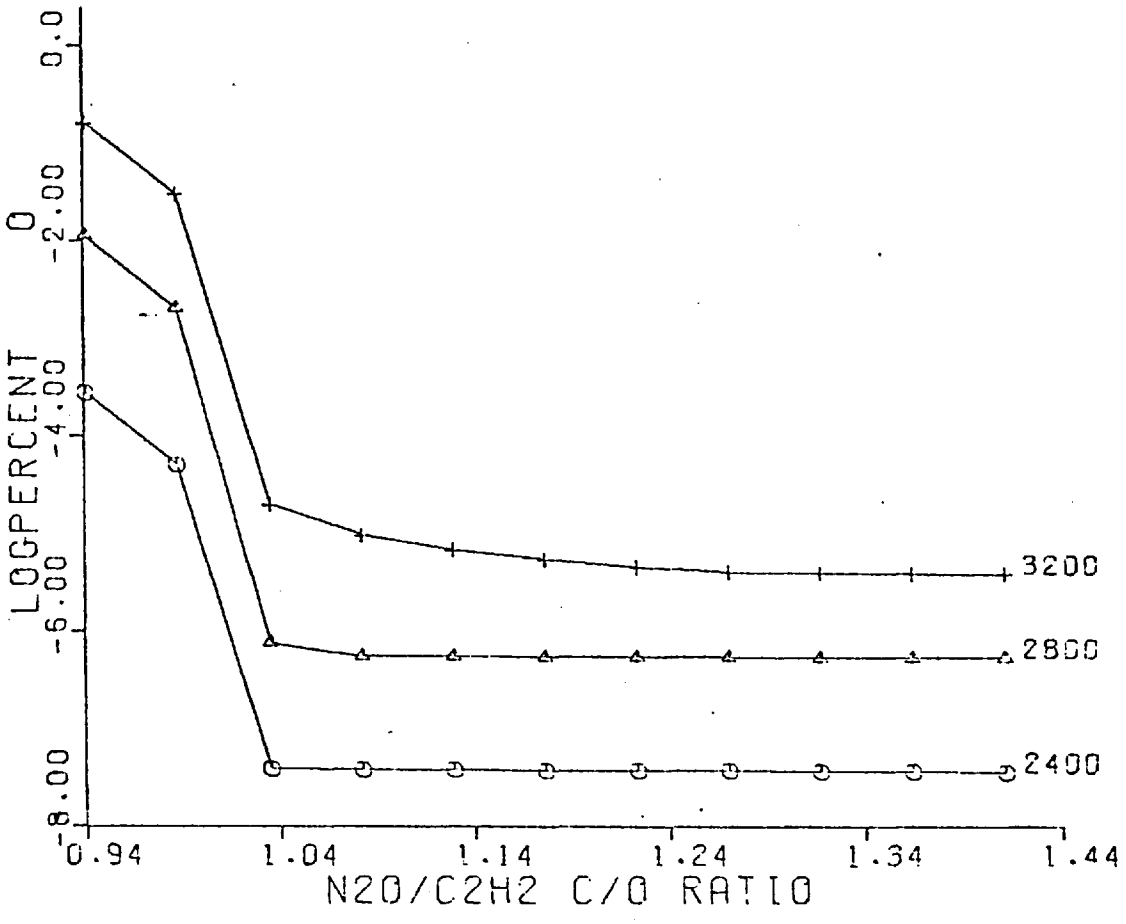

Fig. 3 Log (% concentration O) vs. C:O ratio.

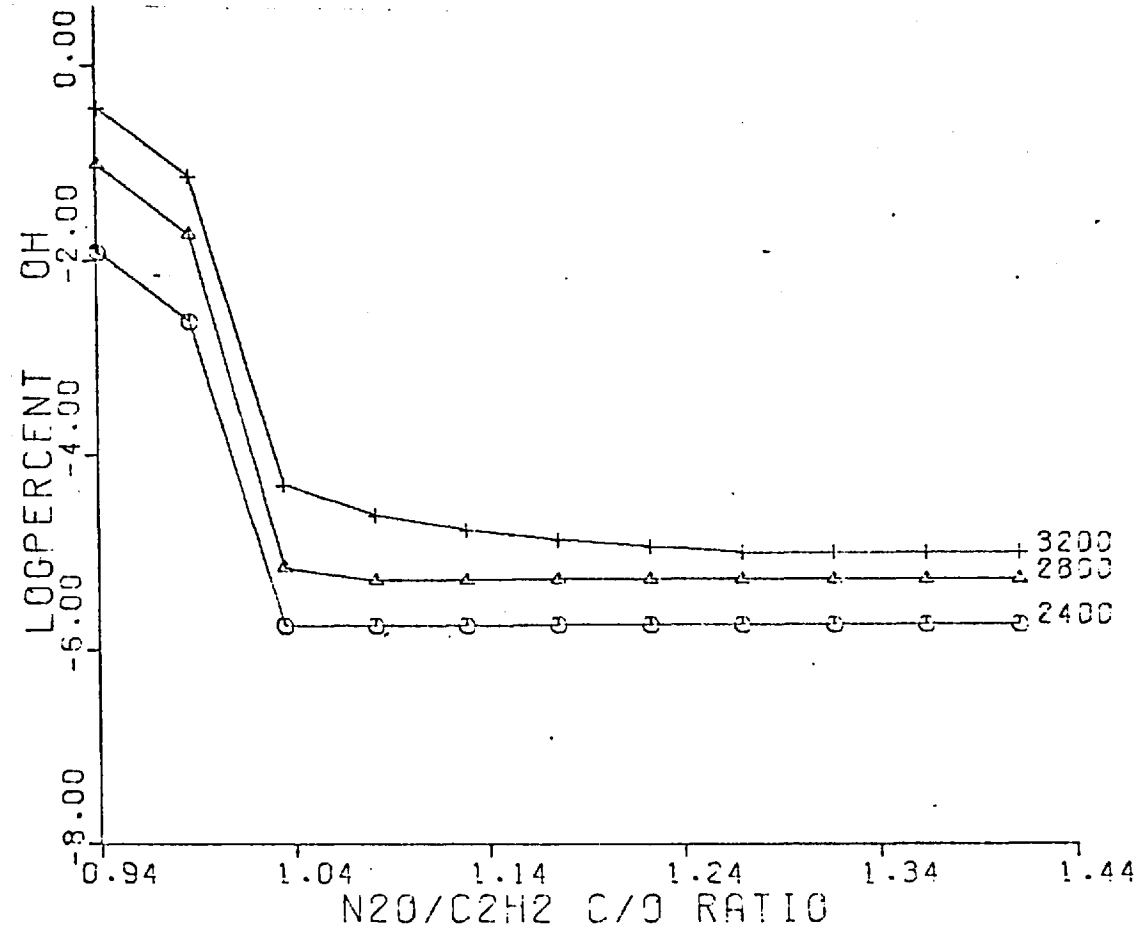

Fig. 4 Log (% concentration OH) vs. C:O ratio.

The atomisation of the metals also exhibits a direct relationship to the concentrations of the carbon containing species particularly atomic carbon (C) (Fig. 5), the cyano radical (CN) (Fig. 6) and HCN (Fig. 7). These in turn are inversely related to the concentrations of atomic oxygen and hydroxyl. This latter relationship may be due to reactions of the type :-

$$C + O = CO$$
$$C + OH = CO + \tfrac{1}{2}H_2$$
$$CN + O = CO + \tfrac{1}{2}N_2$$
$$CN + OH = CO + \tfrac{1}{2}N_2 + \tfrac{1}{2}H_2$$
$$HCN + O = CO + \tfrac{1}{2}N_2 + \tfrac{1}{2}H_2$$
$$HCN + OH = CO + \tfrac{1}{2}N_2 + H_2$$

which are all highly exothermic in view of the high heat of formation of carbon monoxide.

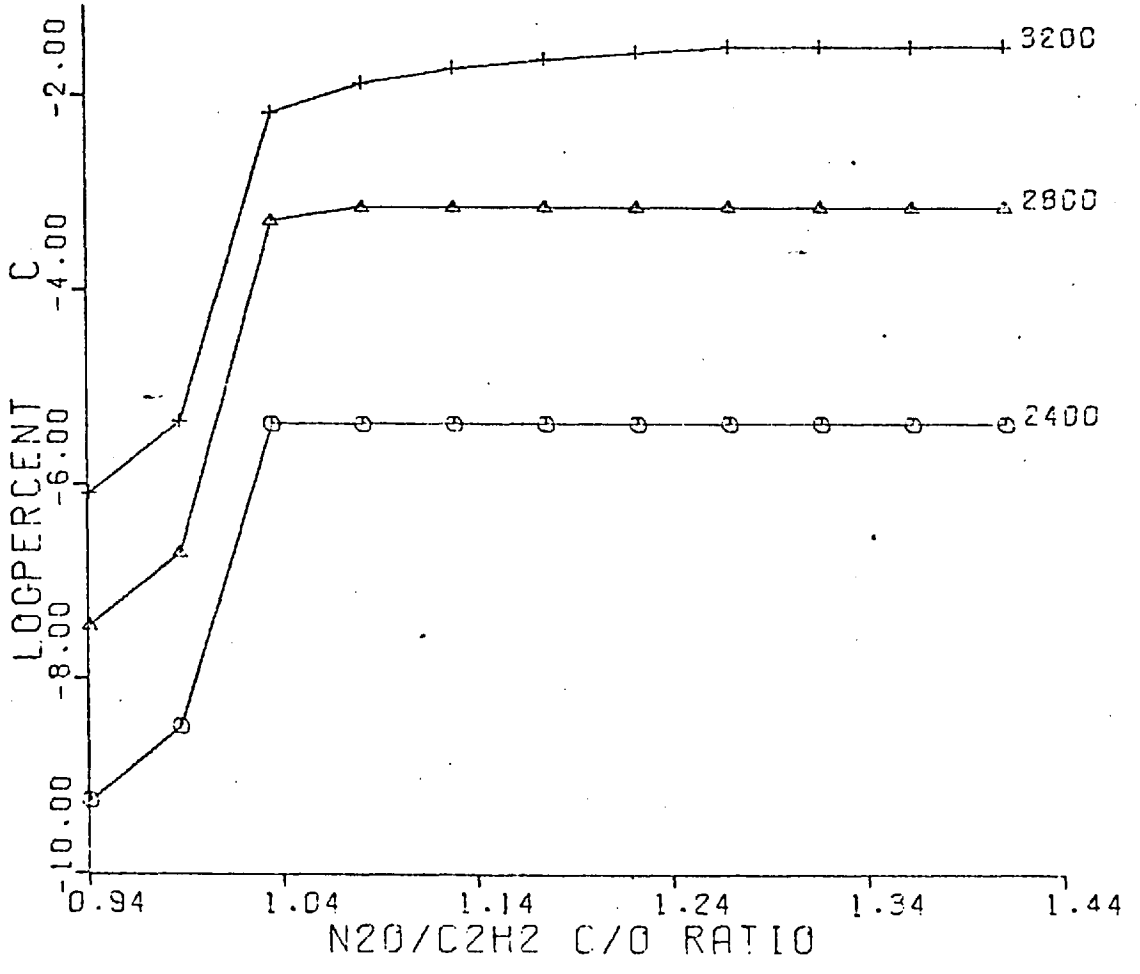

Fig. 5 Log (% concentration C) vs. C : O ratio.

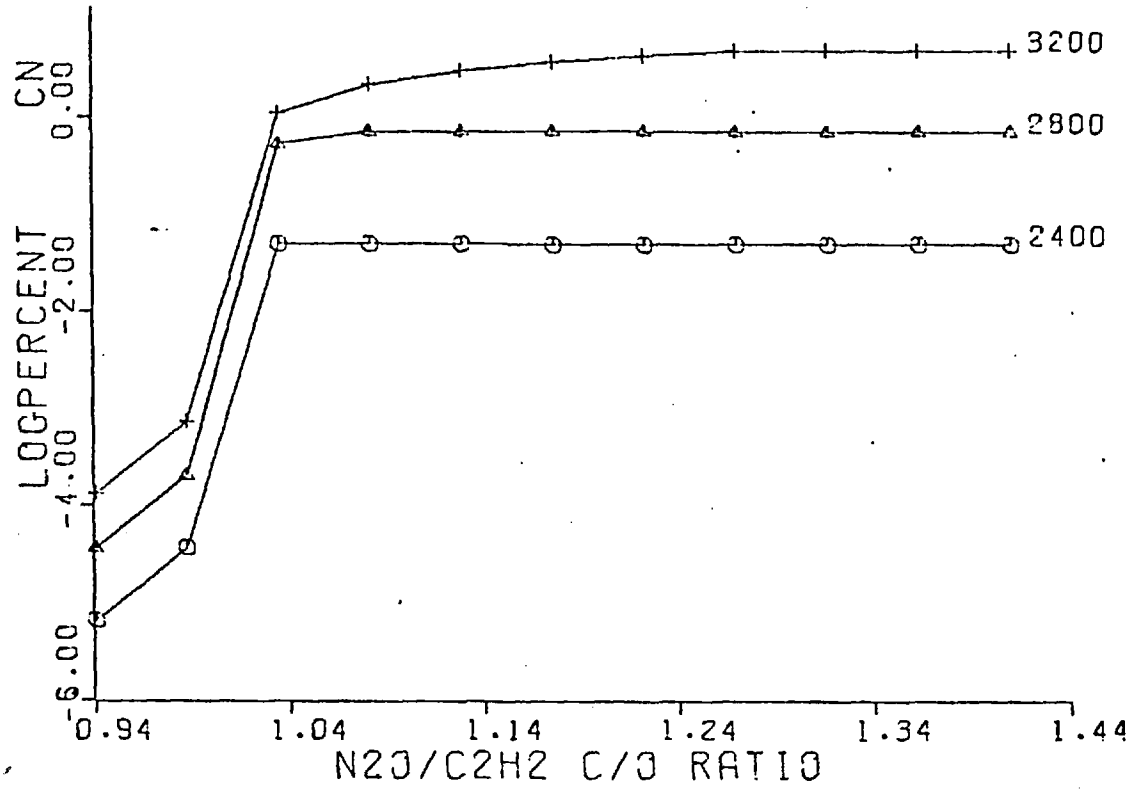

Fig 6 Log (% concentration CN) vs. C:O ratio.

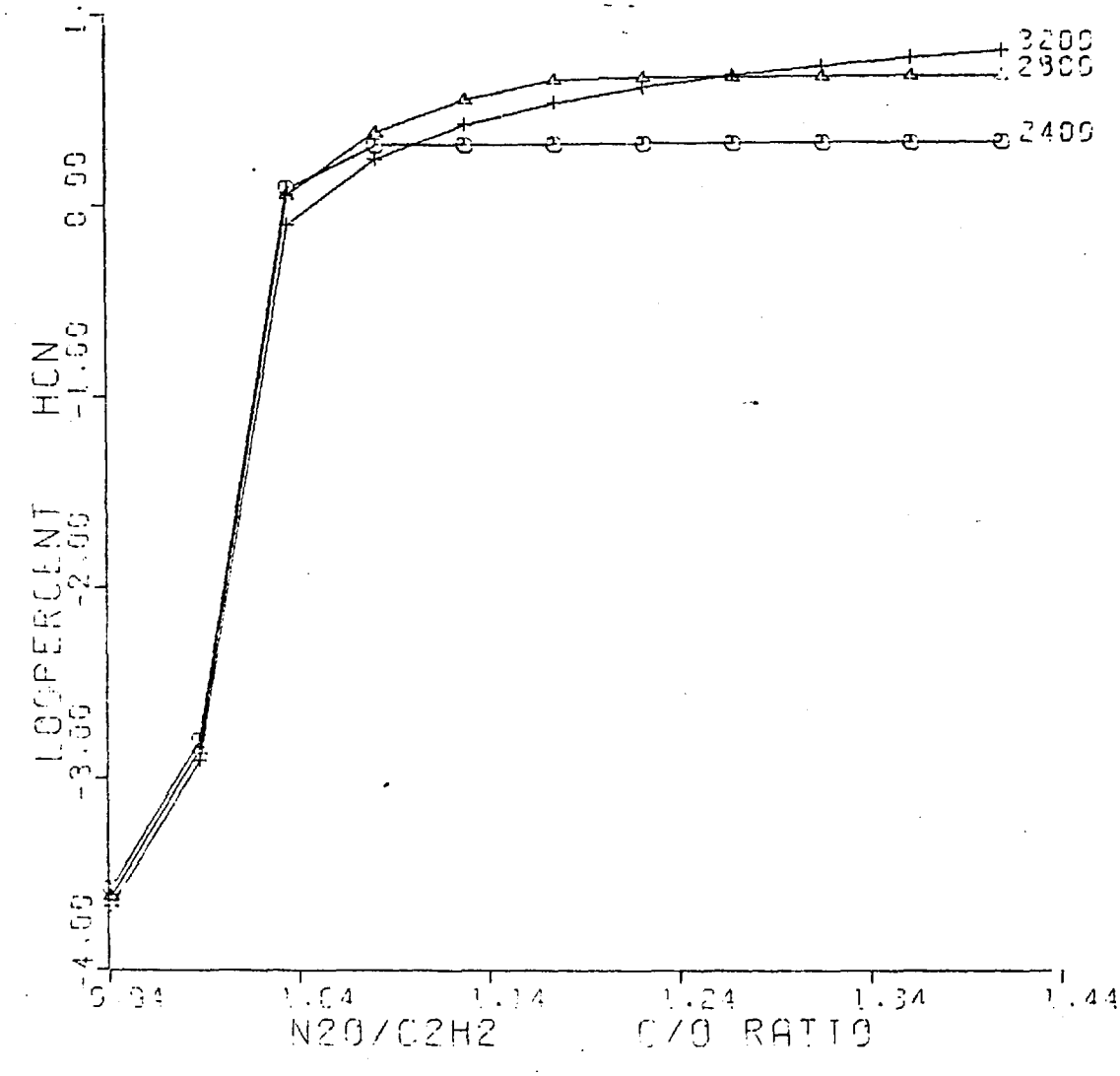

Fig 7 Log (% concentration HCN) vs. C:O ratio.

The direct relationship between the concentrations of the carbon species and the degrees of atomisation of the metals may be explained by consideration of reactions such as

$$C + MO = CO + M$$

$$CN + MO = CO + M + \tfrac{1}{2}N_2$$

$$HCN + MO = CO + M + \tfrac{1}{2}N_2 + \tfrac{1}{2}H_2$$

This type of reaction will always be exothermic because the heat of formation of carbon monoxide (II.I eV) is significantly greater than that of even the most stable metal monoxide. In view of the formation of carbon monoxide in all the reactions between carbon containing species and oxygen it would be expected that this species would be a major constituent of the flame and in fact constitutes ca. 40% of the flame by volume. The concentrations of the major species in the stoichiometric and fuel rich flames are listed in Tables Ia and b.

The identity of the principal reducing species is unknown but the concentrations of HCN and CN in all the nitrous oxide-acetylene flames studied are at least two orders of magnitude greater than those of atomic carbon. However, comparison of results in the nitrousoxide-acetylene and oxygen-acetylene flames (the only difference being the presence or absence of HCN and CN) show that,at the same temperature and carbon : oxygen ratio, a greater degree of atomisation is obtained in the latter flame. This would appear to indicate that the principal reducing species is atomic carbon. Concentrations of all carbon species increase until the carbon : oxygen ratio reaches unity. Above this ratio they are a maximum and approximately constant and the excess carbon is present as solid carbon.

Table 1

a) Concentrations of the major species of the stoichiometric nitrous oxide-acetylene flame (C:O ratio 0.9412) volume per cent.

Species	2400°K	2800°K	3200°K
CO	38.28	37.79	36.39
CO_2	6.06×10^{-1}	5.35×10^{-1}	4.29×10^{-1}
C	5.62×10^{-10}	3.44×10^{-8}	8.26×10^{-7}
O	2.84×10^{-4}	1.14×10^{-2}	1.63×10^{-1}
OH	1.23×10^{-2}	9.75×10^{-2}	3.75×10^{-1}
CN	6.74×10^{-6}	3.59×10^{-5}	1.37×10^{-4}
HCN	2.69×10^{-4}	2.38×10^{-4}	2.16×10^{-4}
H	7.03×10^{-1}	3.46	10.48
H_2	19.71	18.04	14.03
H_2O	1.81	1.73	1.25
N_2	38.88	38.32	36.79
NO	1.02×10^{-3}	1.24×10^{-2}	7.09×10^{-2}
Solid carbon*	0.0	0.0	0.0

* Weight per cent of carbon present.

Table 1

b) Concentrations of the major species of the fuel rich nitrous oxide-acetylene flame (C:O ratio 1.179) volume per cent.

Species	2400°K	2800°K	3200°K
CO	38.48	37.81	36.08
CO_2	8.00×10^{-5}	2.70×10^{-5}	2.54×10^{-5}
C	4.29×10^{-6}	6.83×10^{-6}	1.37×10^{-2}
O	3.75×10^{-8}	5.76×10^{-7}	9.73×10^{-6}
OH	1.76×10^{-6}	5.13×10^{-6}	2.36×10^{-5}
CN	4.88×10^{-2}	6.61×10^{-1}	2.09
HCN	2.12	4.57	3.49
H	7.64×10^{-1}	3.61	11.08
H_2	23.26	19.66	15.70
H_2O	2.81×10^{-4}	9.55×10^{-5}	8.34×10^{-5}
N_2	35.12	32.96	31.15
NO	1.28×10^{-7}	5.79×10^{-7}	3.89×10^{-6}
Solid carbon*	9.40	0.0	0.0

* Weight per cent of carbon present.

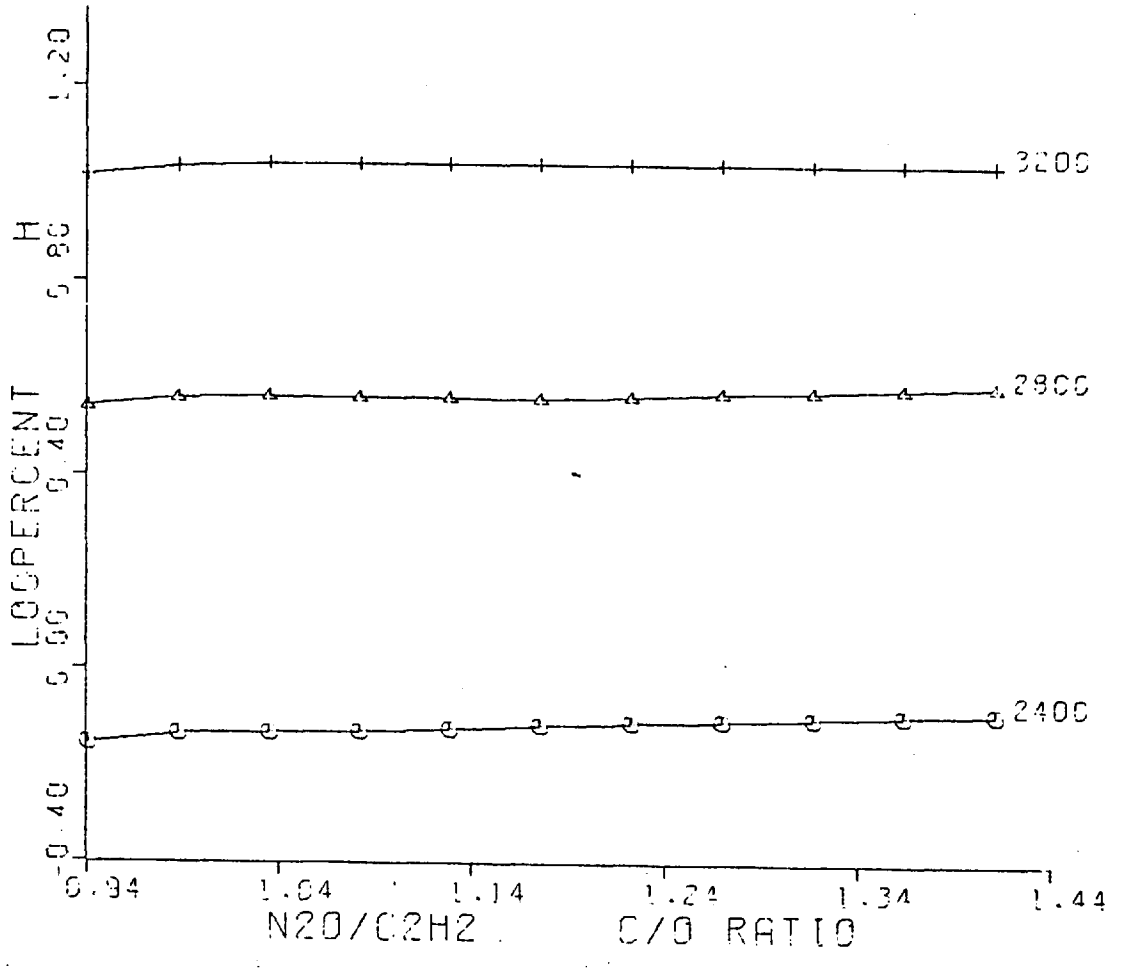

Fig 8 Log (% concentration H) vs C:O ratio.

It is unlikely that hydrogen species such as atomic hydrogen play a major role in the atomisation process described thus far in spite of their large concentrations (Fig. 8), because they can only form products with the oxidising species that are still oxidising in nature, namely hydroxyl and water via reactions of the type

$$H + O = OH$$

$$H + OH = H_2O$$

As would be expected and as is observed in practice the effect of the addition of water to the flame is to make it more fuel lean because there is an increase in the total oxygen content and, as a result, a lowering of the carbon :

oxygen ratio. The concentration of the major carbon containing species carbon monoxide is increased at the expense of the other carbon species such as CN. This effect is especially marked in the stoichiometric and slightly fuel rich (less than 6.25%) where the increase in the oxygen content reduces the carbon : oxygen ratio to below unity.

At the lower temperatures in the flames with a carbon : oxygen ratio not exceeding unity the principal aluminium species is solid Al_2O_3. However, above 2700°K (the melting point of Al_2O_3) in such flames and in all flames with a carbon : oxygen ratio of greater than unity the major aluminium species is atomic aluminium (Al). The other main aluminium species present are AlO, AlH, AlOH and Al_2O. Anomalously high concentrations of atomic aluminium are found in the stoichiometric flame which are a result of the lack of entrained air in the 'ideal' flames studied which in practice resemble flame-shielded flames.

The principal silicon species, especially at the lower flame temperatures, in the flames of carbon : oxygen ratio less than unity is gaseous silicon monoxide (SiO). In the fuel rich flames the principal silicon species is atomic silicon (Si) even at low temperatures. The molecular species Si_2 and Si_3 were not found to be present to any appreciable extent in any flames (all concentrations less than 10^{-10}%).

The results of the calculations for the nitrous oxide-acetylene flame indicate that the atomisation of refractory metals in the flame is due largely to chemical reduction and not solely to thermal dissociation of the oxide species.

The major evidence for this is that the temperature dependence of the degrees of atomisation at carbon : oxygen ratios greater than unity is small and considerably less than at carbon : oxygen ratios below unity. Moreover, if the atomisation were principally due to thermal dissociation of the oxide species, then the degrees of atomisation in the cooler fuel rich flames should be smaller than those in the stoichiometric flame, which has a maximum theoretical temperature of 3228°K (96). In practice, however, they are found to be somewhat higher.

The trends shown in the calculations are in good agreement with those observed in practice. Using conventional and nitrogen or argon shielded nitrous oxide-acetylene flames (the latter being the closest approximation to the 'ideal' flames considered in these calculations) Kirkbright, Sargent and West (100) observed significant absorption of aluminium in the stoichiometric flame but this absorbance was enhanced as the flame was made more fuel rich. In the case of silicon almost no absorbance was observed in the stoichiometric flame but the absorbance increased rapidly as the flame became more fuel rich.

It is impossible to compare the results flame for flame based on the flow rates used in view of the often quite large errors in the readings taken on commercially available flowmeters. At large degrees of fuel richness the absorbance for both elements decreased and this is undoubtedly due to the substantial drop in temperature in very fuel rich flames. The lack of data for temperature variation with changing flame composition prevents comparison with the computed concentrations at the same temperatures.

5.2 Air-acetylene

Air was considered to be a mixture of nitrogen and oxygen in the ratio 4 : 1 by volume, carbon dioxide being neglected.

The flame reaction is :-

$$6\ N_2 + 3/2\ O_2 + C_2H_2\ (+\ 0.3750\ H_2O) = 6\ N_2 + 2CO + H_2O$$

A range of flames was studied by varying the number of moles of acetylene from 1.0 to 2.0 in steps of 0.10. Thus DIV0 = 7.8750 and the normalising factor DIV = 7.8750 + RED(INDEX). As before the B(J) values are given by :-

Carbon B(1) = 2x RED(INDEX) / DIV

and FRAC(1) = 2.0000 ADD(1) = 0.0000

Hydrogen B(2) =(2x RED(INDEX) + 0.7500) / DIV

and FRAC(2) = 2.0000 ADD(2) = 0.7500

Oxygen B(3) = 3.3750 / DIV

and FRAC(3) = 0.0000 ADD(3) = 3.3750

Nitrogen B(4) = 12.0000 / DIV

and FRAC(4) = 0.0000 ADD(4) = 12.0000

The metals were studied at concentrations of 0.0001 gram atom per mole feed and FRAC and ADD data were unnecessary.

The ratio of carbon to total oxygen is given by :-

RATIO(INDEX) = 2x RED(INDEX) / 3.3750

and equals 0.5926 in the stoichiometric flame. It equals unity when RED(INDEX) = 3.3750 / 2 = 1.6875 i.e. when the flame is 68.75 % fuel rich. As before this figure only applies to this system and in general varies with the amount of water reaching the flame.

As in the case of the nitrous oxide-acetylene flame the

degrees of atomisation of both aluminium and silicon are markedly dependent on the flame composition (Figs. 9-10). As before they are inversely related to the concentrations of the oxidising species atomic oxygen (Fig. 11) and hydroxyl (Fig. 12). They are also directly related to the concentrations of the carbon containing species atomic carbon (Fig. 13), cyano (Fig. 14) and HCN (Fig. 15), and these are in turn inversely related to the concentrations of the oxidising species. The concentration of atomic hydrogen exhibits the same behaviour as in the nitrous oxide-acetylene flame and it is therefore unlikely to be a major reducing species.

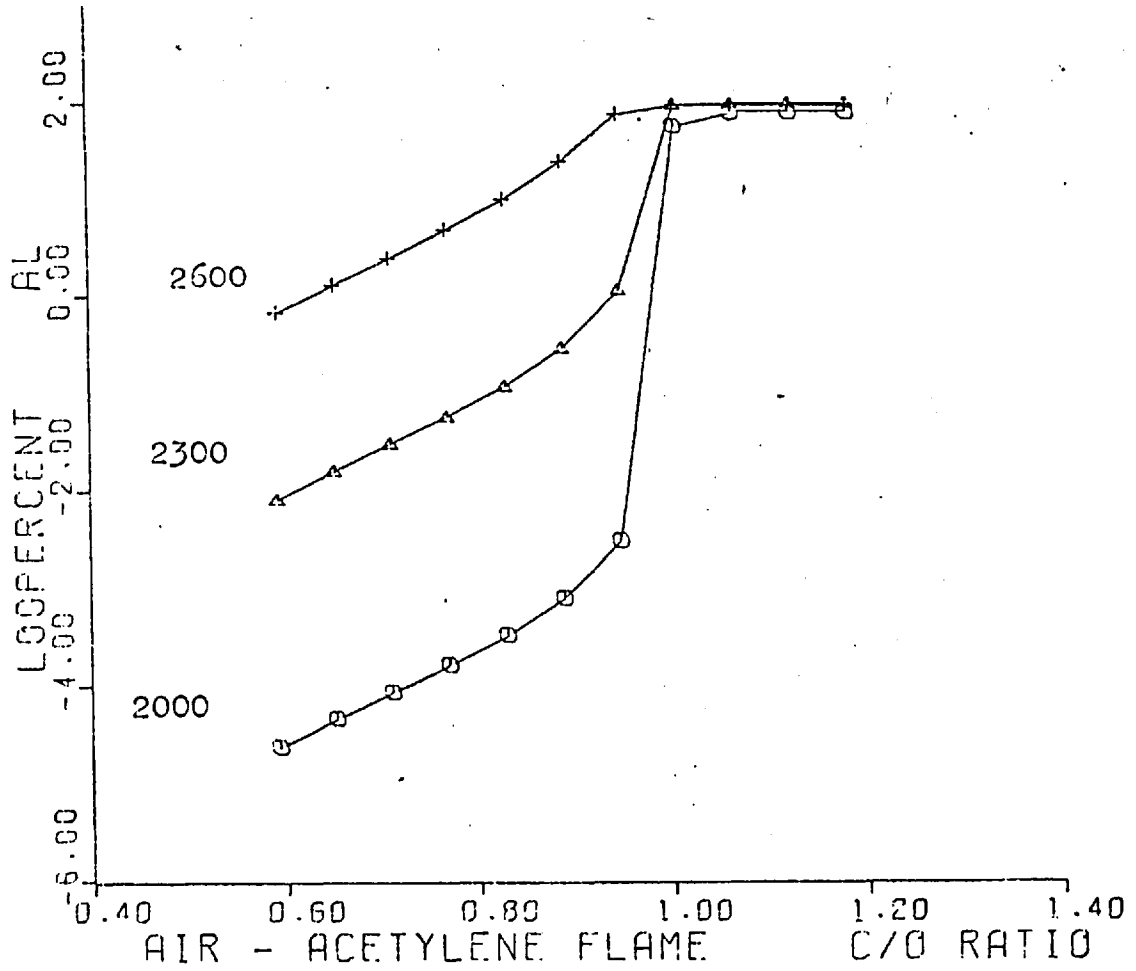

Fig. 9. Log (% atomisation of Aluminium) vs. C : O ratio.

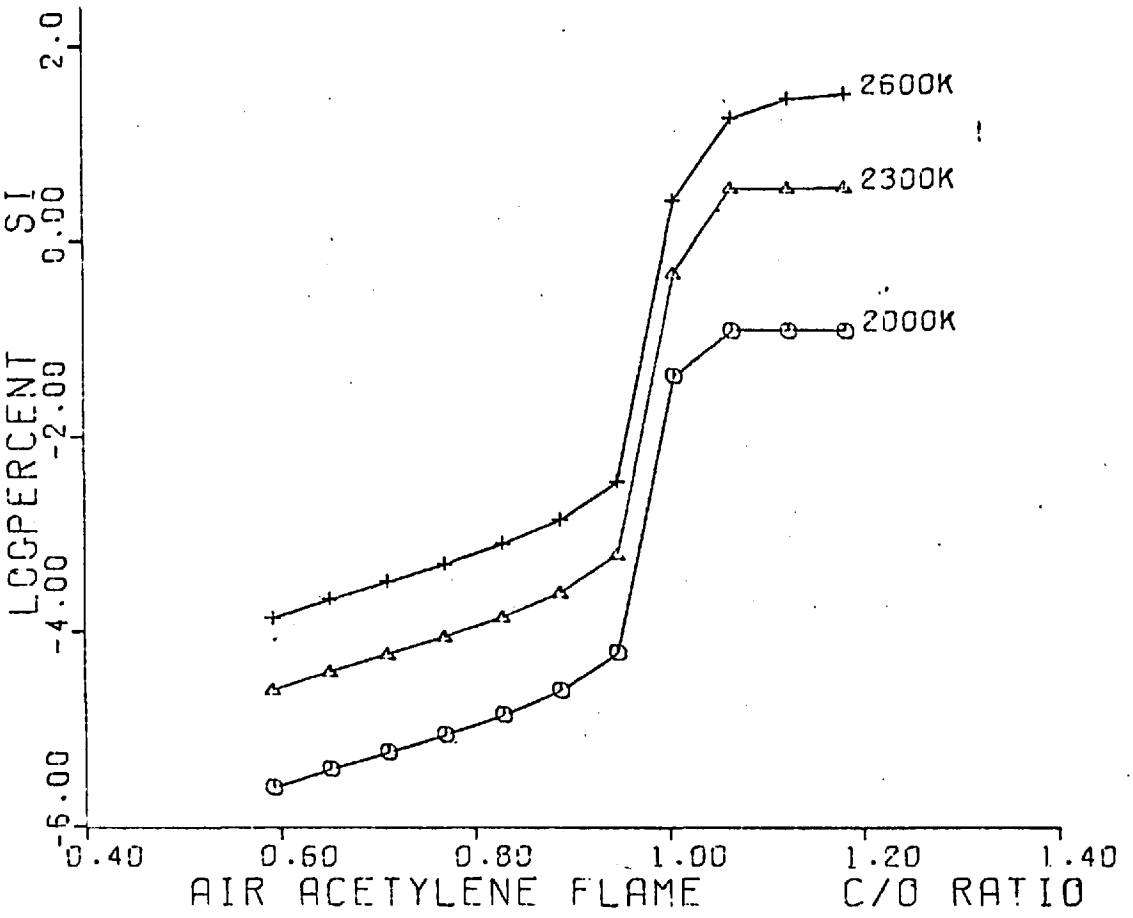

Fig. 10 Log (% atomisation of Silicon) vs. C : O ratio

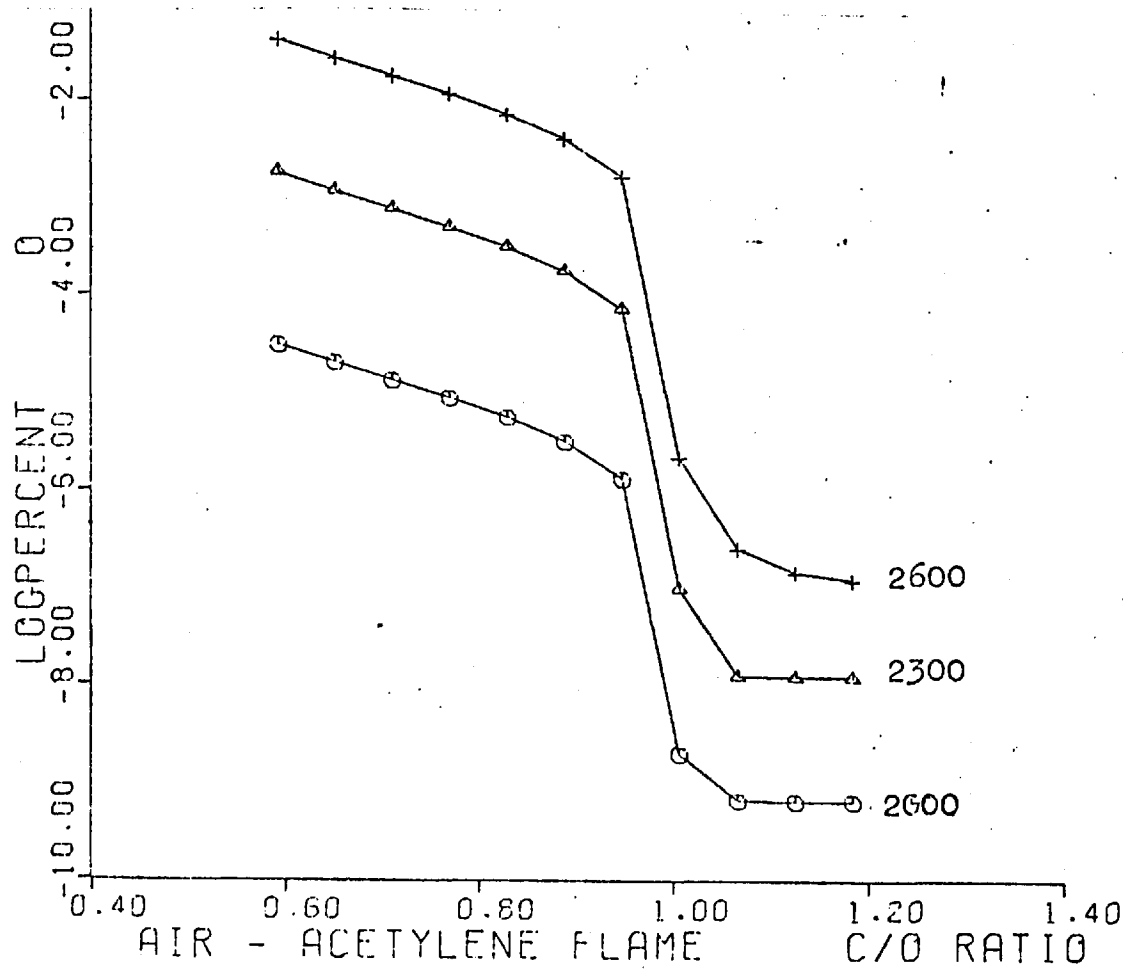

Fig. 11 Log(% concentration O) vs. C : O ratio.

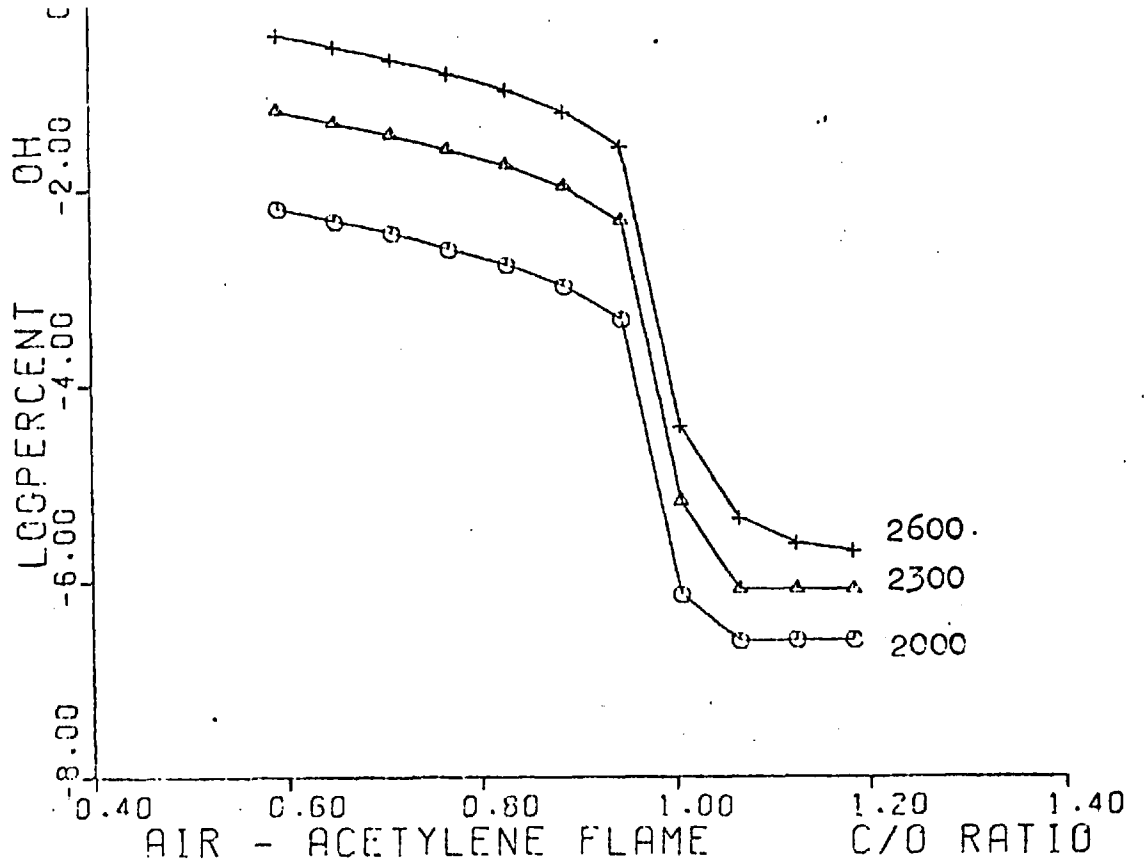

Fig. 12 Log(% concentration OH) vs. C : O ratio.

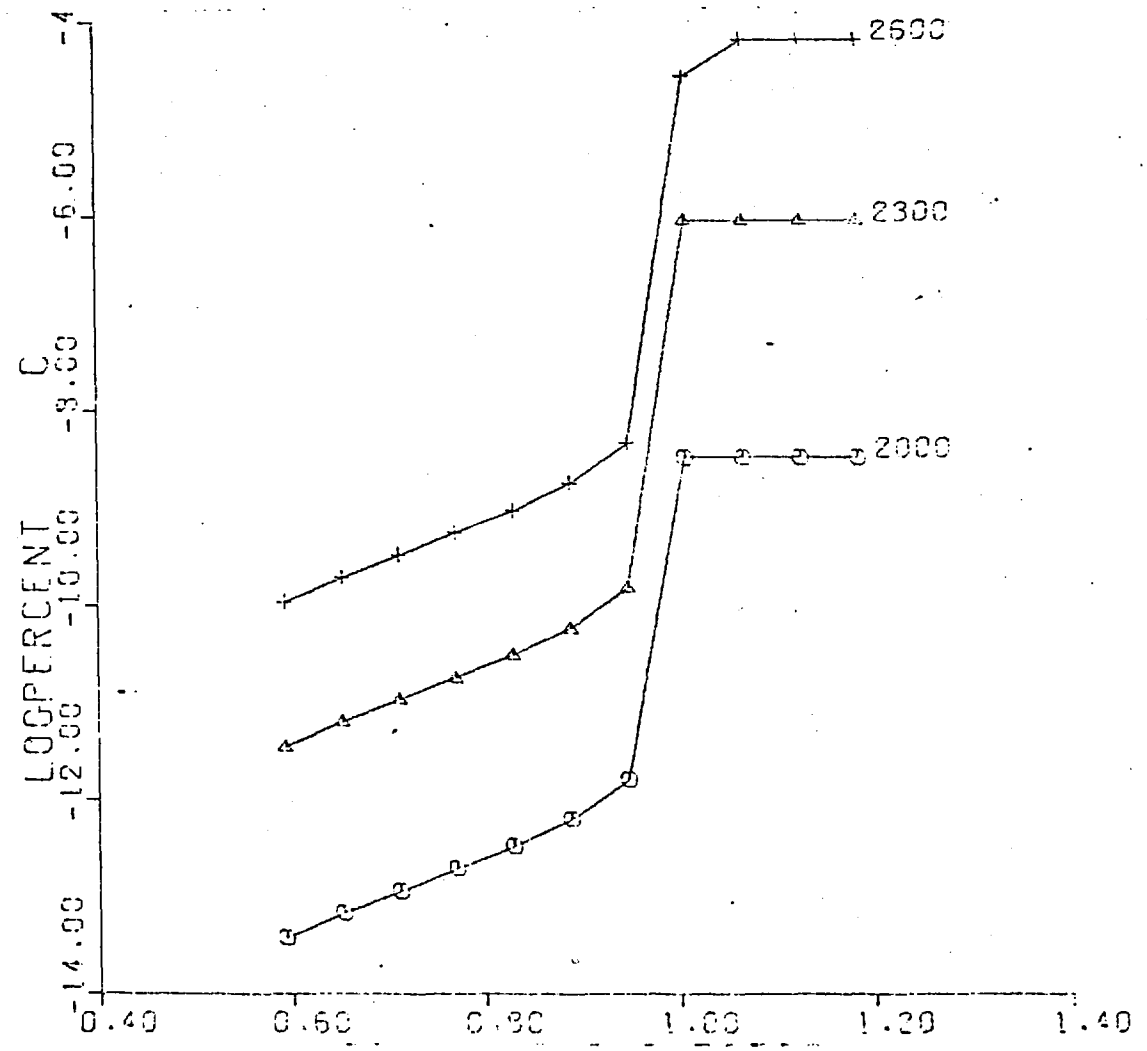

Fig. 13. Log (% concentration C) vs. C : O ratio.

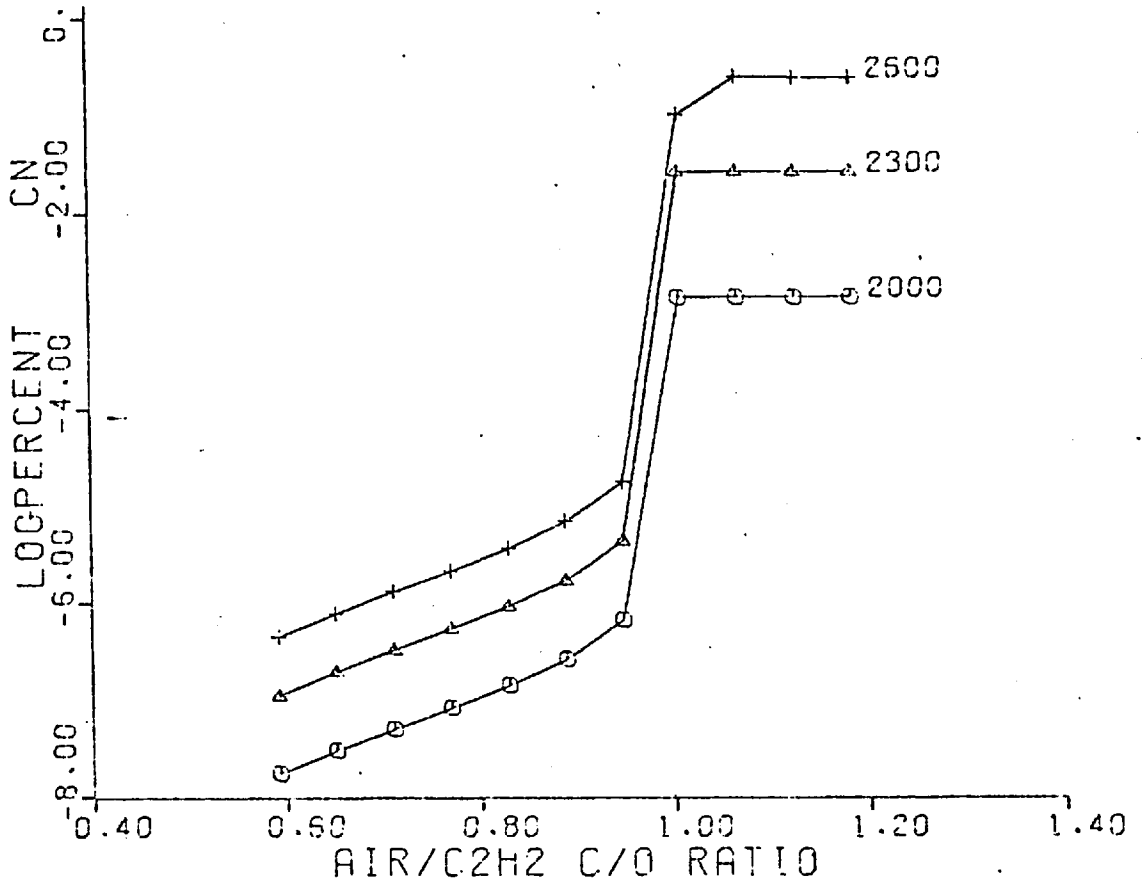

Fig. 14. Log (% concentration CN) vs. C : O ratio.

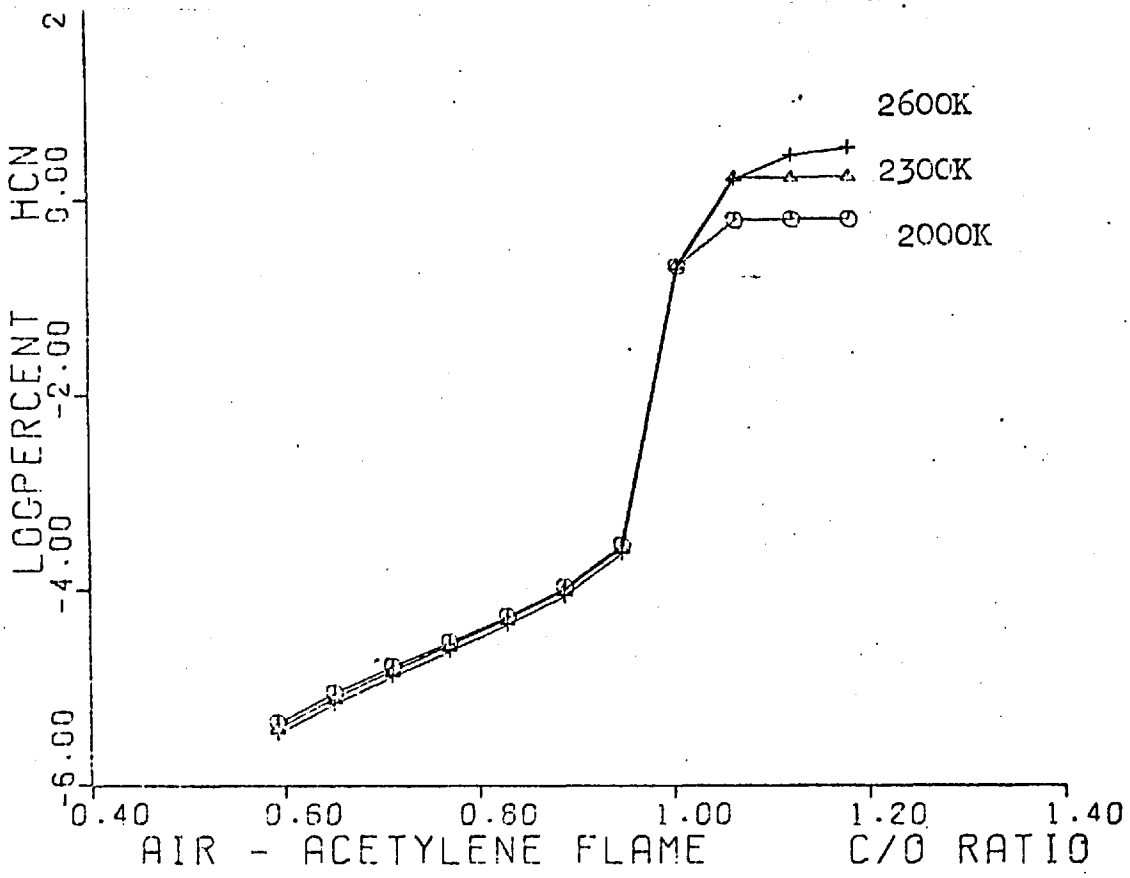

Fig. 15. Log (% concentration HCN) vs. C : O ratio

These results are to be expected from consideration of reactions of the type previously described for the nitrous oxide-acetylene flame. The critical factor is again the ratio of carbon to total oxygen and, due to the greater proportion of oxygen in the stoichiometric flame (relative to the nitrous oxide-acetylene flame) , this ratio does not equal unity until the flame is 68.75 % fuel rich. At this degree of fuel richness the flame is considerably cooler than the temperature of 2523°K quoted as the maximum theoretical temperature of the stoichiometric flame(96). The concentrations of the major species in the stoichiometric and fuel rich flames are listed in Table II.

High concentrations of HCN and CN appear to be present in the air-acetylene flame although they do not seem to have been reported in the literature as being major constituents of the flame. This is presumably because the stoichiometric air-acetylene flame is some 700°K cooler than the stoichiometric nitrous oxide-acetylene flame, and, an air-acetylene flame with a carbon : oxygen ratio of greater than unity will probably be even more than 700° cooler than a nitrous oxide-acetylene of similar carbon : oxygen ratio in which the characteristic red CN emission would be observed. Since the species concerned are at a maximum concentration in flames of carbon : oxygen ratio greater than unity no CN emission is observed because the temperature is too low for appreciable excitation of CN radicals. Also the main emission bands for HCN lie close to the infrared where the emission spectrum of the flame tends to be somewhat complex and this would tend to make measurements of HCN emission difficult.

Table II

a) Concentrations of the major species of the stoichiometric air- acetylene flame (C:O ratio 0.5926) volume per cent.

Species	2000°K	2300°K	2600°K
CO	15.72	16.06	16.32
CO_2	5.61	5.24	4.86
C	3.82×10^{-14}	3.38×10^{-12}	1.11×10^{-10}
CN	1.76×10^{-8}	1.09×10^{-7}	4.56×10^{-7}
H	3.83×10^{-2}	2.19×10^{-1}	8.40×10^{-1}
H_2	5.59	5.18	4.83
H_2O	9.05	9.32	9.11
HCN	4.46×10^{-6}	3.81×10^{-6}	3.51×10^{-6}
O	3.09×10^{-5}	1.84×10^{-3}	4.15×10^{-2}
O_2	2.17×10^{-5}	1.40×10^{-3}	3.23×10^{-2}
OH	6.41×10^{-3}	6.59×10^{-2}	3.81×10^{-1}
N_2	63.99	63.90	63.48
NO	7.45×10^{-4}	1.22×10^{-2}	1.00×10^{-1}
Solid carbon*	0.0	0.0	0.0

* Weight per cent of carbon present.

Table II

b) Concentrations of the major species of the fuel rich air-acetylene flame (C:O ratio 1.0667) volume per cent.

Species	2000°K	2300°K	2600°K
CO	29.21	29.16	28.97
CO_2	2.22×10^{-4}	6.44×10^{-5}	5.37×10^{-5}
C	3.34×10^{-9}	9.07×10^{-7}	3.15×10^{-5}
CN	1.38×10^{-3}	2.60×10^{-2}	1.16×10^{-1}
H	6.96×10^{-2}	4.05×10^{-1}	1.57
H_2	18.45	17.66	16.98
H_2O	6.36×10^{-4}	2.15×10^{-4}	1.99×10^{-4}
HCN	6.35×10^{-1}	1.69	1.67
O	6.58×10^{-10}	1.25×10^{-8}	2.59×10^{-7}
O_2	9.84×10^{-15}	6.41×10^{-14}	1.25×10^{-12}
OH	2.48×10^{-7}	8.24×10^{-7}	4.44×10^{-6}
N_2	51.61	50.98	50.61
NO	1.42×10^{-8}	7.35×10^{-8}	5.58×10^{-7}
Solid carbon*	4.10	1.8×10^{-1}	0.0

* Weight per cent of carbon present.

As would be expected the effect of the addition of water to the flame is to make it more fuel lean. The proportion of oxygen is increased, and the concentration of carbon monoxide increases at the expense of the other carbon containing species such as C, CN etc. as in the nitrous oxide-acetylene flame.

Since in all cases the temperature of the air-acetylene flame is less than the melting point of Al_2O_3 this species is predominant in all flames with a carbon : oxygen ratio less than unity. In more fuel rich flames (those more than 68.75 % fuel rich) the principal aluminium species is atomic aluminium. This is further evidence for atomisation by chemical reduction rather than thermal dissociation of oxide species. Other aluminium species present are AlH, AlO, Al_2O, and AlOH (all gaseous) but these represent less than 1 % of the total aluminium.

In all air-acetylene flames the principal silicon species is gaseous silicon monoxide (SiO). This is largely due to the low temperature of the flame because, even when the carbon : oxygen ratio exceeds unity, the maximum degree of atomisation of silicon does not exceed 20 %. As in the nitrous oxide-acetylene flame the molecular species Si_2 and Si_3 were not found to be present to any appreciable extent.

From the results of the computer calculations for the air-acetylene flame it would appear to be possible to determine aluminium and even silicon by atomic absorption spectroscopy in a fuel rich (more than 70 %) flame since the degrees of atomisation are sufficient. However, the flames considered

are more fuel rich than their practical counterparts using the same fuel to oxident ratios because air entrainment is not considered in this study. The high acetylene flow rates required to produce the 'ideal' fuel rich air-acetylene flame (carbon : oxygen ratio greater than unity) would result in a very low flame temperature (less than 2000°K). This in turn would probably result in a very small degree of atomisation of the elements particularly silicon.

There are several reports in the literature of obtaining enhanced absorbances in the fuel rich air-acetylene flame. Gatehouse and Willis (71) observed an enhancement for tin, and Allan (47) for tin, chromium and ruthenium in an incandescent air-acetylene flame. David (101) observed at least a 100-fold increase in molybdenum absorption.

It should be noted that the monoxide dissociation energies of these metals are all less than 6 eV. Metals with monoxide dissociation energies greater than about 6 eV require the higher temperatures of the nitrous oxide-acetylene and oxygen-acetylene flames to effect significant atomisation. Silicon (monoxide dissociation energy 8.5 eV) is in this latter group of elements and cannot be determined by atomic absorption spectroscopy even in the fuel rich air-acetylene flame. It is meaningless to discuss aluminium (monoxide dissociation energy 4.6 eV) in this respect since the calculations indicate that the monoxide is a comparitively minor species the major species being atomic aluminium or solid Al_2O_3 depending on the composition of the flame.

The absence of the monoxide from such an atomisation

process may also account for the substantial atomisation of tin and arsenic (monoxide dissociation energies 5.4 eV and 4.9 eV respectively) in the cool air-hydrogen and even the nitrogen-hydrogen diffusion flames. Molybdenum (monoxide dissociation energy 5.0 eV) is not atomised in these cool relatively oxidising flames and requires the hot, reducing nitrous oxide-acetylene flame to effect significant atomisation. Unfortunately data for these elements and their monoxides and other species was not available and this effect could not be investigated.

5.3 Oxygen-acetylene

The stoichiometric flame reaction is :-

$$3/2\ O_2 + C_2H_2\ (+ 0.075\ H_2O) = 2CO + H_2O$$

Thus DIV0 = 1.5750 and DIV = 1.5750 + RED(INDEX). A range of flames was studied by varying the number of moles of acetylene fron 1.0 to 2.0 in steps of 0.10. In the absence of nitrogen the metal becomes element 4 and the B(J) values are given by :-

Carbon B(1) = 2x RED(INDEX) / DIV

and FRAC(1) = 2.0000 ADD(1) = 0.0000

Hydrogen B(2) = (2x RED(INDEX) + 0.15) / DIV

and FRAC(2) = 2.0000 ADD(2) = 0.1500

Oxygen B(3) = 3.0750/ DIV

and FRAC(3) = 0.0000 ADD(3) = 3.0750

The metal concentration was 0.0001 gram per mole feed as before. The ratio of carbon to total oxygen is given by :-

RATIO(INDEX) = 2x RED(INDEX) / 3.0750

and is equal to 0.6422 in the stoichiometric flame. It equals unity when RED(INDEX) = 3.0750 / 2 = 1.5375 i.e. when the flame is 53.75 % fuel rich. As before this value will in general vary with the amount of water reaching the flame.

The oxygen-acetylene flame has been used (90,102-7) for the determination of many elements,including those subject to refractory oxide formation,by both thermal emission and atomic absorption spectroscopy. Substantial enhancement in both atomic line emission and absorption of many elements has been observed in the expanded interconal zone formed in the fuel rich premixed flame.

In view of the high burning velocity of the oxygen-acetylene flame it is desirable to burn only very fuel rich mixtures in order to avoid explosive flashbacks. Cowley, Fassel and Kniseley (106) have used a flame mixture of 0.80 moles oxygen and 1,00 moles acetylene, and the use of such fuel rich mixtures is associated with a considerable reduction of the flame temperature from the maximum theoretical value of 3383^{o}K (108). This flame has a carbon : oxygen ratio of 1.25 and ethanolic solutions of the analyte elements were nebulised which further increases this ratio. These studies were made using premixed flames with the Kniseley burner (103). In this burner air entrainment at the base of the premixing tube introduces nitrogen into the mixture prior to combustion and up to 25 % of the total premixed gas is nitrogen. For this reason nitrogen containing species , particularly the cyano radical (CN),are observed in such flames and they are

therefore not strictly comparable with the 'ideal' oxygen-acetylene flames studies in these calculations.

Fiorino, Fassel and Kniseley (107) have used a long path burner capable of supporting an oxygen-acetylene flame without such a high degree of air entrainment and also a nitrous oxide-acetylene flame. They have used this burner to compare these two flames with respect to their use as atom reservoirs for refractory oxide forming elements.

The concentrations of the carbon containing species present, particularly atomic carbon, follow the same trends associated with their concentrations in the other acetylene flames studied, but the species CN and HCN are of course absent due to the absence of nitrogen fron the flame constituents. The concentration of atomic carbon (Fig. 16) increases rapidly at a carbon : oxygen ratio of unity and above this ratio it is a maximum and approximately constant as in the other acetylene flames. As before the excess carbon is present as solid. The concentrations of the oxidising species such as atomic and molecular oxygen (Figs. 17-18) and hydroxyl (Fig. 19) are inversely related to the carbon species concentrations as before, falling rapidly at a carbon : oxygen ratio of unity and being a minimum and approximately constant above this ratio.

The experimental evidence of Cowley, Fassel and Kniseley (106) points to a very low free-oxygen content in the flame gases leaving the primary reaction zone of the fuel rich flame. The computer calculations of low concentrations of

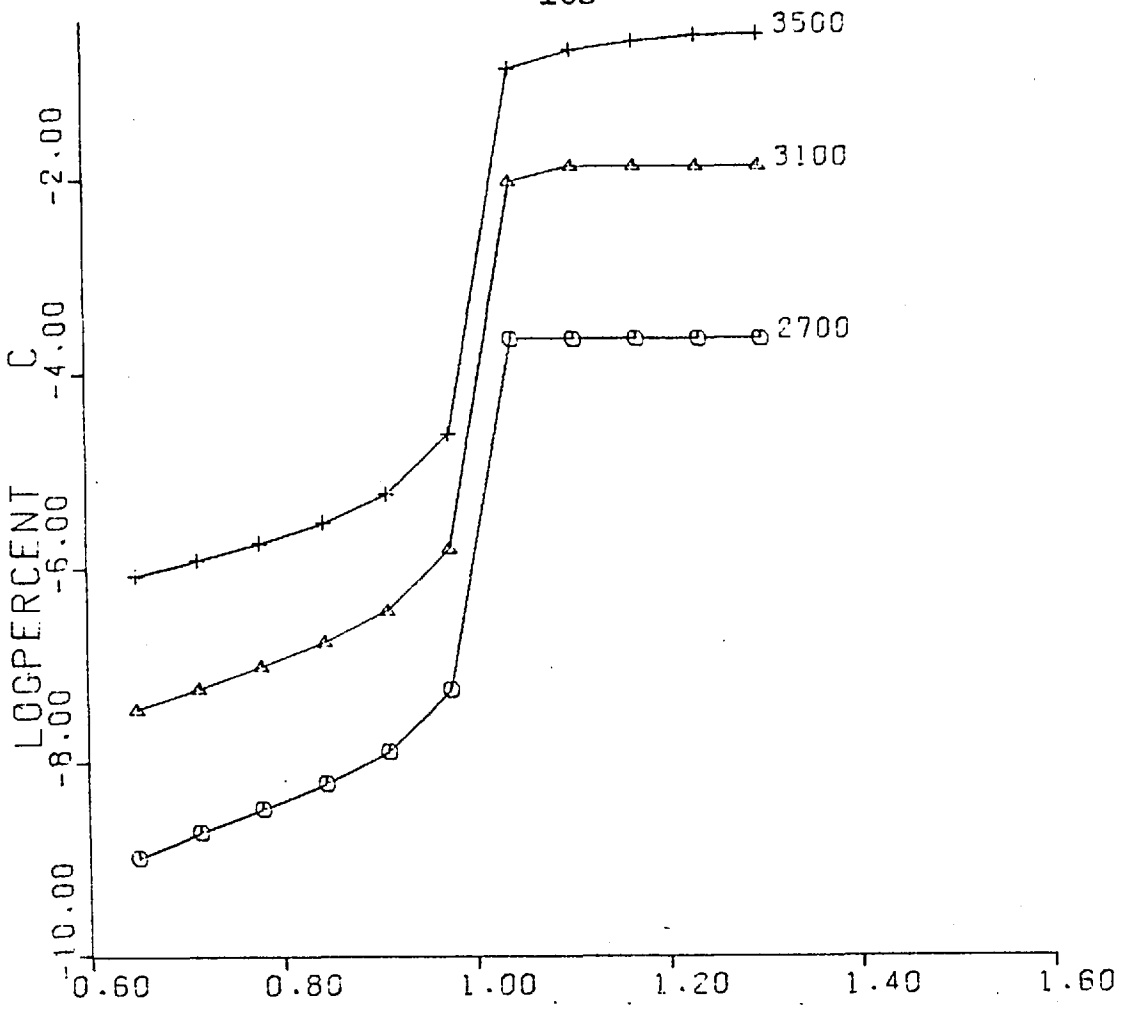

Fig. 16 Log (% concentration C) vs. C : O ratio.

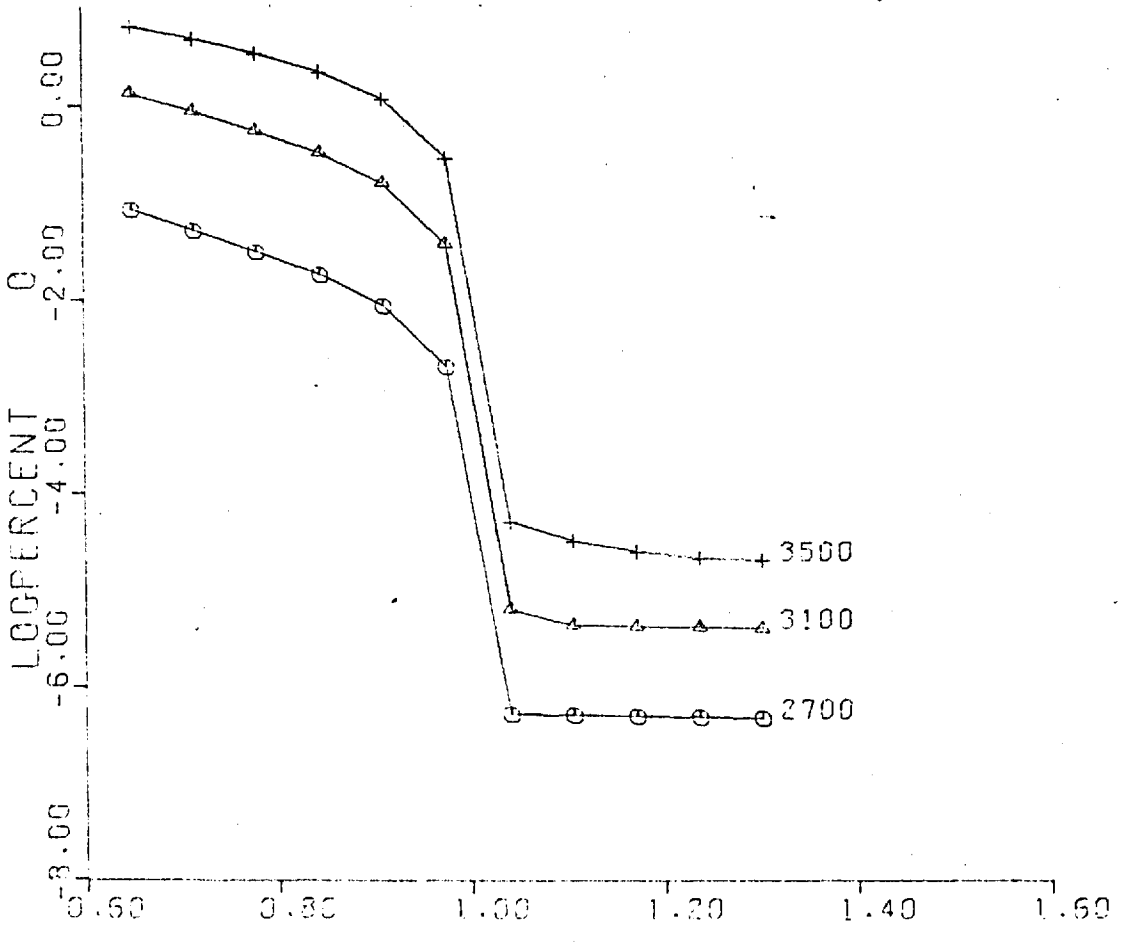

Fig. 17 Log (% concentration O) vs. C : O ratio.

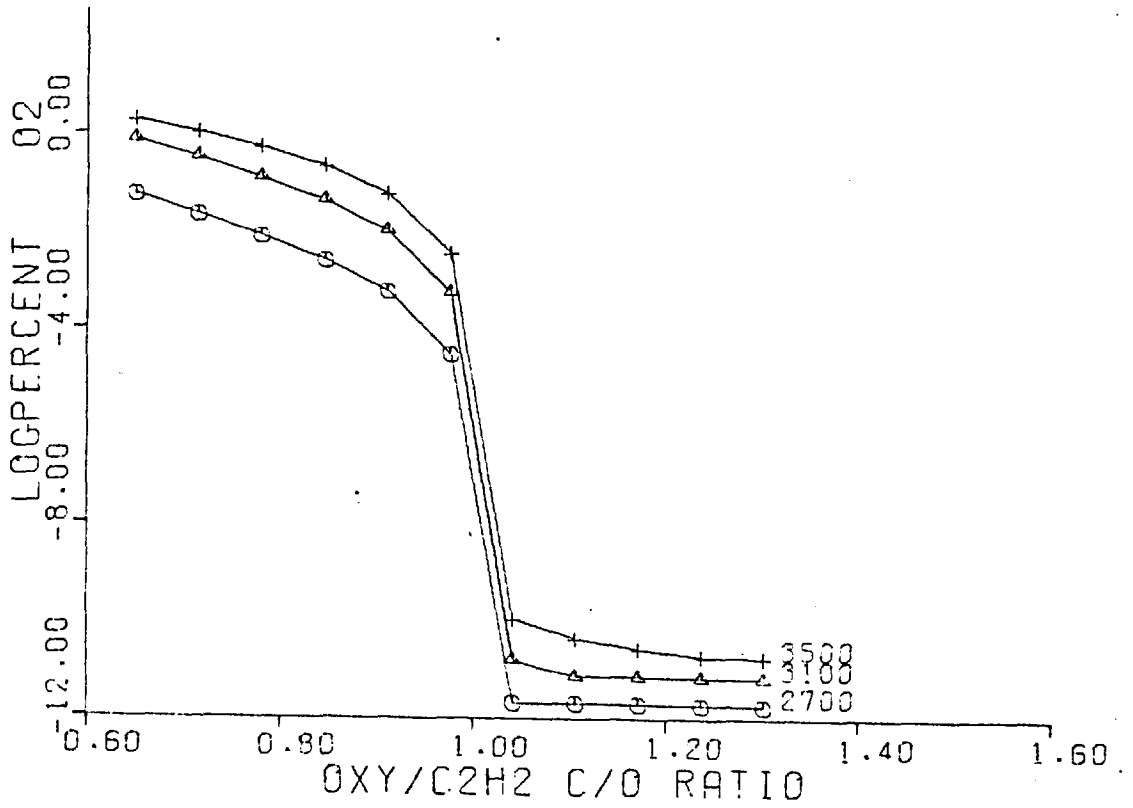

Fig. 18 Log (% concentration O_2) vs. C : O ratio.

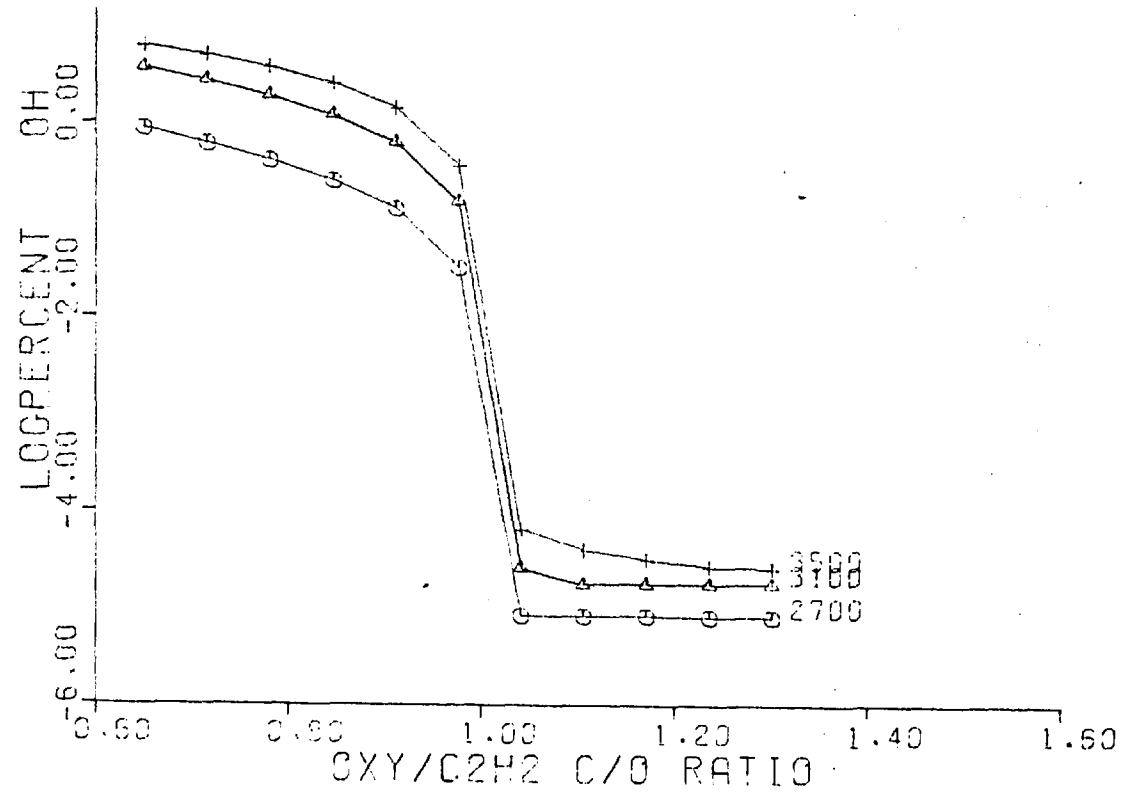

Fig. 19 Log (% concentration OH) vs. C : O ratio.

oxidising species in the interconal zone of the fuel rich flame are therefore in good agreement with experimental observations. The concentrations of the major species in the stoichiometric and fuel rich flames are listed in Table III.

The degrees of atomisation of aluminium and silicon (Figs. 20-21) again exhibit a direct relationship with the concentrations of the reducing carbon containing species and are inversely related to the concentrations of the oxidising species. The concentration of atomic hydrogen follows the same trends as in the other acetylene flames and this species is again unlikely to play a major part in the atomisation process.

The predominant aluminium species at the lower temperatures in the range studied (total range 2600°K - 3500°K) is solid aluminium oxide(Al_2O_3),as in the other acetylene flames at lower temperatures,when the carbon : oxygen ratio is less than unity. In flames with a carbon : oxygen ratio of greater than unity the predominant aluminium species at all temperatures is atomic aluminium.

The main silicon species at all temperatures in flames of carbon : oxygen ratio less than unity and at the lower temperatures of the flames of carbon : oxygen ratio greater than unity is gaseous silicon monoxide (SiO). At the higher temperatures in the latter flames the principal silicon species is atomic silicon.

It is found that, at equivalent carbon : oxygen ratios (greater than unity) and temperatures, the degrees of

Table III

a) Concentrations of the major species of the stoichiometric oxygen-acetylene flame (C:O ratio 0.6520) volume per cent.

Species	2700°K	3100°K	3500°K
CO	51.20	50.38	47.30
CO_2	12.81	9.72	4.25
C	1.08×10^{-9}	3.53×10^{-8}	8.79×10^{-7}
H	2.00	7.04	17.78
H_2	12.45	11.09	9.15
H_2O	20.52	15.81	6.58
O	8.68×10^{-2}	1.41	6.82
O_2	5.86×10^{-2}	8.06×10^{-1}	1.94
OH	8.75×10^{-1}	3.75	6.16
Solid carbon*	0.0	0.0	0.0

* Weight per cent of carbon present.

Table III

b) Concentrations of the major species of the fuel rich oxygen-acetylene flame (C:O ratio 1.172) volume per cent.

Species	2700°K	3100°K	3500°K
CO	61.08	58.63	53.76
CO_2	8.64×10^{-5}	3.40×10^{-5}	1.79×10^{-5}
C	2.28×10^{-4}	1.36×10^{-2}	2.70×10^{-1}
H	3.32	11.11	24.48
H_2	34.64	27.55	17.36
H_2O	3.23×10^{-4}	1.18×10^{-4}	4.62×10^{-5}
O	4.90×10^{-7}	4.23×10^{-6}	2.53×10^{-5}
O_2	1.87×10^{-12}	7.30×10^{-12}	2.67×10^{-11}
OH	8.25×10^{-6}	1.78×10^{-5}	3.15×10^{-5}
Solid carbon*	11.9	6.66	0.0

* Weight per cent of carbon present.

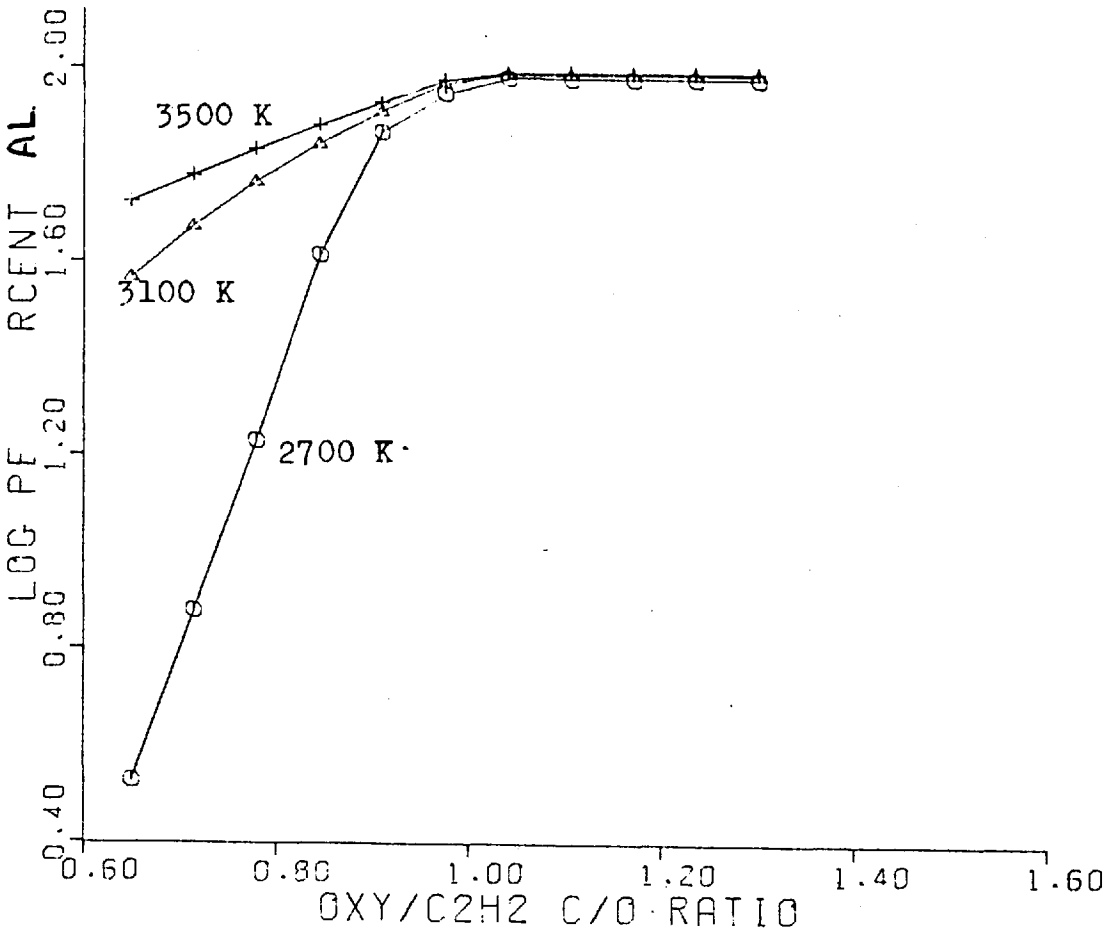

Fig. 20 Log (% atomisation of Aluminium) vs. C : O ratio

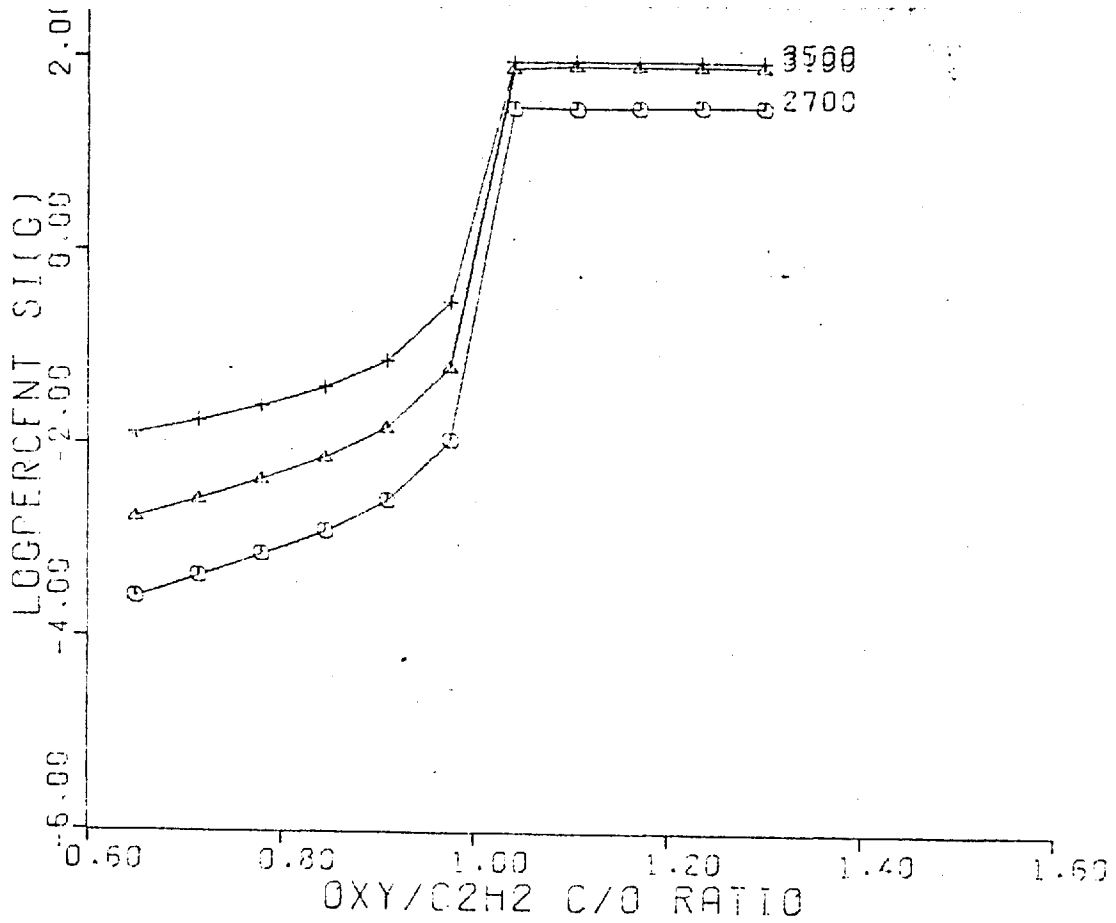

Fig. 21 Log (% atomistaion of Silicon) vs. C : O ratio

atomisation of aluminium in the oxygen-acetylene flame is approximately equal to that in the nitrous oxide-acetylene flame, and that of silicon is somewhat greater in the oxygen-acetylene flame. Moreover the concentrations of atomic carbon in the two flames (after correction of the carbon concentration in the nitrous oxide-acetylene flame to account for the extra 40 % nitrogen species) are approximately equal. These results would tend to indicate that the principal reducing species in acetylene flames is atomic carbon since CN and HCN are absent from the oxygen-acetylene flame.

The calculations are in good agreement with the experimental results obtained by Fiorino, Fassel and Kniseley (167) who compared detection limits in atomic absorption in the oxygen-acetylene and nitrous oxide-acetylene flames using a burner capable of supporting both flames. They determined some fourteen elements, and, in most cases, the oxygen-acetylene flame gave limits of detection comparable to those obtained in the nitrous oxide-acetylene flame. In seven cases the oxygen-acetylene flame was found to give lower detection limits. They also found that the absorbance for strong monoxide forming elements depended on the fuel to oxident ratio.

They note however that the nitrous oxide-acetylene flame is easier to operate. Its substantially lower burning velocity allows greater flexibility with respect to mixture composition and total gas flow. They suggest that the oxygen-acetylene flame be used only when there is substantial background emission from the nitrous oxide-acetylene flame causing a noisy signal. This is especially evident in the region of strong CN emission.

CHAPTER 6

SOME LESS COMMON ANALYTICAL FLAMES

6.1 Nitrous oxide-hydrogen

Many instances appear in the literature of comparisons of results obtained in flame spectroscopic analysis under varying experimental conditions leading to apparent discrepancies. The differences arise because of variations in flame composition, burner design and occasionally use of different techniques of measurement e.g. emission or absorption. One such instance is the nitrous oxide-hydrogen flame about which conflicting reports have appeared in the literature of late (109-111). Dagnall, Thompson and West (109) have reported its use as an efficient atom reservoir for the flame emission determination of aluminium and a number of other elements using a circular laminar flow burner. On the other hand Willis et al. (110) have used it in atomic absorption without finding any particular advantage over the flames in general use. The Free Energy Minimisation technique was therefore applied to this flame in an attempt to provide a more objective evaluation of its capabilities as an atom reservoir for refractory elements.

The flame reaction is :-

$$N_2O + H_2 \ (+ 0.0625\ H_2O\ ) = N_2 + H_2O$$

and a range of flames was studied by varying the number of moles of hydrogen from 1.0 to 2.0 in steps of 0.10. Thus DIVO = 1.0625 and DIV = 1.0625 + RED(INDEX). The

amounts of the elements in one mole feed are given by :-

Hydrogen B(1) = (2x RED(INDEX) + 0.1250) / DIV

and FRAC(1) = 2.0000 ADD(1) = 0.1250

Oxygen B(2) = 1.0625 / DIV

and FRAC(2) = 0.0000 ADD(2) = 1.0625

Nitrogen B(3) = 2.0000 / DIV

and FRAC(3) = 0.0000 ADD(3) = 2.0000

In the absence of carbon oxygen becomes element two . The metal concentrations are again 0.0001 gram atom per mole and FRAC and ADD data are unnecessary.

In the acetylene flames heretofore described it is found that there is a sharp increase in the degrees of atomisation of aluminium and silicon at the compesition corresponding to a carbon : oxygen ratio of unity. At this composition there is also an increase in the concentrations of the carbon containing species atomic carbon, cyano and HCN and a decrease in the concentrations of the oxidising species atomic oxygen and hydroxyl. The concentration of atomic hydrogen however exhibited a linear dependence on the carbon : oxygen ratio. In the case of the nitrous oxide-hydrogen flame the highly reducing carbon species are all absent unless an organic solvent is nebulised into the flame and, even then, the carbon : oxygen ratio is small and never approaches unity. This is apparent from consideration of the flame reaction :-

$$N_2O + H_2 (+ 0.1\ C_6H_6) = \text{Products}$$

The figure of 0.1 mole of solvent per mole nitrous oxide was calculated from practical uptake rates for organic solvents and benzene was selected since it contains no oxygen and will therefore give the maximum carbon : oxygen ratio.

The carbon to oxygen ratio is given by :-

$$6 \times 0.1 / 1.0 = 0.6$$

which is insufficient to effect substantial atomisation of refractory elements.

From consideration of the flame reaction it is apparent that the hydrogen analogue to the carbon : oxygen ratio , namely the ratio H_2 : O is already unity in the stoichiometric flame even when water is nebulised because the ratio of H_2 : O in water is of course unity. The only effect of the addition of water to the flame is to cause a slight cooling since water does not make the flame more fuel lean as it does the acetylene flames. It would therefore be expected that there should not be the sharp increase in the degrees of atomisation of the metals but that they should exhibit an approximately linear dependence on the H_2 : O ratio (Figs. 22-23) and this found to be the case.

As would also be expected the concentrations of atomic hydrogen (which must be regarded as the principal reducing species) exhibit a similar direct , almost linear dependence on the H_2 : O ratio. The concentrations of the oxidising species atomic and molecular oxygen and hydroxyl exhibit an inverse , approximately linear dependence on the H_2 : O ratio. These trends are shown in Figs. 24-27.

The maximum theoretical temperature of the nitrous oxide-hydrogen flame is 2920°K (110) but the composition was calculated for temperatures up to 3300°K so that a direct comparison with the nitrous oxide-acetylene flame at equivalent temperatures. The concentrations of the major species in the stoichiometric and fuel rich nitrous oxide-hydrogen flames are shown in Table IV.

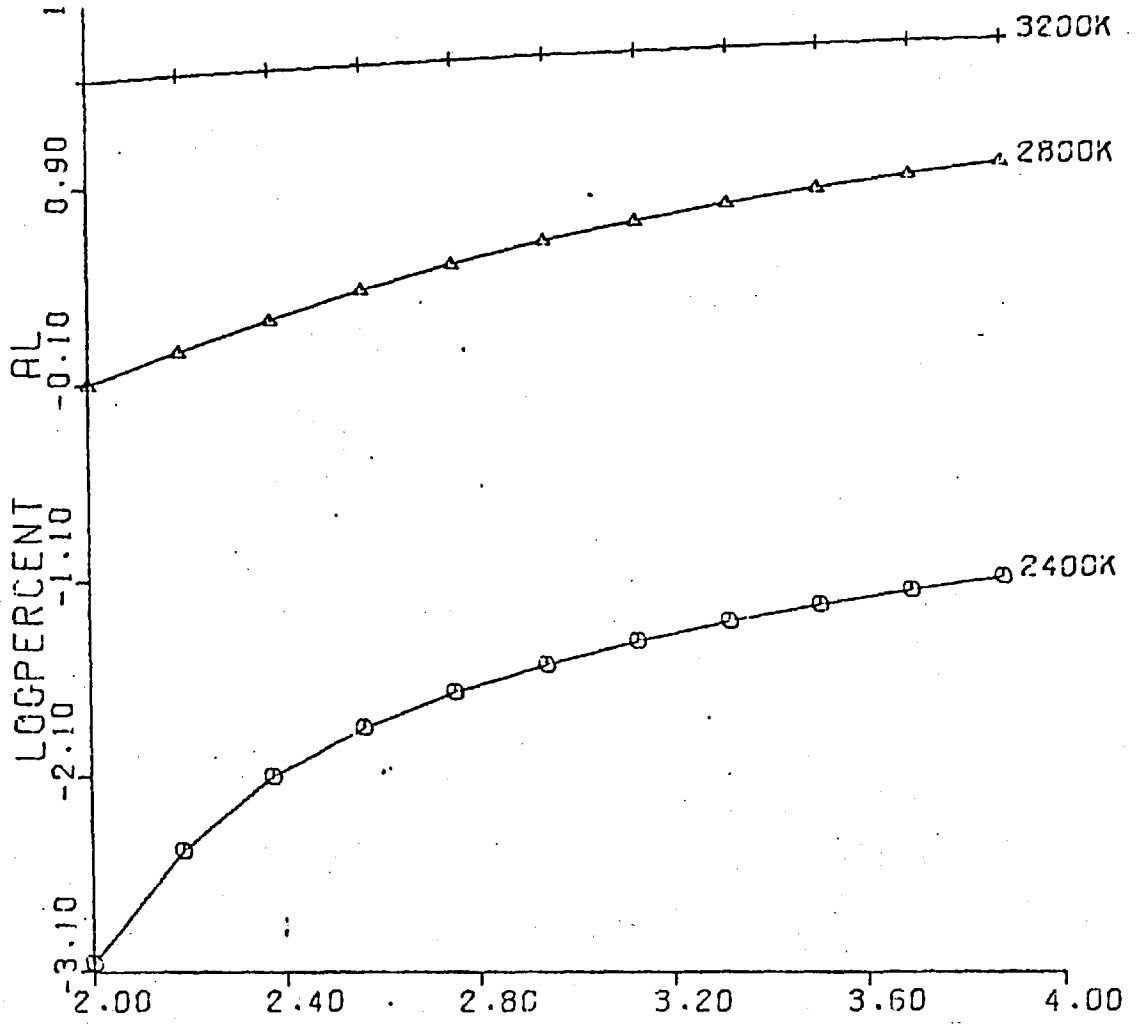

Fig 22 Log (% atomisation of Aluminium) vs. H : O ratio

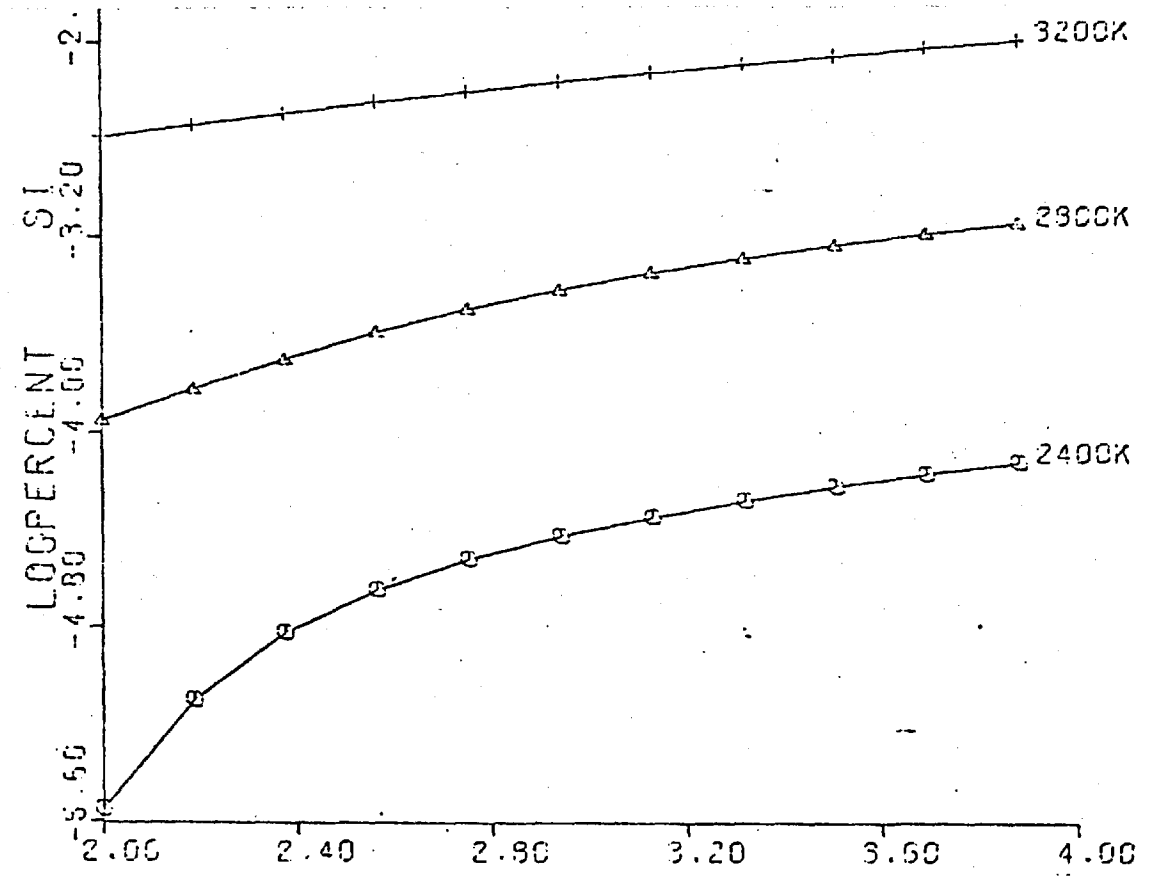

Fig. 23 Log (% atomisation of Silicon) vs. H : O ratio

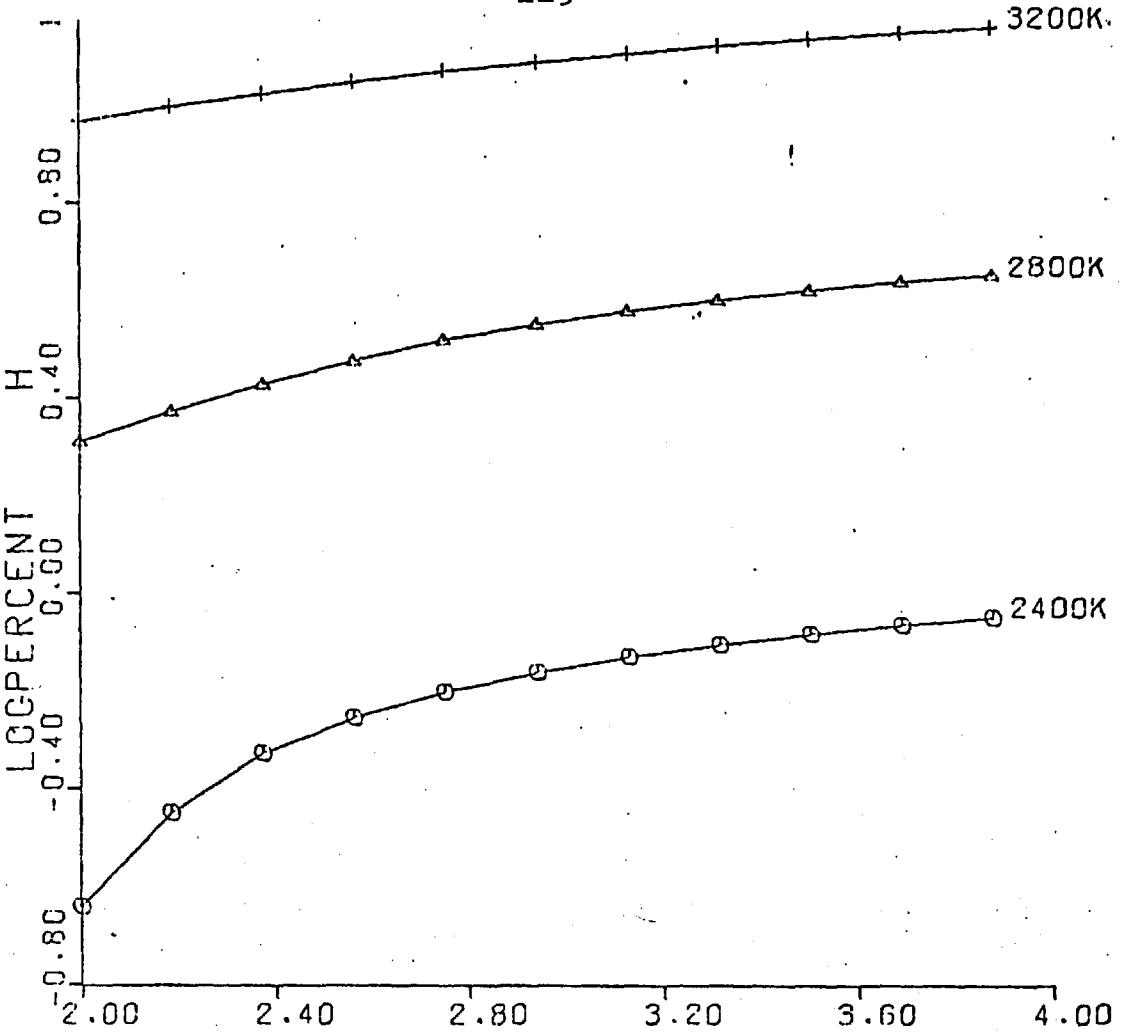

Fig 24 Log (% concentration H) vs. H : O ratio

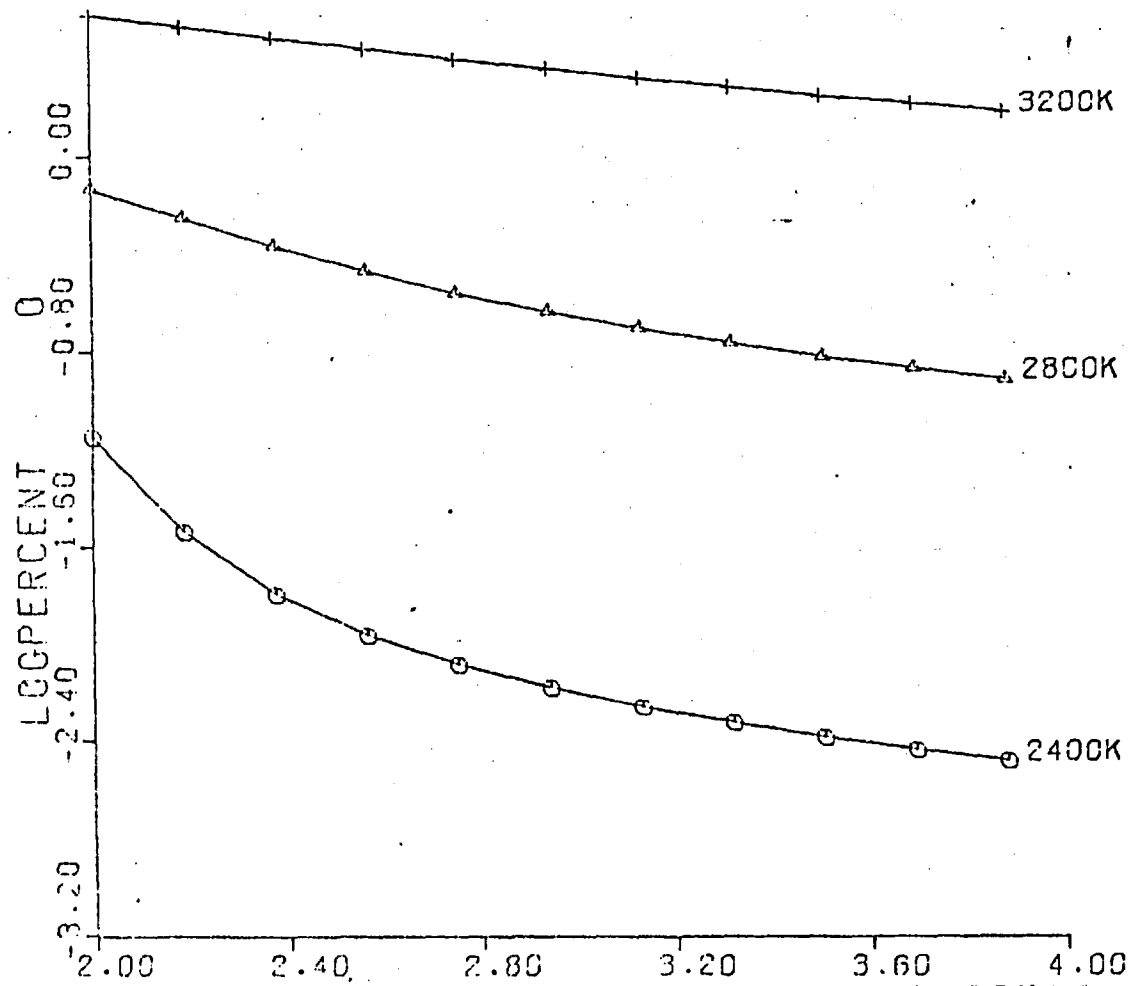

Fig. 25. Log(Concentration (%) O) vs. H : O ratio

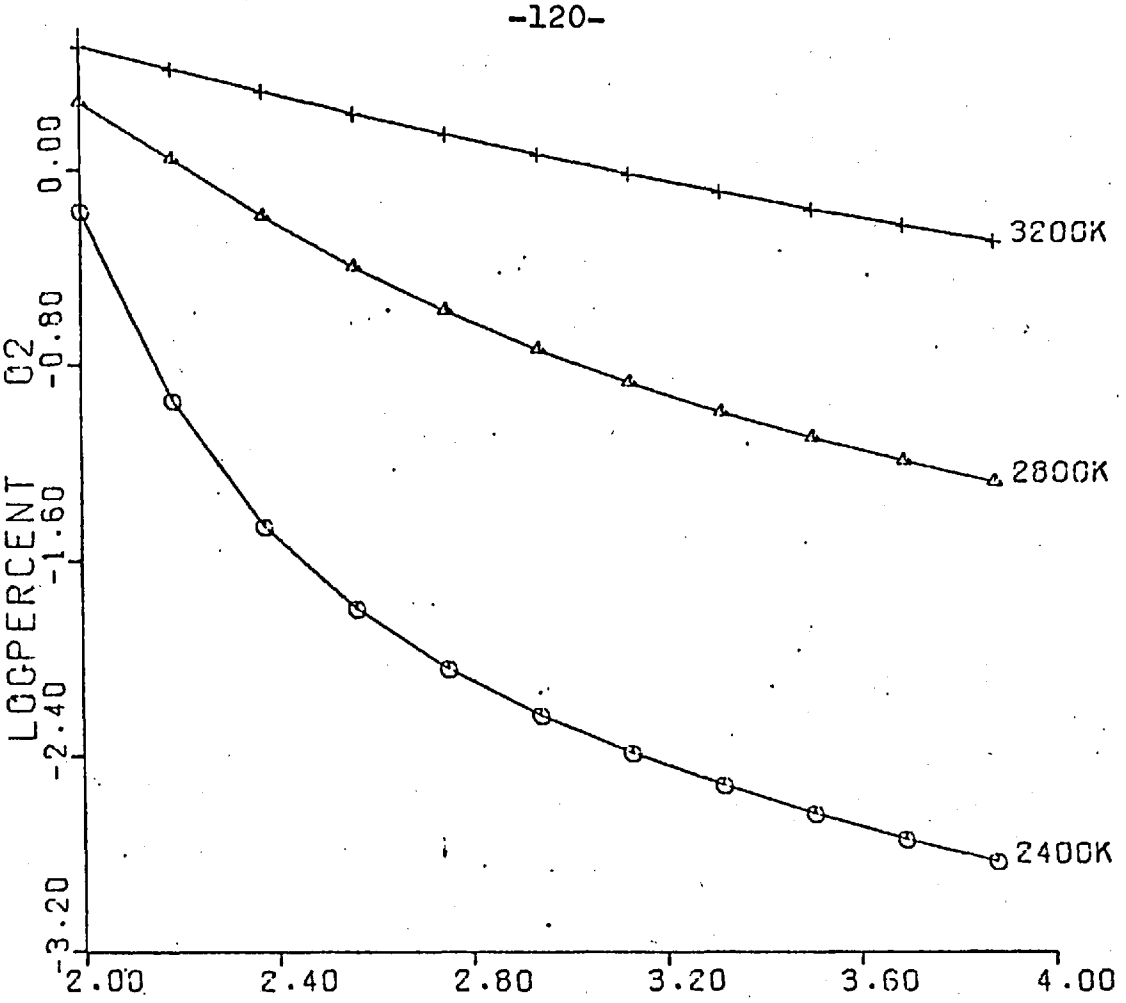

Fig. 26 Log (% concentration O_2) vs. H : O ratio

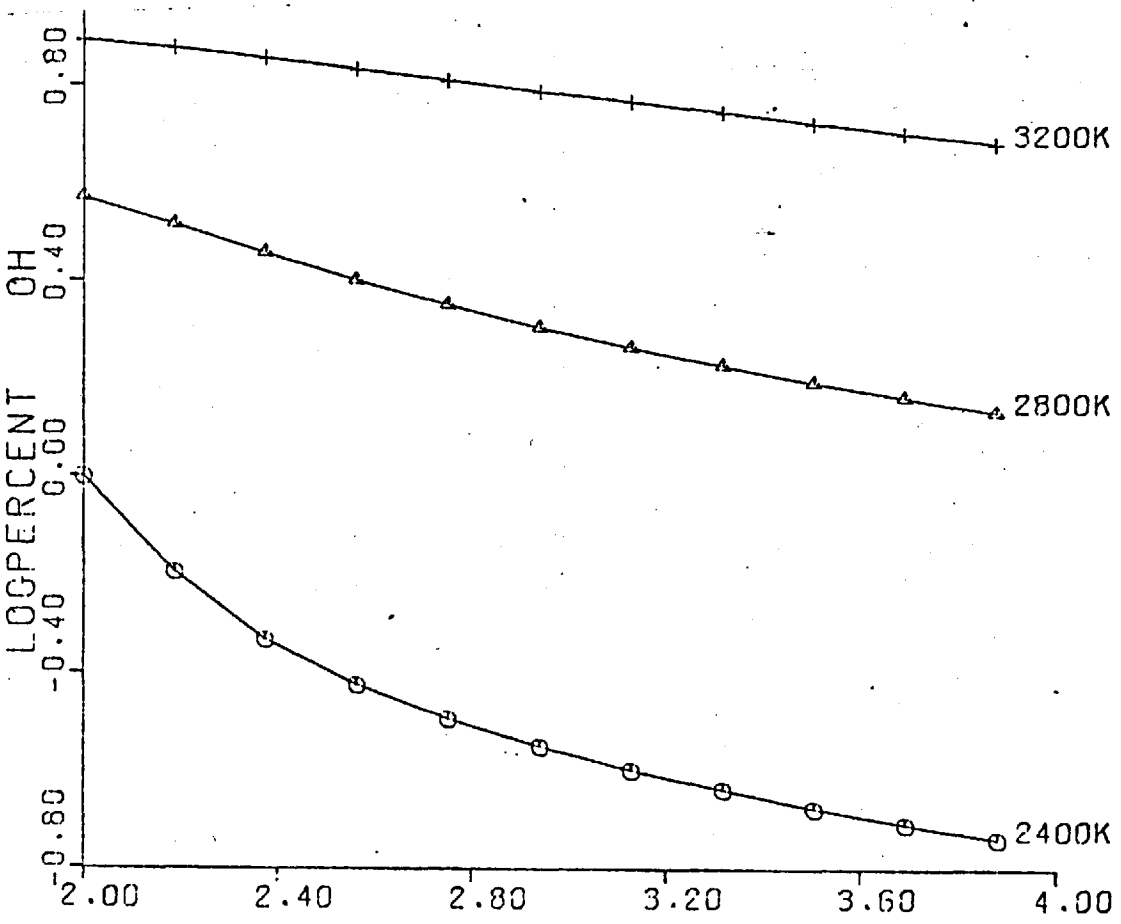

Fig. 27 Log (% concentration OH) vs. H : O ratio

Table IV

a) Concentrations of major species of the stoichiometric Nitrous oxide-hydrogen flame (H:O ratio 2) in volume per cent

Species	2400°K	2800°K	3200°K
H	2.29×10^{-1}	2.04	9.35
H_2	2.10	6.26	11.16
H_2O	48.03	39.28	23.30
O	7.10×10^{-2}	7.42×10^{-1}	3.82
O_2	6.80×10^{-1}	1.90	3.19
OH	1.00	3.74	7.81
N_2	47.61	45.15	39.64
NH	6.81×10^{-6}	1.23×10^{-4}	9.13×10^{-4}
NO	2.81×10^{-1}	8.74×10^{-1}	1.72

b) Concentrations of major species of the fuel rich Nitrous oxide-hydrogen flame (H:O ratio 4) in volume per cent.

Species	2400°K	2800°K	3200°K
H	8.97×10^{-1}	4.49	14.54
H_2	32.13	30.41	27.01
H_2O	34.30	31.86	22.53
O	3.31×10^{-3}	1.24×10^{-1}	1.52
O_2	1.48×10^{-3}	5.31×10^{-2}	5.10×10^{-1}
OH	1.83×10^{-1}	1.37	4.85
N_2	32.47	31.56	28.43
NH	2.20×10^{-5}	2.27×10^{-4}	1.20×10^{-3}
NO	1.08×10^{-2}	1.22×10^{-1}	5.82×10^{-1}

From these results it may be assumed that the high temperature, low background nitrous oxide-hydrogen flame is somewhat oxidising in nature due to the high concentrations of the oxidising species studied in even the fuel rich flame. It would seem therefore that any atomisation of refractory oxide forming elements that may occur is due pricipally to thermal dissociation of the oxide species rather than the chemical reduction associated with acetylene flames. Some chemical reduction must take place since the degrees of atomisation of the elements studied were greater in the cooler fuel rich flames,although the differences were by no means so marked as in the case of the acetylene flames.

The nitrous oxide-hydrogen flame may well be satisfactory for the determination of elements that are readily atomised (109). It may also be of use for reducing some chemical interferences that are encountered in flame atomic emission and absorption spectroscopic analysis without producing a high degree of ionisation (110,111). However,its value as an atom reservoir for the determination of elements prone to refractory oxide formation is decidedly questionable. In these instances the degree of atomisation was found to be markedly temperature dependent, and hence will depend largely on burner design and flame characteristics. The results may thus explain why Willis et al. (110) found less ionisation of calcium at low concentrations in a long path nitrous oxide-hydrogen flame than did Dagnall et al. (109) using a circular flame.

6.2 Oxygen-cyanogen

The high temperature oxygen-cyanogen flame has been used in atomic absorption (112) and thermal emission spectroscopic (113) determination of several elements. Vallee and Bartholomay (113) observed emission of many elements including aluminium, but Robinson (112) observed no atomic absorption of aluminium and noticed improvements in sensitivity over the oxygen-hydrogen flame only in the cases of vanadium and platinum.

The maximum theoretical temperature of the stoichiometric flame has been calculated by Gaydon and Wolfhard (96) at 4853°K, and experimentally determined temperatures are in good agreement with this figure. Thomas, Gaydon and Brewer (114) calculated the temperature by determination of the distribution of the vibration intensity of cyanogen bands which yielded a value of 4800°K ± 200°K and a value of 4640°K ± 50°K has been obtained by the line reversal method (115).

The flame reaction is :-

$$C_2N_2 + O_2 \ (+ 0.05\ H_2O\ ) = CO + N_2$$

and a range of flames was studied by varying the number of moles of cyanogen from 0.5 to 1.5 in steps of 0.10. Thus DIVO = 1.0500 and DIV = 1.0500 + RED(INDEX).

The flame composition is altered considerably by the introduction of water because there is not only substantial cooling but several important hydrogen containing species e.g. H, H_2, HCN, OH, H_2O which are absent in the water-free flame. The effect of the addition of water on the composition of the stoichiometric flame is shown in Table V which lists the concentrations of the major species in the stoichiometric

flames with and without the addition of water.

The amounts of the elements present in one mole feed are given by :-

Carbon B(1) = 2x RED(INDEX) / DIV

and FRAC(1) = 2.0000 ADD(1) = 0.0000

Oxygen B(2) = 2.0500 / DIV

and FRAC(2) = 0.0000 ADD(2) = 2.0500

Nitrogen B(3) = 2x RED(INDEX) / DIV

and FRAC(3) = 2.0000 ADD(2) = 0.0000

Hydrogen B(4) = 0.1000 / DIV

and FRAC(4) = 0.0000 ADD(4) = 0.1000

So that the flame could be studied without water, hydrogen becomes element 4 to simplify the data, and oxygen becomes element 2. The metals were present at levels of 0.0001 gram atom per mole feed and FRAC and ADD data are unnecessary as before. The flame is unusual in that the amount of hydrogen is dependent only on the amount of water, and that the amount of nitrogen depends only on the amount of fuel gas and has no contribution from DIVO.

The carbon : oxygen ratio is given by :-

RATIO(INDEX) = 2x RED(INDEX) / 2.0500

and equals 0.9756 in the stoichiometric flame. It equals unity when RED(INDEX) = 2.0500 / 2 = 1.0250 i.e. when the flame is 2.5 % fuel rich.

The concentrations of atomic carbon (Fig. 28) and cyano (Fig. 29) follow identical trends to those associated with the acetylene flames studied. In the case of cyano there is an increase in concentration of two orders of magnitude

Table V

a) Concentrations of the major species of the oxygen-cyanogen flame in volume per cent.

Species	4100°K	4500°K	4900°K
CO	66.40	65.87	64.58
CO_2	8.64×10^{-3}	6.52×10^{-3}	5.23×10^{-3}
C	1.52×10^{-2}	8.94×10^{-2}	3.82×10^{-1}
C_2	3.42×10^{-5}	2.42×10^{-4}	1.16×10^{-3}
CN	1.47×10^{-1}	3.59×10^{-1}	7.30×10^{-1}
O	1.39×10^{-1}	4.15×10^{-1}	1.06
O_2	6.09×10^{-5}	1.41×10^{-4}	2.99×10^{-4}
N	1.45×10^{-1}	5.12×10^{-1}	1.46
N_2	33.13	32.72	31.73
NO	1.43×10^{-2}	2.73×10^{-2}	4.73×10^{-2}

Table V

b) Concentrations of the major species of the stoichiometric oxygen-cyanogen flame with the addition of water in volume per cent.

Species	4100°K	4500°K	4900°K
CO	63.48	63.31	62.27
CO_2	8.04×10^{-2}	2.35×10^{-2}	9.61×10^{-3}
C	1.49×10^{-3}	2.28×10^{-2}	1.93×10^{-1}
C_2	3.30×10^{-7}	1.59×10^{-5}	2.98×10^{-4}
CN	1.41×10^{-2}	8.97×10^{-2}	3.62×10^{-1}
H	3.12	3.14	3.13
H_2	2.72×10^{-2}	8.33×10^{-3}	3.01×10^{-3}
H_2O	2.96×10^{-4}	2.74×10^{-5}	4.17×10^{-6}
HCN	1.32×10^{-4}	2.48×10^{-4}	3.53×10^{-4}
O	1.35	1.56	2.02
O_2	5.76×10^{-3}	2.00×10^{-3}	1.09×10^{-3}
OH	2.16×10^{-2}	7.68×10^{-3}	3.65×10^{-3}
N	1.42×10^{-1}	5.01×10^{-1}	1.43
N_2	31.64	31.33	30.48
NO	1.36×10^{-1}	1.00×10^{-1}	8.84×10^{-2}

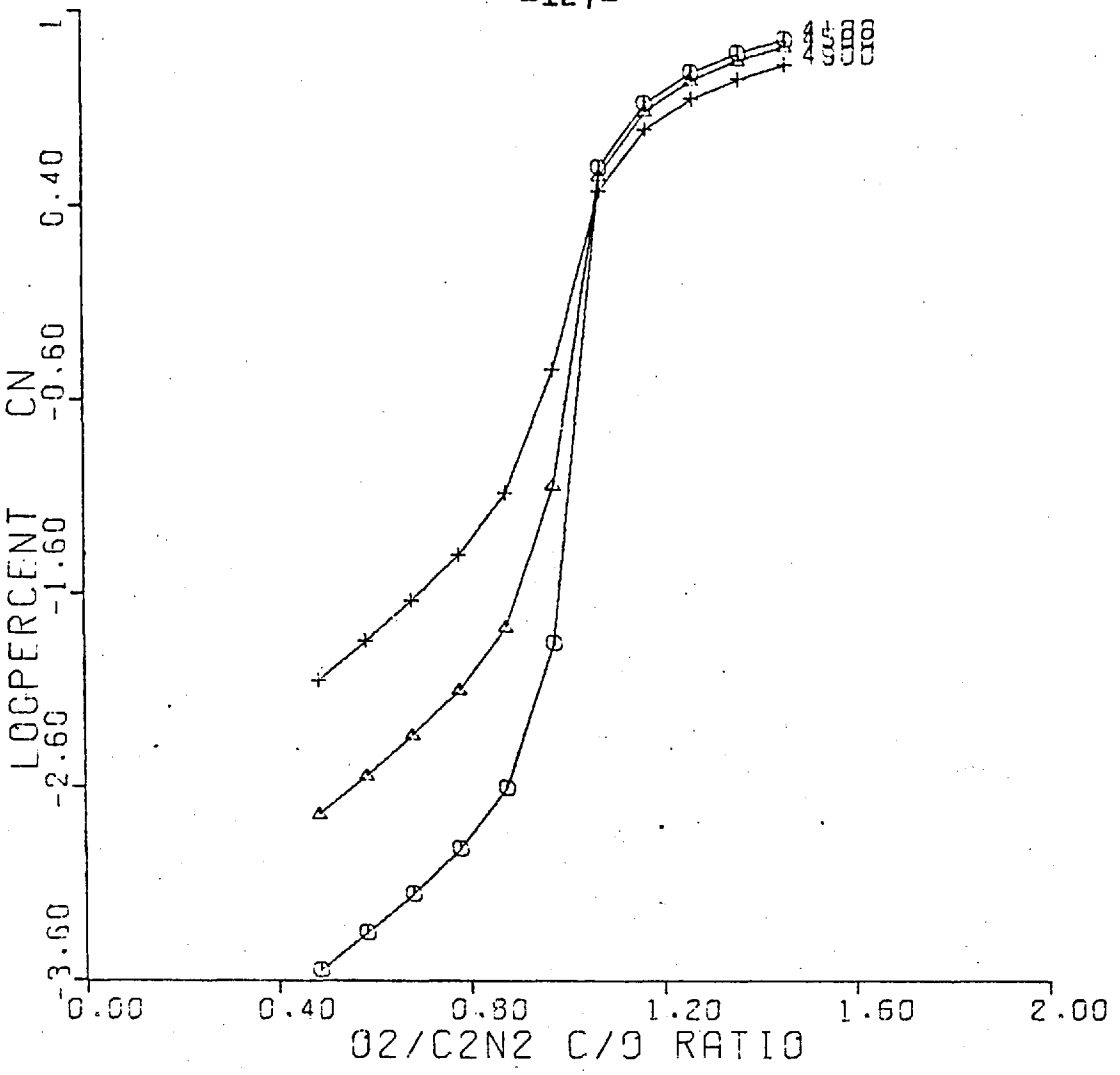

Fig. 28 Log (% concentration CN) vs. C : O ratio.

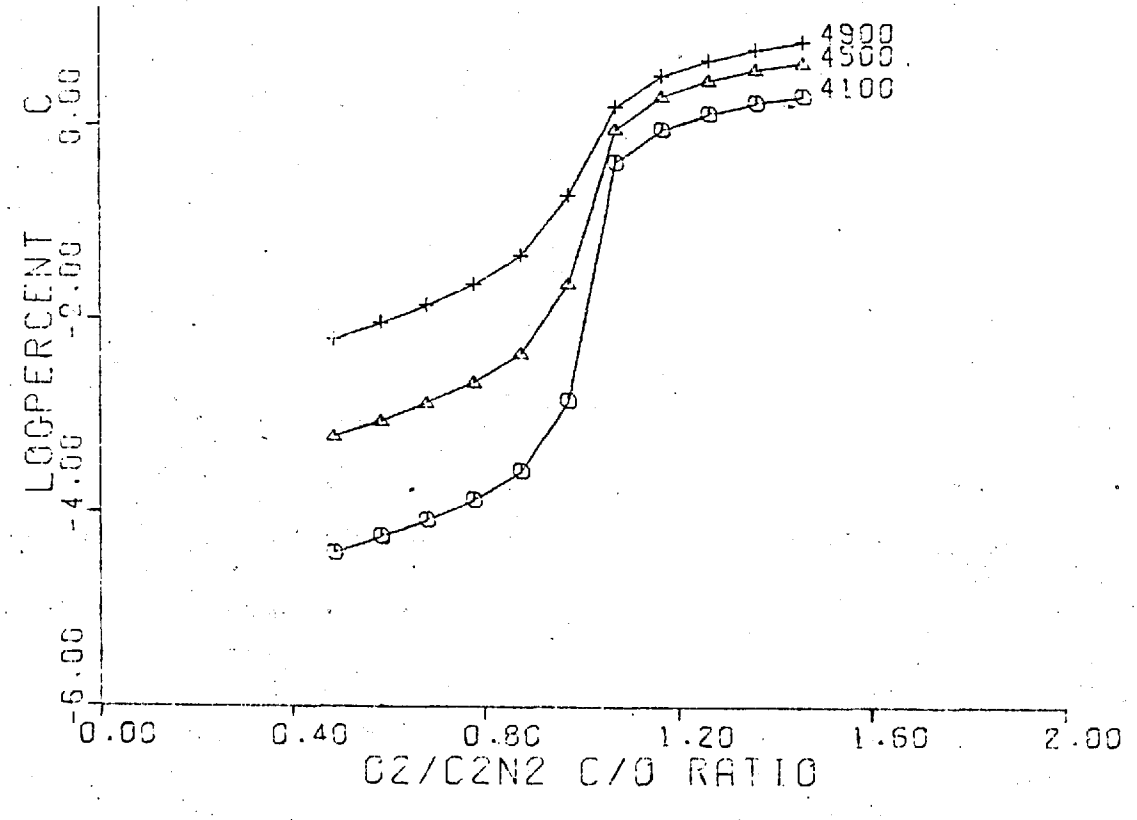

Fig. 29 Log (% concentration C) vs. C : O ratio

at a carbon to oxygen ratio of unity. Identical trends are followed in the flames with and without the addition of water although the concentrations of the carbon species are higher in the flames without water because these flames contain less oxygen. At carbon : oxygen ratios of greater than unity the concentration of CN decreases with rise in temperature as do the other carbon species concenrtations except that of atomic carbon which increases with rise in temperature. A possible explanation for this is that no solid carbon can be formed because the temperature is too high, and, at this high temperature, the molecular carbon containing species tend to dissociate. Thus the concentration of atomic carbon which of course cannot dissociate will tend to rise with rise in temperature.

The concentrations of the oxidising species atomic oxygen (Fig. 30) and hydroxyl (Fig.31) also exhibit identical behaviour to that observed in acetylene flames. The concentrtaion of hydroxyl is considerably smaller than in acetylene flames since hydrogen is available only from the water. The concentrations of molecular oxygen and hydroxyl decrease with increase in temperature at carbon : oxygen ratios of less than unity but increase with increase in temperature when the carbon : oxygen ratio exceeds unity. The concentration of atomic oxygen is directly related to temperature throughout. This is presumably due to the variations in the carbon species concentrations described above.

The degree of atomisation of silicon (Fig. 32) is again markedly dependent on the flame composition and silicon is

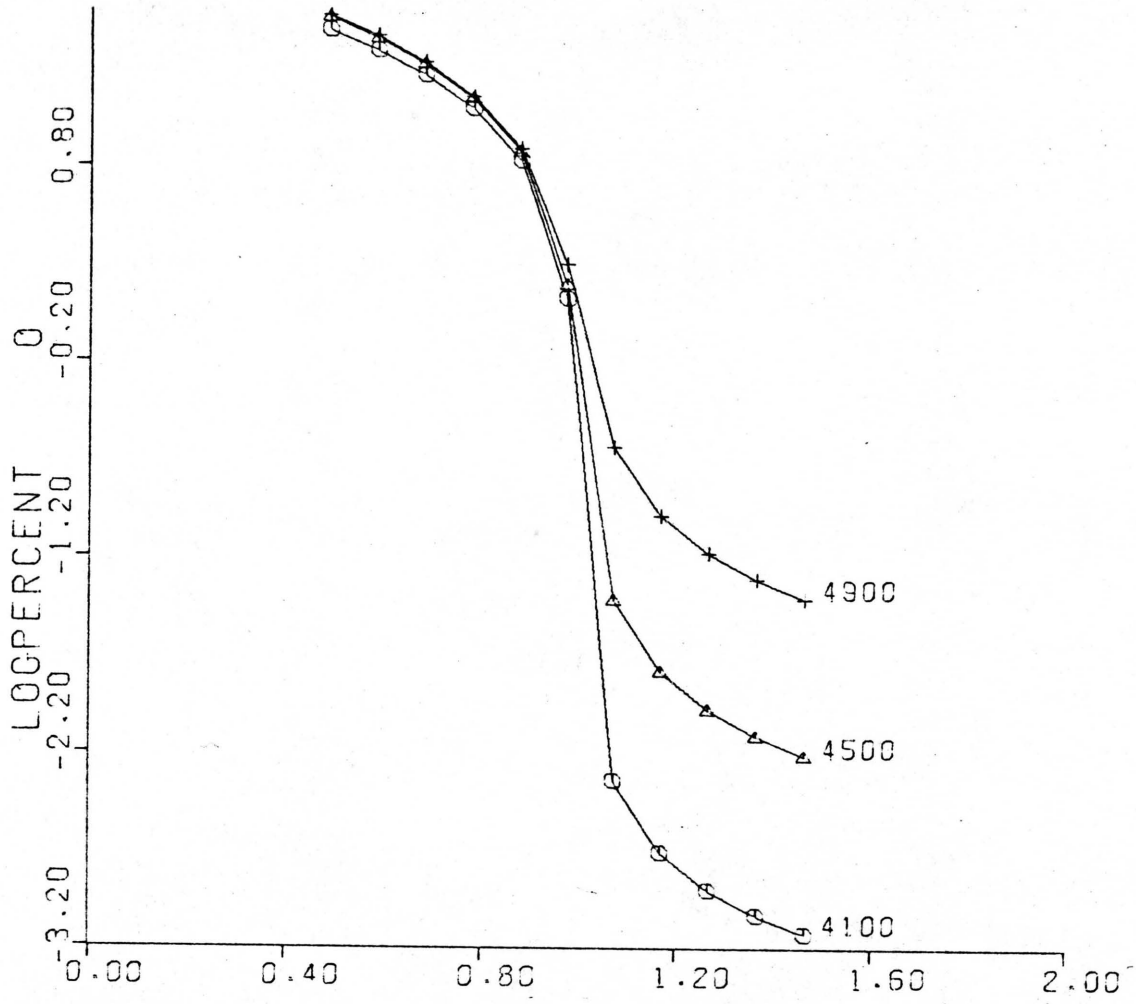

Fig. 30 Log (% concentration O) vs. C : O ratio.

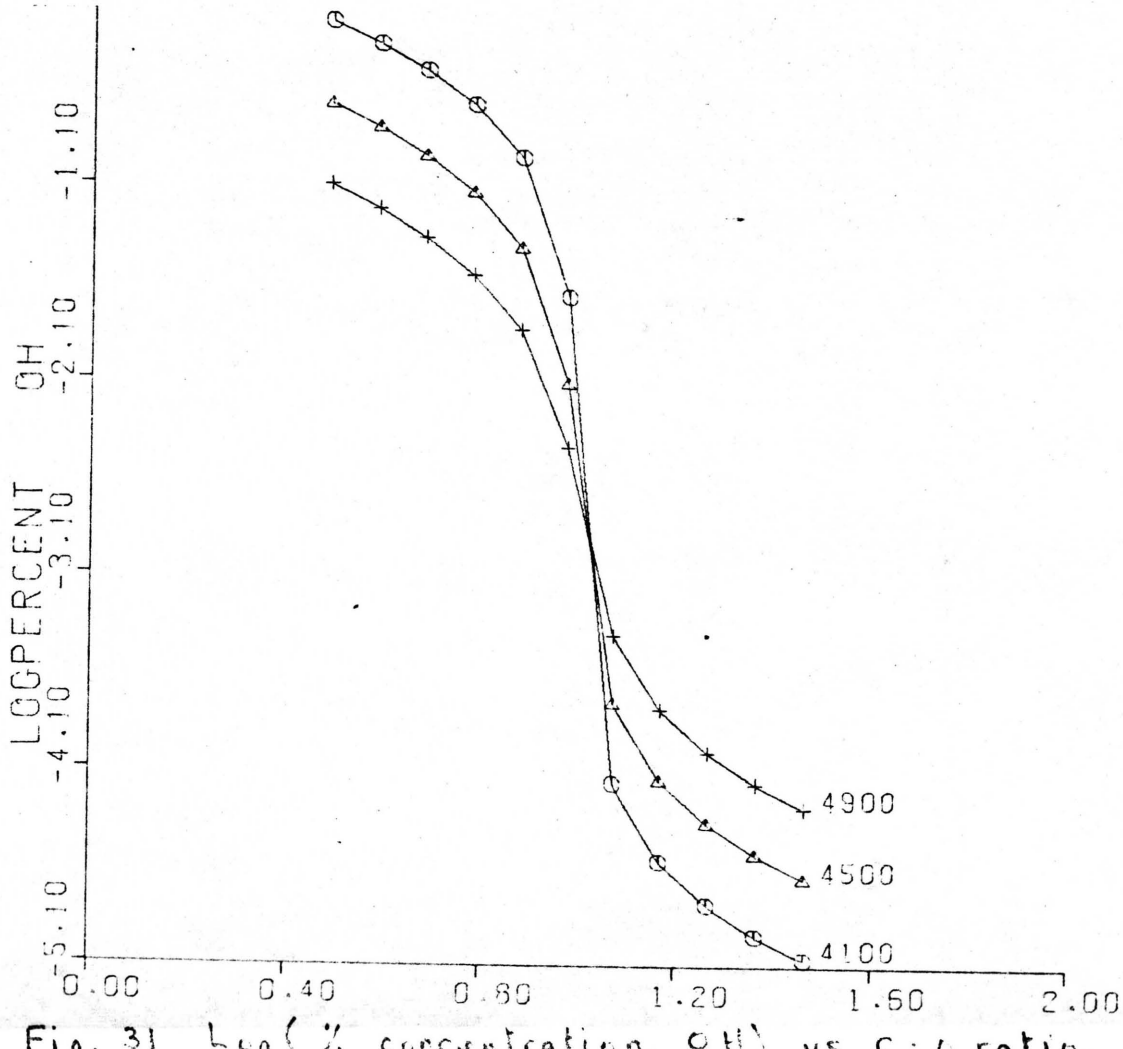

Fig. 31 Log (% concentration OH) vs C : O ratio.

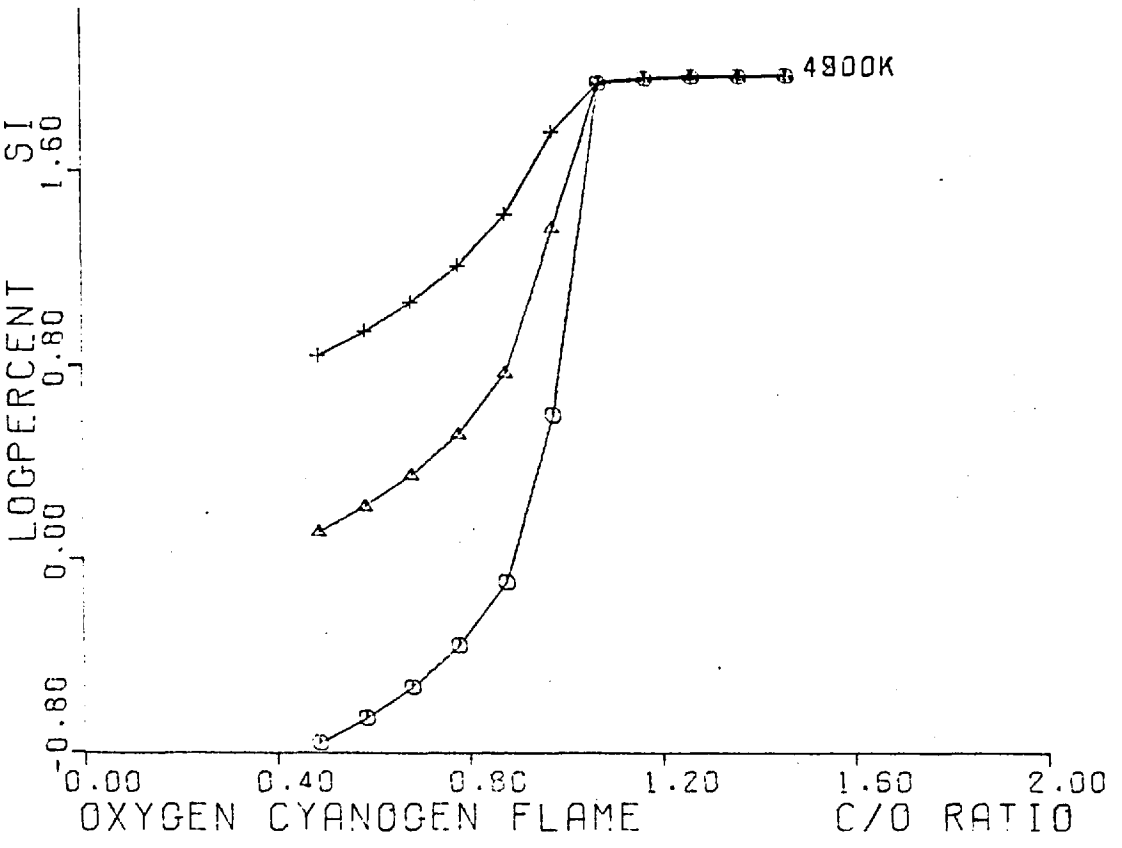

Fig. 32 Log (% atomisation of Silicon) vs. C : O ratio.

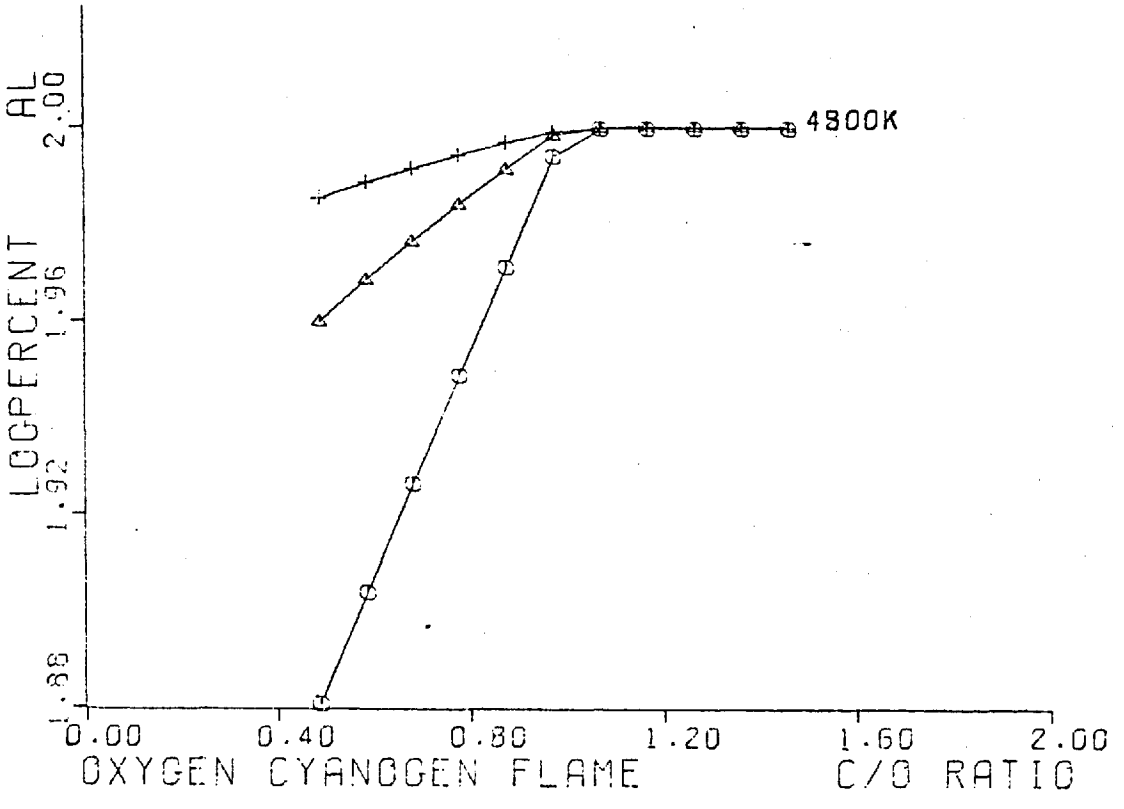

Fig. 33 Log (% atomisation of ALuminium) vs. C : O ratio

completely atomised at all temperatures studied (4000°K - 4900°K) when the carbon : oxygen ratio exceeds unity. Until this ratio reaches unity the principal silicon species is gaseous silicon monoxide (SiO). This is further evidence for atomisation by chemical reduction in flames of carbon containing fuels rather than thermal dissociation since even a temperature of 4900°K is insufficient to atomise silicon completely until the carbon : oxygen ratio exceeds unity.

As would be expected from consideration of the results obtained from the other carbon containing flames the principal aluminium species at all temperatures is atomic aluminium (Fig. 33). The JANAF tables do not contain data for condensed Al_2O_3 for the temperature range considered , but this species may be safely omitted since it does not appear at temperatures above its melting point (2700°K) in the acetylene flames studied. Aluminium is atomised to the extent of 70 % at the lowest temperature (4000°K) in the most fuel lean flame studied (carbon : oxygen = 0.4878) and, at a carbon : oxygen ratio of greater than unity, it is atomised to the extent of 99.9 % even at 4000°K. The other aluminium species present to any extent are AlO, AlOH and AlH in the fuel lean flames and only AlH in the fuel rich flames.

The oxygen-cyanogen flame is the hottest flame that has found use in analytical flame spectroscopy. However, a temperature of 5200°K has been reported for the ozone-cyanogen flame according to the reaction :-

$$3\ C_2N_2 + 2\ O_3 = 6\ CO + 3N_2$$

by Streng and Grosse (116).

Very high temperatures may also be obtained by combustion of the nitrile of acetylene dicarboxylic acid C_4N_2 with oxygen or ozone. The heat of formation of cyanogen is 73.6 kcal / mole (gaseous state at 298°K) and that of carbon subnitride (C_4N_2) under the same conditions is 149.8 kcal / mole, and this presumable accounts for the increase in temperature,

The oxygen flame reaction is :-

$$C_4N_2 + 2O_2 = 4CO + N_2$$

and the flame has a temperature of 5261°K (117).

The ozone flame reaction is :-

$$C_4N_2 + 4/3\ O_3 = 4CO + N_2$$

and the flame has a temperature of 5516°K (117). This latter flame has not been used in flame emission studies because the gas mixture tends to decompose explosively to form nitrogen and carbon powder.

6.3 Miscellaneous Hydrocarbon Flames

i) Some other flames of various hydrocarbons were studied but do not merit extensive discussion since the same trends are observed as in the other flames previously described viz. nitrous oxide-acetylene and air-acetylene. This is to be expected since the computer is clearly unable to distinguish between flame types, and merely distributes the available carbon, hydrogen, oxygen and nitrogen to the species considered to give the composition corresponding to minimum free energy. The only variable therfore is flame temperature.

i) Nitric oxide-acetylene

This flame has been used by Manning (118) for the determination of aluminium by atomic absorption spectroscopy, and yielded absorbances some 60% higher than the nitrous oxide-acetylene flame. This is presumably due to its higher temperature of 3353°K. It has a low burning velocity of 87 cm/sec.

The flame reaction is :-

$$2\ NO + C_2H_2\ (+\ 0.1250\ H_2O) = CO + N_2 + H_2$$

The composition is very similar to that of the nitrous oxide-acetylene flame the principal difference being the smaller proportion of nitrogen since the nitric oxide molecule has only one nitrogen atom compared to the two of the nitrous oxide molecule.

ii) Nitrous oxide-propane

The flame reaction is :-

$$3\ N_2O + C_3H_8\ (+\ 0.1875\ H_2O) = 3\ CO + 3\ N_2 + 4\ H_2$$

The red CN emission characteristic of the nitrous oxide-acetylene flame is not observed to such an extent in the propane flame. This is explained by the fact that concentrations of CN increase with rise in temperature. The temperature of this flame is lower than that of the nitrous oxide -acetylene flame, and the CN concentration is therefore lower. This drop in temperature also decreases the emission from the already smaller CN concentration, and so a marked drop in the emission is observed. The composition of the nitrous oxide-propane and the degrees of atomisation of aluminium and silicon therein are listed in Table VI.

Table VI

b) Concentrations of the major species of the stoichiometric nitrous oxide-propane flame in volume per cent

Species	2400°K	2700°K	3000°K
CO	29.09	28.75	27.92
CO_2	2.09×10^{-1}	1.86×10^{-1}	1.66×10^{-1}
C	9.43×10^{-10}	2.34×10^{-8}	3.05×10^{-2}
CN	9.78×10^{-6}	3.64×10^{-5}	1.03×10^{-4}
H	9.86×10^{-1}	3.44	9.06
H_2	38.79	37.07	33.19
H_2O	1.62	1.58	1.42
HCN	5.49×10^{-4}	5.11×10^{-4}	4.61×10^{-4}
O	1.29×10^{-4}	2.24×10^{-3}	2.18×10^{-2}
O_2	2.25×10^{-6}	3.92×10^{-5}	3.77×10^{-4}
OH	7.83×10^{-3}	3.90×10^{-2}	1.34×10^{-1}
N_2	29.30	28.93	28.08
NO	4.02×10^{-4}	2.76×10^{-3}	1.26×10^{-2}
Solid C*	0.0	0.0	0.0
%Al	12.47	87.18	91.06
%Si	2.02×10^{-3}	1.05×10^{-2}	3.99×10^{-2}

* Moles per mole feed.

Table VI

b) Concentrations of the major species of the fuel rich nitrous oxide-propane flame in volume per cent.

Species	2400°K	2700°K	3000°K
CO	27.87	27.48	26.59
CO_2	4.20×10^{-5}	2.41×10^{-5}	2.10×10^{-5}
C	4.29×10^{-6}	1.65×10^{-4}	2.19×10^{-3}
CN	4.11×10^{-2}	2.34×10^{-1}	6.71×10^{-1}
H	1.04	3.60	9.50
H_2	43.26	40.62	36.52
H_2O	3.78×10^{-4}	2.34×10^{-4}	2.08×10^{-4}
HCN	2.44	3.44	3.15
O	2.71×10^{-8}	3.04×10^{-7}	2.90×10^{-6}
O_2	9.94×10^{-14}	7.19×10^{-13}	6.65×10^{-12}
OH	1.74×10^{-6}	5.53×10^{-6}	1.86×10^{-5}
N_2	24.99	24.03	23.12
NO	7.80×10^{-8}	3.40×10^{-7}	1.51×10^{-6}
Solid C*	4.48×10^{-2}	0.0	0.0
%Al	82.80	94.23	96.25
%Si	8.75	43.67	75.02

* Moles per mole feed.

iii) Air-propane

As before air was considered to be a mixture of nitrogen and oxygen in the ratio 4 : 1 by volume , carbon dioxide being neglected. The flame reaction is :-

$$C_3H_8 + 5\ O_2 + 20\ N_2\ (+\ 1.25\ H_2O) = 3CO_2 + 4\ H_2O + 20\ N_2$$

for which the maximum theoretical temperature is 2198°K (108). The stoichiometric flame has a carbon : oxygen ratio of less than 0.3 (equals 0.3 in the absence of water) and is therefore rather oxidising in nature. Its low temperature and oxidising nature make it clearly unsuitable for the flame spectroscopic determination of any but the most easily atomisable elements.

A carbon : oxygen ratio of unity is achieved only when the flame is some 275 % fuel rich. It is unlikely that such a flame would be supported on conventional burners. Moreover its temperature would be extremely low, and it would be totally unsuitable for any spectroscopic measurements viz. atomic absorption, flame emission.

The composition of the stoichiometric flame is listed in Table VII.

Table VII

Concentrations of the major species of the stoichiometric air-propane flame in volume per cent.

Species	1600°K	1900°K	2200°K
CO	1.91×10^{-2}	1.80×10^{-1}	8.72×10^{-1}
CO_2	10.60	10.42	9.67
C	7.23×10^{-24}	4.67×10^{-19}	1.43×10^{-15}
CN	5.74×10^{-16}	6.63×10^{-13}	1.08×10^{-10}
H	5.69×10^{-5}	2.19×10^{-3}	3.13×10^{-2}
H_2	1.12×10^{-2}	7.67×10^{-2}	3.11×10^{-1}
H_2O	18.57	18.46	18.00
HCN	2.73×10^{-13}	4.30×10^{-11}	1.67×10^{-9}
O	1.55×10^{-5}	9.25×10^{-4}	1.77×10^{-2}
O_2	1.19×10^{-2}	9.77×10^{-2}	4.35×10^{-1}
OH	3.85×10^{-3}	4.48×10^{-2}	2.61×10^{-1}
N_2	70.78	70.68	70.22
NO	4.70×10^{-3}	3.95×10^{-2}	1.81×10^{-1}
%Si	1.92×10^{-14}	6.86×10^{-9}	3.73×10^{-7}

CHAPTER 7

ATOMISATION OF LITHIUM AND MAGNESIUM AND INTERFERENCE FROM SILICON IN THE NITROUS OXIDE-ACETYLENE AND AIR-ACETYLENE FLAMES.

The previous calculations have shown that both aluminium and silicon are incompletely atomised in air- and nitrous oxide-acetylene flames especially when the carbon:oxygen ratio is less than unity. Both elements form condensed oxide species at the lower temperatures, and these species may interfere in the atomisation process of other elements by occlusion. There is also the possibility of the formation of stable compounds such as mixed oxides, and of scatter of the incident radiation by the condensed particles. The available JANAF thermochemical tables contained no date for aluminate species (mixed oxides with Al_2O_3) but data was available for silicate species of lithium and magnesium.

These two elements are of interest also because they are only partially atomised in air-acetylene flame but are more than 95% atomised in the nitrous oxide-acetylene flame. In the case of lithium this is mainly due to the formation of gaseous lithium hydroxide, presumably from the reaction:-

$$Li + OH \rightarrow LiOH$$

In the case of magnesium the principal species at low temperatures in flames of carbon to oxygen ratio less than unity is condensed magnesium oxide. The other main magnesium species are the gaseous oxide M_gO and hydroxide

M

MgOH. These observations are in quite good agreement with the results obtained by de Galan and Winefordner. (119) The concentrations of the lithium and magnesium species with respect to percentage of total metal are listed in tables X a-d

Table X

a) Concentrations of Lithium Species in the Stoichiometric Air-acetylene flame (C:O ratio 0.5926).

Species	2000°K	2200°K	2500°K
Li	3.0	6.7	16.6
Li^+	2.7×10^{-14}	1.1×10^{-12}	8.3×10^{-11}
LiH	4.8×10^{-2}	8.9×10^{-2}	1.7×10^{-1}
LiN	9.1×10^{-3}	2.0×10^{-1}	4.8×10^{-1}
LiOH	96.8	92.9	82.5
LiO	3.1×10^{-3}	1.0×10^{-1}	1.6×10^{-1}

b) Concentrations of magnesium species in the stoichiometric air-acetylene flame (C:O ratio 0.5926).

Species	2000°K	2200°K	2500°K
Mg	9.5	97.5	94.9
MgN	1.4×10^{-4}	3.1×10^{-3}	5.8×10^{-3}
MgH	3.3×10^{-2}	3.7×10^{-1}	3.9×10^{-1}
MgO	9.4×10^{-2}	2.0	4.5
MgOH	7.5×10^{-3}	1.0×10^{-1}	1.4×10^{-1}
MgO(c)	90.1	0.0	0.0

c) Concentrations of Lithium Species in the fuel rich Air-acetylene flame (C:O ratio 1.0667).

Species	2000°K	2200°K	2500°K
Li	94.6	95.1	95.5
Li^+	8.4×10^{-13}	1.5×10^{-11}	1.7×10^{-10}
LiO	2.1×10^{-6}	2.6×10^{-6}	5.5×10^{-6}
LiH	2.7	2.4	1.9
LiOH	1.2×10^{-1}	2.3×10^{-2}	5.3×10^{-3}
LiN	2.5	2.5	2.5

d) Concentrations of Magnesium Species in the fuel rich Air-acetylene flame (C:O ratio 1.0667).

Species	2000°K	2200°K	2500°K
Mg	99.3	99.3	99.2
MgN	1.3×10^{-3}	2.8×10^{-3}	7.1×10^{-3}
MgH	6.2×10^{-1}	6.9×10^{-1}	7.7×10^{-1}
MgO	2.1×10^{-5}	1.9×10^{-5}	2.3×10^{-5}
MgOH	3.0×10^{-6}	1.8×10^{-6}	1.6×10^{-6}
MgO(c)	0.0	0.0	0.0

In the hotter nitrous oxide-acetylene flame, even when the carbon to oxygen ratio is less than unity, the magnesium oxide is vapourised and the lithium hydroxide almost completely dissociated. The concentrations of the species of both elements are listed in tables XI a-d.

Table XI

a) Concentrations of Lithium Species in the stoichiometric Nitrous oxide-acetylene flame (C:O ratio 0.9412) in per cent Lithium present.

Species	2400°K	2800°K	3200°K
Li	58.2	79.9	90.1
Li^+	1.0×10^{-10}	6.0×10^{-9}	1.1×10^{-9}
LiO	1.9×10^{-2}	9.5×10^{-2}	2.5×10^{-1}
LiH	1.32	1.42	1.22
LiOH	39.1	16.8	6.46
LiN	1.32	1.77	1.92

b) Concentrations of Lithium Species in the fuel rich Nitrous oxide-acetylene flame (C:O ratio 1.1765) in per cent Lithium present.

Species	2400°K	2800°K	3200°K
Li	95.6	96.2	96.7
Li^+	1.7×10^{-10}	7.3×10^{-9}	1.2×10^{-7}
LiO	4.1×10^{-6}	5.6×10^{-6}	1.2×10^{-5}
LiH	2.34	1.78	1.36
LiOH	9.2×10^{-3}	1.0×10^{-3}	3.1×10^{-4}
LiN	2.06	1.98	1.92

c) Concentrations of Magnesium Species in the stoichiometric Nitrous oxide-acetylene flame (C:O ratio 0.9412) in per cent magnesium present.

Species	2400°K	2800°K	3200°K
Mg	99.0	98.6	98.3
MgN	4.7×10^{-3}	1.3×10^{-2}	2.6×10^{-2}
MgO	1.8×10^{-1}	4.5×10^{-1}	7.8×10^{-1}
MgH	7.9×10^{-1}	8.7×10^{-1}	8.5×10^{-1}
MgOH	1.3×10^{-2}	1.8×10^{-2}	1.8×10^{-2}
MgO(c)	0.0	0.0	0.0

d) Concentrations of Magnesium Species in the fuel rich Nitrous oxide-acetylene flame (C:O ratio 1.1765) in per cent Magnesium present.

Species	2400°K	2800°K	3200°K
Mg	99.1	99.1	99.1
MgN	4.4×10^{-3}	1.2×10^{-2}	2.4×10^{-2}
MgO	2.4×10^{-5}	2.2×10^{-5}	3.5×10^{-5}
MgH	8.6×10^{-1}	9.1×10^{-1}	8.9×10^{-1}
MgOH	1.9×10^{-6}	9.1×10^{-7}	8.2×10^{-7}
MgO(c)	0.0	0.0	0.0

The effect of a 1000 fold excess of silicon on the atomisation of Lithium and Magnesium was investigated in both flames.

The extra species considered were condensed Li_2SiO_3 and $Li_2Si_2O_5$ $MgSiO_3$ and Mg_2SiO_4 . The concentrations of the species are listed in tables XII a-d.

Table XII

a) Concentrations of Lithium species in the presence of a 1000 fold mole excess of silicon in the stoichiometric Nitrous oxide-acetylene flame (C:O ratio 0.9412) in per cent Lithium present.

Species	2400°K	2800°K	3200°K
Li	95.7	96.2	96.7
Li^+	1.7×10^{-10}	7.3×10^{-9}	1.2×10^{-7}
LiN	2.12	2.07	2.00
LiO	3.7×10^{-6}	1.7×10^{-5}	1.1×10^{-4}
LiOH	7.6×10^{-3}	3.1×10^{-3}	2.8×10^{-3}
LiH	2.17	1.72	1.32
$Li_2SiO_3(c)$	0.0	0.0	0.0
$Li_2Si_2O_5(c)$	0.0	0.0	0.0
$SiO_2(c)$*	0.0	0.0	0.0

* Weight per cent silicon present.

b) Concentrations of Lithium species in the presence of a 1000 fold mole excess of silicon in the fuel rich Nitrous oxide-acetylene flame (C:O ratio 1.1765) in per cent Lithium present.

Species	2400°K	2800°K	3200°K
Li	95.6	96.3	96.8
Li^+	1.7×10^{-10}	7.3×10^{-9}	1.2×10^{-7}
LiN	2.06	1.95	1.86
LiO	3.5×10^{-6}	5.1×10^{-6}	1.0×10^{-5}
LiOH	7.8×10^{-3}	9.2×10^{-4}	2.6×10^{-4}
LiH	2.34	1.75	1.31
$Li_2SiO_3(c)$	0.0	0.0	0.0
$Li_2Si_2O_5(c)$	0.0	0.0	0.0
$SiO_2(c)$*	0.0	0.0	0.0

c) Concentrations of Magnesium species in the presence of a 1000 fold mole excess of silicon in the stoichiometric Nitrous oxide-acetylene flame (C:O ratio 0.9412) in per cent Magnesium present.

Species	2400°K	2800°K	3200°K
Mg	99.1	98.8	98.5
MgN	4.7×10^{-3}	1.3×10^{-2}	2.6×10^{-2}
MgO	1.3×10^{-1}	3.3×10^{-1}	5.8×10^{-1}
MgH	7.9×10^{-1}	8.8×10^{-1}	8.6×10^{-1}
MgOH	9.6×10^{-3}	1.3×10^{-2}	1.4×10^{-2}
MgO(c)	0.0	0.0	0.0
$MgSiO_3(c)$	0.0	0.0	0.0
$Mg_2SiO_4(c)$	0.0	0.0	0.0
$SiO_2(c)$*	0.0	0.0	0.0

* Weight per cent silicon present.

d) Concentrations of Magnesium species in the presence of a 1000 fold mole excess of silicon in the fuel rich Nitrous oxide-acetylene flame (C:O ratio 1.1765) in per cent Magnesium present.

Species	2400°K	2800°K	3200°K
Mg	99.1	99.1	99.1
MgN	4.4×10^{-3}	1.2×10^{-2}	2.4×10^{-2}
MgO	2.4×10^{-5}	2.2×10^{-5}	3.4×10^{-5}
MgH	8.6×10^{-1}	9.1×10^{-1}	8.9×10^{-1}
MgOH	1.8×10^{-6}	8.9×10^{-7}	8.1×10^{-7}
MgO(c)	0.0	0.0	0.0
$MgSiO_3(c)$	0.0	0.0	0.0
$Mg_2SiO_4(c)$	0.0	0.0	0.0
$SiO_2(c)$*	0.0	0.0	0.0

* Weight per cent silicon present.

The results indicate that all the silicate species are totally absent from both flames as is condensed silicon dioxide. Thus both chemical interference and interference by occlusion are ruled out. It would appear therefore that there should be no interference from silicon in the nitrous oxide-acetylene flame in the determination of both magnesium and lithium. Any apparent interference which may occur should therefore be negative and due to viscosity variations in the sample solutions.

The same excess of silicon was examined in the air-acetylene flame and the species concentrations are shown in tables XIII a-d.

Table XIII

a) Concentrations of Lithium species in the presence of a 1000 fold mole excess of silicon in the stoichiometric air-acetylene flame (C:O ratio 6.5926) in per cent Lithium present.

Species	2000°K	2200°K	2500°K
Li	89.7	70.5	41.7
Li^+	8.0×10^{-13}	1.1×10^{-11}	2.1×10^{-10}
LiN	2.62	2.03	1.16
LiO	1.1×10^{-4}	1.7×10^{-2}	7.8×10^{-2}
LiOH	5.40	25.9	56.5
LiH	2.25	1.49	6.2×10^{-1}
$Li_2SiO_3(c)$	0.0	0.0	0.0
$Li_2Si_2O_5(c)$	0.0	0.0	0.0
$SiO_2(c)$*	54.6	49.3	0.0

b) Concentrations of Lithium species in the presence of a 1000 fold mole excess of silicon in the fuel rich air-acetylene flame (C:O ratio 1.0667) in per cent Lithium present.

Species	2000°K	2200°K	2500°K
Li	94.7	95.1	95.7
Li^+	8.4×10^{-13}	1.5×10^{-11}	4.8×10^{-10}
LiN	2.53	2.51	2.44
LiO	1.5×10^{-6}	9.7×10^{-6}	2.6×10^{-6}
LiOH	8.3×10^{-2}	1.7×10^{-2}	2.5×10^{-3}
LiH	2.72	2.33	1.87
$Li_2Si0^3(c)$	0.0	0.0	0.0
$Li_2Si_2O_5(c)$	0.0	0.0	0.0
$SiO_2(c)$*	0.0	0.0	0.0

c) Concentrations of Magnesium species in the presence of a 1000 fold mole excess of silicon in the stoichiometric air-acetylene flame (C:O ratio 0.5926) in per cent Magnesium present.

Species	2000°K	2200°K	2500°K
Mg	99.5	99.4	98.4
MgN	1.4×10^{-3}	3.1×10^{-3}	7.5×10^{-3}
MgH	5.4×10^{-1}	6.0×10^{-1}	5.6×10^{-1}
MgO	1.2×10^{-3}	3.4×10^{-2}	9.3×10^{-1}
MgOH	1.5×10^{-4}	2.8×10^{-3}	3.9×10^{-2}
MgO(c)	0.0	0.0	0.0
SiO_2(c)*	54.6	49.3	0.0
$MgSiO_3$(c)	0.0	0.0	0.0
$MgSiO_5$(c)	0.0	0.0	0.0

d) Concentrations of Magnesium species in the presence of a 1000 fold mole excess of silicon in the fuel rich air-acetylene flame (C:O ratio 1.0667) in per cent Magnesium present.

Species	2000°K	2200°K	2500°K
Mg	99.4	99.3	99.2
MgN	1.3×10^{-3}	2.8×10^{-3}	7.0×10^{-3}
MgH	6.2×10^{-1}	6.9×10^{-1}	7.5×10^{-1}
MgO	1.5×10^{-5}	1.4×10^{-5}	1.4×10^{-5}
MgOH	2.2×10^{-6}	1.3×10^{-6}	7.5×10^{-7}
MgO(c)	0.0	0.0	0.0
SiO_2(c)*	0.0	0.0	0.0
$MgSiO_3$(c)	0.0	0.0	0.0
$MgSi_2O_5$(c)	0.0	0.0	0.0

* Weight per cent silicon present.

The results indicate that there is a substantial increase in the degree of atomisation of lithium at all temperatures in the air-acetylene* flame in the presence of a 1000 fold mole excess of silicon. Neither of the condensed silicate species considered is present, but there are significant amounts of condensed silicon dioxide at the lower temperatures considered (lower than 2400°K).

The degree of atomisation of lithium under these conditions appears to be inversely related to temperature when the condensed silicon dioxide is present and directly related to temperature when it is absent. This direct temperature dependence is also observed in the flame containing only lithium. The degree of atomisation of lithium is also inversely related to the amount of condensed silicon dioxide present.

These results would tend to indicate that silicon is acting as a releasing agent and is consuming the oxidising species to form silicon monoxide and silicon dioxide (gaseous and condensed) thus shifting the equilibria of reactions such as :-

$$Li + OH = LiOH$$

to the left. It would be expected therefore that the atomic absorption of lithium in the stoichiometric air-acetylene flame should be enhanced in the presence of large excesses of silicon. There is a further complication however in that, although neither of the condensed silicate species is formed, there could presumably be some interaction between the lithium atomic vapour and the condensed silicon dioxide.

* stoichiometric flame only.

There could also be the apparent negative interference due to the increase in viscosity of solutions containing large excesses of silicon.

In the fuel rich flame the concentrations of the oxidising species atomic oxygen and hydroxyl are already low and therefore the effect of the excess of silicon is negated since there is no condensed silicon dioxide. As a result the degrees of atomisation of lithium are approximately the same as those in the fuel rich flame in the absence of silicon. The only type of interference possible would therefore appear to be the alteration in the viscosity of the sample solution containing large amounts of silicon.

Similar behaviour is observed in the stoichiometric air-acetylene flame with magnesium in the presence of a 1000 fold mole excess of silicon. Magnesium is almost completely atomised in the stoichiometric flame and condensed magnesium oxide is totally absent at temperatures of 2000^{o}K (the lowest studied) and above. As in the case of lithium in the fuel rich flame the excess of silicon has virtually no effect on the degree of atomisation of magnesium.

These observations suggest that atomisation of some elements could be improved by selectively removing oxidising species from the flame with an element that forms stable oxide species. It is of course desirable that the oxide species formed should be gaseous to obviate problems of occlusion and scatter of the incident radiation in atomic absorption and atomic fluorescence spectroscopy. This therefore affords evidence, on theoretical grounds, of the

action of releasing agents such as those in quite common use including lanthanum and strontium. Unfortunately the relative efficiencies of such releasing agents and the prediction of the most suitable one is not possible at this time because of insufficient thermodynamic data for the elements and oxide species concerned.

CHAPTER 8

CONCLUSIONS AND SUGGESTIONS FOR FUTURE WORK

The calculations have shown that the main requirements for a flame to be an efficient atom reservoir for refractory elements are a high temperature and to be of a carbon containing fuel such that the ratio of carbon to oxygen is greater than unity. Both the nitrous oxide-acetylene and the oxygen-acetylene flames are capable of fulfilling these requirements. In the case of the nitrous oxide-acetylene flame a carbon : oxygen ratio in excess of unity is achieved in a flame that is less than 10 % fuel rich, and there is only a small drop in the temperature from that in the stoichiometric flame. In the case of the oxygen-acetylene a flame over 50% fuel rich is required, and there is a greater drop in the flame temperature. Thus , although the temperature of the stoichiometric nitrous oxide-acetylene flame is lower than that of the stoichiometric oxygen-acetylene flame, the nitrous oxide-acetylene flame of carbon : oxygen ratio greater than unity is probably hotter than an oxygen-acetylene flame of the same carbon : oxygen ratio.

Moreover the nitrous oxide-acetylene flame has a considerably lower burning velocity than the oxygen-acetylene flame (180 cm/sec as against 2,480 cm/sec) and is therefore less likely to cause explosive flashbacks. For these reasons the nitrous oxide-acetylene flame remains the most widely used flame for the determination of metals that are prone to the formation of refractory oxides.

In view of its lower temperature the air-acetylene flame is quite adequate for the determination of elements that are readily atomised only in the absence of refractory oxide forming metals. The calculations showed that it is not capable of atomising silicon and aluminium completely and this could lead to interference. It is sufficiently hot however for significant amounts of nitrogen containing species such as CN and HCN to be formed.

The nitrous oxide-hydrogen flame is shown not to be an efficient atom reservoir for refractory elements, and this appears to be due to the lack of the carbon species present in the acetylene flames. Which of these species is the principal reducing species cannot be determined unequivocally, but the high degrees of atomisation of aluminium and silicon in the fuel rich oxygen-acetylene flames would tend to suggest that atomic carbon is the main species, since CN and HCN are absent from such flames. This might perhaps be established if it were possible to compare the capabilities of the nitrogen/oxygen/acetylene and argon/oxygen/acetylene flames of atomising refractory elements. After corrections are made for temperature etc. the only difference would appear to be the presence or absence of CN and HCN. This involves the design of a burner capable of supporting a flame such as :-

$$2\,N_2 + O_2 + C_2H_2 \rightarrow \text{Products}$$

so that a carbon : oxygen ratio of unity may be obtained without the use of very fuel rich flames.

The lack of thermodynamic data from the available JANAF tables prevented a thorough study of the effects of releasing agents, and other interesting phenomena such as the efficient atomisation in cool oxidising flames of tin and arsenic but not molybdenum, although their monoxide dissociation energies are similar. As more data becomes available it may be possible to solve such problems. The concentrations of ionic species in the flame such as NO^+ could also be calculated as could degrees of ionisation of metals in the flame when such data becomes available as it is now beginning to do.

REFERENCES

1. A. Walsh, Spectrochimica Acta, 1955, 7, 108.
2. C.Th.J. Alkemade and J.M.W. Milatz, Appl. Sci. Res., 1955, 4B, 289.
3. R. Bunsen, Ann. Chem. Pharm., 1859, 111, 257.
4. G. Kirchhoff, Pogg. Ann., 1860, 109, 275.
5. J. Fraunhofer, Ann. Pkysik, 1817, 56, 264.
6. P.J.T. Zeegers, R. Smith and J.D. Winefordner, Anal. Chem., 1968, 40, 13, 26A.
7. S. Talansky, High Resolution, Spectroscopy, Methuen, London, 1947.
8. W.G. Jones and A. Walsh, Spectrochimica Acta, 1960, 16, 249.
9. W.T. Elwell and J.A.F. Gidley, Atomic Absorption Spectroscopy, Pergamon Press, 1966.
10. S. Greenfield, I.Ll. Jones and C.T. Berry, Analyst, 1964, 89, 713.
11. V.A.Fassel, V.G. Mossotti, W.E.L. Grossman and R.N. Kniseley, Spectrochimica Acta, 1966, 22, 347.
12. R.M. Dagnall, K.C. Thompson and T.S. West, Talanta, 1967, 14, 557.
13. R.M. Dagnall, K.C. Thompson and T.S. West, Talanta, 1967, 14, 1467.
14. R.M. Dagnall, K.C. Thompson and T.S. West, Talanta, 1968, 15, 677.
15. J.E. Allan, Spectrochimica Acta, 1961, 17, 467.
16. C.Th.J. Alkemade, Thesis, Utrecht, 1954.

17. W.J. Kirston and G.O.B. Bertilsson, Anal. Chem., 1966, 38, 649.

18. B.V. L'vov, Spectrochimica Acta, 1961, 17, 761.

19. D.N. Hingle, G.F. Kirkbright and T.S. West, Talanta, 1968, 15, 199.

20. T.S. West and X.K. Williams, Anal, Chim. Acta, 1969, 45, 27.

21. V.A. Fassel and R.H. Wendt, Anal. Chem., 1966, 38, 337

22. B.J. Russell, J.P. Shelton and A. Walsh, Spectrochimica Acta, 1957, 8, 317.

23. J.V. Sullivan and A. Walsh, Spectrochimica Acta, 1966, 22, 1843.

24. E.L. Nichols and H.L. Howes, Phys. Rev., 1923, 22, 425 and 1924, 23, 472.

25, C.Th.J. Alkemade, Proc. Xth colloquium Spectroscopium Internationale, 1962, Spartan Books, Washington D.C., 1963,p143.

26. J.D. Winefordner and T.J. Vickers, Anal. Chem., 1964, 36, 161.

27. J.D. Winefordner and R.A. Staab, Anal. Chem., 1964, 36, 165.

28. J.D. Winefordner and R.A. Staab, Anal. Chem., 1964, 36, 1367.

29. J.D. Winefordner, J.M. Mansfield and C. Veillon, Anal. Chem., 1965, 37, 1049.

30. N. Omenetto and G. Rossi, Spectrochimica Acta, 1969, 24B, 95.

31. J.D. Winefordner, M.L. Parsons, J.M. Mansfield and W.J. McCarthy, Spectrochimica Acta, 1967, 23B, 37.

32. D.R. Jenkins, Spectrochimica Acta, 1967, 23B, 167.

33. J.D. Winefordner, W.J. McCarthy and M.L. Parsons, Spectrochimica Acta, 1967, 23B, 25.

34. A.C.G. Mitchell and M.W. Zemansky, Resonance Radiation and Excited Atoms, University Press, Cambridge,1961.

35. J.I. Dinnin, Anal. Chem., 1967, 39, 1491.

36. D.N. Armentrout, Anal. Chem., 1966, 38, 1235.

37. T.S. West and X.K. Williams,Anal. Chim. Acta, 1968,42,29.

38. R.M. Dagnall, T.S. West and P. Young, Talanta, 1966, 13, 803.

39 R.M. Dagnall, K.C. Thompson and T.S. West, ,Anal. Chim. Acta, 1966, 36, 269

40 R.M. Dagnall, K.C. Thompson and T.S. West, Talanta, 1967, 14, 551.

41. R.F. Browner, R.M. Dagnall,and T.S. West, Anal. Chim. Acta, 1969, 45, 163.

42. C. Veillon, J.M. Mansfield, M.L. Parsons and J.D. Winefordner, Anal. Chem., 1966, 38, 204.

43. R.M. Dagnall, K.C. Thompson and T.S. West, Anal. Chim. Acta., 1966, 36, 269.

44. M.D, Amos and J.B. Willis, Spectrochimica Acta, 1966, 22, 1325.

45. C.S. Rann and A.W. Hambly, Anal. Chim. Acta., 1965, 32, 346.

46. C.L. Chakrabarti, Anal. Chim. Acta, 1968, 42, 379.

47. J.E. Allan, Spectrochimica Acta, 1962, 18, 259.

48 H. Bode, Z. anal. Chem., 1954, 143, 182.

49. H. Mabuchi and H. Nakahara, Bull. Chem. Soc. Japan, 1963, 36, 151.

50. H.M.N.H. Irving and R.S. Ramakrishna, Anal. Chim. Acta, 1970, 49, 9.

51. G.F. Kirkbright and W.K. Ng, Anal. Chim. Acta, 1966, 35, 116.

52. M.S. Cresser and T.S. West, Analyst, 1968, 93, 595.

53, L. Futekov and N. Jordanov, Talanta, 1965, 12, 371.

54. L. Futekov and N. Jordanov, Talanta, 1966, 13, 163.

55. H. Goto and Y Kakita, Sci. Rep. Res. Inst., Tohuku Univ. Ser. A, 1959, 11, 1.

56 J.A. Deans and J.L. Simms, Anal. Chem., 1963,35,699

57. C.L. Chakrabarti, Anal. Chim. Acta, 1967, 39, 293.

58. H. Bode, Z. anal. Chem, 1955, 144, 90, 165.

59. G. Nakagawa, J. Chem. Soc. Japan, Pure Chem. Sect., 1960, 81, 1255.

60. J.A. Deans and W.L. Carnes, Analyst, 1962, 87, 745.

61. P.T. Gilbert Jnr., Proc. Xth Colloquium Spectroscopium Internationale, p171, Spartan, Washington D.C.,1963.

62. W, Slavin, C. Sebens and S. Sprague, Atomic Absorption Newsletter, 1965, 4,341.

63. K. Röhre, Z. anal. Chem., 1924, 65, 109.

64. E. Schaaf, Z. anal. Chem., 1943, 136, 298.

65. E.B. Sandell, Colorimetric Determination of Trace Metals, Interscience, New York, 1959.

66. H.J. Morris and H.O. Calvery, Ind. Eng. Chem. Anal. Ed., 1937, 9, 447.

67. H. Bode, Z. anal. Chem., 1954, 142, 414.

68. P.F. Wyatt, Analyst, 1955, 80, 368.

69. W. Fischer and W. Harre, Angew. Chem., 1954,66, 165.

70. E.E. Pickett and S.R. Koirtyohann, Spectrochimica Acta, 1968, 23B, 235.

71. B.M. Gatehouse and J.B. Willis, Spectrochimica Acta, 1961, 17, 710.

72. R.F. Browner, R.M. Dagnall and T.S. West, Anal, Chim. Acta, 1970, 50, 375.

73. R.M. Dagnall and T.S. West, Talanta, 1964, 11, i553.

74. H.H. Lockwood, Anal. Chim. Acta, 1954, 10, 97.

75. H. Bode, Z. anal. Chem., 1955, 144, 165.

76. H.V. Hart, Analyst, 1951, 76, 693.

77. A.D. Maynes and W.A.E. McBryde, Anal. Chem., 1957, 29, 1259.

78. P.W. West and J.K. Carlton, Anal. Chim. Acta, 1952, 6, 406.

79. R.M. Dagnall, T.S. West and P. Young, Anal. Chem., 1966,38, 358.

80. R.S. Hobbs, G.F. Kirkbright, M. Sargent and T.S. West, Talanta, 1968, 15, 997.

81. P.T. Gilbert, Bulletin 753A, Beckman Instruments Inc., Fullerton, California, 1961.

82. K.L. Cheng, R.H. Bray amd S.W. Melsted, Anal. Chem., 1955, 27, 24.

83. L.A. Haddock, Analyst, 1934, 59, 163.

84 J.W. Robinson, Atomic Absorption Spectroscopy, Marcel Dekker, New York.

85. T.S. West and X.K. Williams, Anal. Chem.,1968,40,35.

86. K.M. Aldous, unpublished work.

87. D Betteridge and T.S. West, Anal. Chim. Acta, 1962, 26, 101.

88. V.A. Fassel, J.O. Rasmuson and T.G. Cowley, Spectrochimica Acta, 1968, 23B, 579.

89. J.E. Allan, Spectrochimica Acta, 1969, 24B, 13.

90. V.A. Fassel and D.W. Golightly, Anal. Chem., 1967, 39, 466.

91. W.B. White, S.M. Johnson and G.B. Dantzig, J. Chem. Phys., 1958, 28, 751.

92. B.R. Kubert,and S.E. Stephanou, Kinetics Equilibria and Performance of High Temperature Systems,pp166-170, edited by G.S. Bahn and E.E. Zukowski, Washington D.C., 1960.

93. C.H. Anderson, Paper presented at the Pittsburgh Conference of Analytical Chemistry and Applied Spectroscopy, 1968.

94. W.G. Parker and H.G. Wolfhard, Fourth International Symposium on Combustion, p 420, Williams and Wilkins Co., Baltimore, 1953.

95. G.F. Kirkbright, M.K. Peters, M. Sargent and T.S. West, Talanta, 1968, 15, 663.

96. A.G. Gaydon and H.G. Wolfhard, 'Flames', Chapman and Hall, London, 1960.

97. R.C. Oliver, S. E. Stephanou and R.W. Baier, Chem. Eng., 1962, Feb. 19, p121.

98. JANAF Interim Thermochemical Tables, Dow Chemical Co., Midland, Michigan.

99. K.M. Aldous, R.F. Browner, R.M. Dagnall and T.S. West, unpublished work.

100. G.F. Kirkbright, M. Sargent and T.S. West, Talanta, 1969, 16, 1467.

101. D.J. David, Nature, 1960, 187, 1109.

102. R.N. Kniseley, A.P. D'Silva and V.A. Fassel, Anal. Chem., 1963, 35, 910.

103. A.P. D'Silva, R.N. Kniseley and V.A. Fassel, Anal. Chem., 1964,36, 1287.

104. W. Slavin and D.C. Manning, Anal. Chem., 1963, 35, 253.

105. V.A. Fassel, R.B. Myers and R.N. Kniseley, Spectrochimica Acta, 1963, 19, 1187.

106. T.G. Cowley, V.A. Fassel and R.N. Kniseley, Spectrochimica Acta, 1968, 23B, 771.

107. J.A. Fiorino, R.N. Kniseley and V.A. Fassel, Spectrochimica Acta, 1968, 23B, 413.

108. R. Mavrodineanu and H. Boiteux, L'analyseSpectral Quantitative par la Flamme, Masson, Paris, 1964.

109. R.M. Dagnall, K.C. Thompson and T.S. West, Analyst, 1969, 93, 153.

110. J.B. Willis, V.A. Fassel and J.A. Fiorino, Spectrochimica Acta, 1969, 24B, 157.

111. M.P. Bratzel Jnr., R.M. Dagnall and J.D. Winefordner, Anal. Chem., 1969, 41, 1527.

112. J.W. Robinson, Anal. Chem., 1961, 33, 1067.

113. B.L. Vallee and A.F. Bartholomay, Anal. Chem., 1956, 28, 1753.

114. N. Thomas, A.G. Gaydon and L. Brewer, J. Chem. Phys., 1952, 20, 369.

115. J.B. Conway, R.H. Wilson Jnr. and A.V. Grosse, J. Amer. Chem. Soc., 1953, 76, 499.

116. A.G. Streng and A.V. Grosse, J. Amer. Chem. Soc., 1957, 79, 5583.

117. A.D. Kirschenbaum and A.V. Grosse, J. Amer. Chem. Soc., 1956, 78, 2020.

118. D.C. Manning, Atomic Absorption Newsletter, 1965, 4, 267.

119. L. de Galan and J.D. Winefordner, J. Quant. Spec. Rad. Trans., L967, 7, 251.

APPENDIX I

ANFLAM

A Fortran IV computer program for the calculation of equilibrium compositions of flames and other systems by the method of Minimsation of Free Energy.

Species considered

Flame species

C	NH_3	Al	MgOH
C_2	NO	AlH	$MgSiO_3(c)$*
C_3	NO_2	AlO	$Mg_2SiO_4(c)$*
CH	N_2O	AlOH	
CH_2	NOH	AlN	
CH_3	C (solid)	AlC	
CH_4		Al_2O	
C_2H_2		Al_2O_2	
C_2H_4		Al_2O_3(solid)	
CO		Si	
CO_2		Si_2	
CHO		Si_3	
CH_2O		SiO	
CN		SiO_2	
C_2N_2		SiO_2(liquid)	
H		Li	
H_2		Li^+	
H_2O		LiH^-	
HO_2		LiO	
HCN		LiOH	
HCNO		LiN	
O		$Li_2SiO_3(c)$*	
O_2		$Li_2Si_2O_5(c)$*	
OH		Mg	
N		MgH	
N_2		MgO	
NH		MgO(solid)	
NH_2		MgN	

* (c) condensed species

```
      PROGRAM ANFLAM (INPUT,OUTPUT,TAPE5=INPUT,TAPE6=OUTPUT,TAPE27,
     1TAPE25)
$IBFTC MAIN
C
C      CALCULATION OF CONCENTRATIONS OF FLAME SPECIES BY MINIMISATION
C                              FREE ENERGY
C
C     READ IN DATA AND CALCULATE F/RT
C
      DIMENSION FRT(60,10),NTEMP(10),TITLE(60),THERM1(60,10),
     1 THERM2(60,10),TEMP(10)
     2,Z(60,10)
      COMMON FRT,KELVIN
      READ(5,1914) NSPECY,KELVIN
 1914 FORMAT(I2,2X,I2)
      DO 10 NS = 1,NSPECY
      DO 11 NT = 1,KELVIN
      READ(5,1000)TITLE(NS),NTEMP(NT),THERM1(NS,NT),THERM2(NS,NT)
 1000 FORMAT (1X,A6,I6,2F10.3)
      TEMP(NT) = NTEMP(NT)
      FRT(NS,NT) = -THERM1(NS,NT)/1.9872 + THERM2(NS,NT)/
     1 (1.9872*TEMP(NT))*1000.0
   11 CONTINUE
   10 CONTINUE
      CALL THERMO
      STOP
      END
```

```
$IBFTC ATHERM
       SUBROUTINE THERMO
      DIMENSION TEMP(10),FRT(60,10),B(10),AW(10),TITLE(60),A(60,10),
     1Y(60),F(60),ALPHA(10),R(10,10),Y1(60),X(41,42),NONCON(10),Z(60,10
     2,KTEMP(10),ZVOL(60,10),SUMZ(10),ETITLE(10),AVEMW(10),WT(10)
     3,FTITLE(5),RED(20),ATOM(60,3,20),RATIO(20),NOUGHT(60)
     4,FRAC(10),ADD(10)
      COMMON FRT,KELVIN
      DO 116 I = 1,60
  116 NOUGHT(I) = -1
      INDEX = 1
      READ(5,119)(FTITLE(I),I=1,4)
  119 FORMAT(4A10)
      READ(5,120)NOMORE,METALS,NOM
  120 FORMAT(I2,2X,I2,2X,I2)
      READ(5,121) NE,NGS,NCS,STEMP,P
  121 FORMAT(3I4,F8.1,F6.2)
      READ(5,140)(ETITLE(I),I=1,NE)
  140 FORMAT(10(1X,A6))
      READ(5,144)(WT(J),J=1,NE)
  144 FORMAT(10F7.3)
      READ(5,9111)NOXY,RED(1),DELTA,DIVO
 9111 FORMAT(I2,3F7.3)
      READ(5,1999)(FRAC(I),ADD(I),I=1,NE)
 1999 FORMAT(2F7.4)
      READ(5,1998)LEAST,MOST,INSTEP
 1998 FORMAT(3I2)
      NS= NGS + NCS
      DO 150 I =1,NS
      READ(5,151)(TITLE(I),Y(I),(A(I,II),II=1,NE))
  151 FORMAT(A6,F6.4,10F6.1)
  150 CONTINUE
C
C     CALCULATE B VALUES FROM FLAME STOICHEOMETRY
C
  414 CONTINUE
      DIV = DIVO + RED(INDEX)
      DO 415 I=1,NE
  415 B(I) =(FRAC(I)*RED(INDEX) + ADD(I))/DIV
      IF(NOM.LE.0) GO TO 417
      DO 416 I=NOM,NE
  416 B(I) = ADD(I)
  417 RATIO(INDEX) = B(1)/B(NOXY)
      WRITE(6,162)(ETITLE(I),I = 1,NE)
  162 FORMAT(1H1,7X,10(3X,A6))
      WRITE(6,163)(B(I),I = 1,NE)
  163 FORMAT(1H0,5X,2HB=,10F9.6)
      WRITE(6,8001)RATIO(INDEX),RED(INDEX)
 8001 FORMAT(1H0,5X,22HFUEL/OXIDANT RATIO IS ,F8.4,5X,F8.4,10H MOLS FUE
     1  )
      T1 = STEMP
      ITEMP = 1
C
C      FIND SOLUTION FOR EACH TEMPERATURE
C
      NGS1 = NGS + 1
      NE1 = NE + 1
      DO 1100 IT =1,KELVIN
      LOOP = 0
```

```
      NONCON(IT) = 0
  260  DO 270 I = 1,NS
       IF ( Y(I) - 1.0E-8 )265,270,270
  265  Y(I) = 0.0
  270 Y1(I) = Y(I)
      LOOP = LOOP + 1
       IF ( LOOP - 100 ) 280,280,275
  275 NONCON (IT) = 1
      GO TO 1085
  280 N = NE1
      IF ( NS - NGS1 ) 350, 300, 300
  300 DO 340 I = NGS1,NS
      IF ( Y(I) ) 320, 340, 320
  320 N = N + 1
  340 CONTINUE
  350 N1 = N + 1
      DO 370 I =1,N
      DO 370 J =1,N1
  370 X(I,J) = 0.0
C
C     FIND VALUES OF ALPHA, R AND F
C
  400 YBAR = 0.0
      DO 420 I = 1,NGS
  420 YBAR = YBAR + Y(I)
      DO 440 I = 1,NGS
      IF(Y(I).EQ.0.0) Y(I) = 1.0E-250
  440 F(I) = Y(I)*(FRT(I,ITEMP) + ALOG(P) + ALOG( Y(I)/YBAR))
      DO 480 J = 1,NE
      ALPHA(J) = 0.0
      DO 460 K = 1,NE
      R(J,K) = 0.0
      DO 460 I = 1,NGS
  460 R(J,K) = R(J,K) + A(I,J)*A(I,K)*Y(I)
      DO 480 I = 1,NGS
  480 ALPHA(J) = ALPHA(J) + A(I,J)*Y(I)
C
C     SET UP THE SYSTEM OF EQUATIONS.
C
C     EQUATIONS FOR GASEOUS SPECIES
C
      DO 550 I = 1,NE
      X(I,N1) = B(I)
      X(I,1) = ALPHA(I)
      II = N - NE + I
      X(NE1,II) = ALPHA(I)
      DO 530 J = 1,NE
      JJ = N - NE + J
  530 X(I,JJ) = R(I,J)
      DO 550 J = 1,NGS
  550 X(I,N1) = X(I,N1) + A(J,I)*F(J)
      DO 570 I = 1,NGS
  570 X(NE1,N1) = X(NE1,N1) + F(I)
      IF ( NS - NGS1 ) 680, 600, 600
C
C     EQUATIONS FOR CONDENSED SPECIES
C
  600 NC = 0
      DO 650 I = NGS1,NS
```

```
      IF ( Y(I) ) 620, 650, 620
  620 NC = NC + 1
      NN = NE1 + NC
      X(NN,N1) = FRT(I,ITEMP)
      DO 640 J = 1,NE
      NJ = N- NE + J
      X(J,NC+1) = A(I,J)
  640 X(NN,NJ) = A(I,J)
  650 CONTINUE
C
C     SOLVE THE SYSTEM OF EQUATIONS
C
  680 CONTINUE
  690 CALL GPIVOT(N,X)
C
C     COMPUTE NEW VALUES
C
      DO 780 I = 1,NGS
      SUM = 0.0
      DO 700 J = 1, NE
      NN = N - NE + J
  700 SUM = SUM + X(NN,N1)*A(I,J)
      IF ( Y1(I) ) 720, 750, 720
  720 Y(I) = Y1(I)*(-FRT(I,ITEMP) - ALOG(P) - ALOG(Y1(I)/YBAR)
     1 + X(I,N1) + SUM )
      GO TO 780
  750  Y(I) = YBAR*EXP(-FRT(I,ITEMP) + SUM)
      IF ( Y(I) - 1.0E-5 ) 770, 770,760
  760 Y(I) = 1.0E-5
      GO TO 780
  770 IF ( Y(I) - 1.0E-35 ) 775,780,780
  775  Y(I) = 1.0E-35
  780 CONTINUE
      IF ( NS - NGS1 ) 850,800,800
  800 NC = 1
      DO 840 I = NGS1,NS
      IF ( Y1(I) ) 820,840,820
  820 NC = NC + 1
      Y(I) = X(NC,N1)
  840 CONTINUE
C
C     ADJUST NEW VALUES TO A POSITIVE SET
C
  850 FLAM = 1.0
      DO 900 I = 1,NS
      IF ( Y(I) ) 855,900,900
  855 IF ( Y(I) - Y1(I) ) 860,900,900
  860 FL = - Y1(I)/ ( Y(I) - Y1(I) )
      IF ( FLAM - FL ) 900,900,880
  880 FLAM = 0.99*FL
  900 CONTINUE
  910 DO 920 I =1,NS
  920 Y(I) = Y1(I) + FLAM*( Y(I) - Y1(I) )
      IF ( NS - NGS1 ) 1050,950,950
  950 DO 1000 I = NGS1,NS
      IF ( Y1(I) ) 955,955,1000
  955 SUM = 0.0
      DO 960 J = 1, NE
      NN = N - NE + J
```

```
  960 SUM=SUM + X(NN,NI)*A(I,J)
      DIF = FRT(I,ITEMP) - SUM
      IF ( DIF ) 980,1000,1000
  980 IF ( ABS (DIF/FRT(I,ITEMP) ) - 1.0E-3 ) 1000,990,990
  990 Y(I) = 1.0E-8
 1000 CONTINUE
C
C     CHECK FOR CONVERGENCE
C
 1050 DO 1070 I = 1,NS
       IF ( ABS( Y(I) - Y1(I)) - 1.0E-6 ) 1070,260,260
 1070 CONTINUE
      IF ( FLAM - 1.0 ) 260,1080,260
 1080 CONTINUE
C
C     STORE VALUES OF Y(I) IN A TWO-DIMENSIONAL ARRAY SO THAT Y(I) CAN
C        BE USED AS INITIAL GUESSES FOR THE NEXT TEMPERATURE
C
      DO 2102 I=1,NS
      Z(I,IT) = Y(I)
 2102 CONTINUE
      KTEMP(IT) = T1
      T1 = T1 + 100.0
      ITEMP = ITEMP + 1
 1100 CONTINUE
      GO TO 1086
C
C     IF SYSTEM FAILS TO CONVERGE PRINT CURRENT VALUES OF CONCENTRATION
C                  AND TERMINATE PROGRAM
C
 1085 WRITE(6,3110)T1
 3110 FORMAT(1X,37HSYSTEM HAS FAILED TO CONVERGE AT TEMP,F6.1/
     11X,40H VALUES OF Y(I) AFTER 50 ITERATIONS ARE      )
      WRITE(6,2555)(TITLE(I),Z(I,IT),I = 1,NS)
 2555 FORMAT(1X,5(A6,1PE12.5))
      STOP
 1086 CONTINUE
C
C     PRINT CONCENTRATIONS OF SPECIES IN MOLES PER MOLE GAS FEED
C
      WRITE(6,2999) (FTITLE(I),I=1,3)
 2999 FORMAT(1H0,6X,29HEQUILIBRIUM CONCENTRATIONS OF ,3A10,28H IN MOLES
     1PER MOLE GAS FEED       )
      WRITE(6,2100)(KTEMP(IT) ,IT = 1,KELVIN)
 2100 FORMAT(1H0,6H TEMP=/1X,10I12)
      DO 6666 I = 1,NS
      WRITE(6,2111)TITLE(I),(Z(I,IT),IT = 1,KELVIN)
 2111 FORMAT(1X,A6,1X,1P10E12.5)
 6666 CONTINUE
      IF(METALS.EQ.0) GO TO 8012
      DO 8000 I = 1,METALS
      K = 1
      DO 8002 KT = LEAST,MOST,INSTEP
      IF(KT.GT.KELVIN) GO TO 8000
      EFFIC = Z(I,KT)*100.0/B(NE)
      EFFIC = EFFIC*A(I,NE)
      IF (EFFIC.LE.0.0) NOUGHT(I) = 1
      IF (EFFIC.LE.0.0)GO TO 8000
      ATOM(I,K,INDEX) = ALOG10(EFFIC)
```

```
 8002 K=K+1
 8000 CONTINUE
      DO 8012  I = 1,METALS
      IF(NOUGHT(I).EQ.-1) GO TO 8012
      K = 1
      DO 8011 KT = LEAST,MOST,INSTEP
      ATOM(I,K,INDEX)  = Z(I,KT)*A(I,NE)
 8011 K = K+1
 8012 CONTINUE
C
C       CALCULATE CONCENTRATIONS IN VOLUME PER CENT
C
      DO 85 IT =1,KELVIN
      SUMZ(IT) = 0.0
      DO 84 I = 1,NGS
      SUMZ(IT) = SUMZ(IT) + Z(I,IT)
   84 CONTINUE
   85 CONTINUE
       DO 88 IT = 1,KELVIN
       DO 87 I =1,NGS
      ZVOL(I,IT) = 100.0*(Z(I,IT)/SUMZ(IT) )
   87 CONTINUE
   88 CONTINUE
      DO 95 IT = 1,KELVIN
      SUMMW = 0.0
      DO 94 I = 1,NGS
      DO 93 J = 1,NE
      SUMMW = SUMMW + ZVOL(I,IT)*A(I,J)*WT(J)
   93 CONTINUE
   94 CONTINUE
      AVEMW(IT) = SUMMW/100.0
   95 CONTINUE
C
C       PRINT CONCENTRATIONS OF SPECIES IN VOLUME PER CENT
C
      WRITE(6,162)(ETITLE(I),I=1,NE)
      WRITE(6,163)(B(I),I = 1,NE)
      WRITE(6,8001)RATIO(INDEX),RED(INDEX)
      WRITE(6,2998) (FTITLE(I),I=1,3)
 2998 FORMAT(1H0,6X,29HEQUILIBRIUM CONCENTRATIONS OF ,3A10,31H IN VOLUME
     1 PERCENT OF PRODUCTS     )
      WRITE(6,2100)(KTEMP(IT),IT=1,KELVIN)
      DO 86 I =1,NGS
   86 WRITE(6,2997)TITLE(I),(ZVOL(I,IT),IT=1,KELVIN)
 2997 FORMAT(1X,A6,1X,1P1OE12.5)
      NSTART = METALS + 1
      DO 9020 NSPEC = NSTART,NGS
      K = 1
      DO 9021 KT = LEAST,MOST,INSTEP
      IF(KT.GT.KELVIN) GO TO 9020
      IF(ZVOL(NSPEC,KT).LE.0.0) NOUGHT(NSPEC) = 1
      IF(ZVOL(NSPEC,KT).LE.0.0) GO TO 9020
      ATOM(NSPEC,K,INDEX) = ALOG10(ZVOL(NSPEC,KT))
 9021 K = K+1
 9020 CONTINUE
      DO 9022 NSPEC = NSTART,NGS
      IF(NOUGHT(NSPEC).EQ.-1) GO TO 9022
      K = 1
      DO 9023 KT = LEAST,MOST,INSTEP
```

```
      ATOM(NSPEC,K,INDEX) = ZVOL(NSPEC,KT)
 9023 K = K+1
 9022 CONTINUE
      WRITE(6,3000)(AVEMW(IT),IT = 1,KELVIN)
 3000 FORMAT(1X,44H AVERAGE MOLECULAR WEIGHTS OF FLAME PRODUCTS  /1X,10(
     1F12.5))
      IF(INDEX.EQ.NOMORE) CALL GLYPHO(ATOM,RED,TITLE,RATIO,FTITLE)
      IF(INDEX.GE.NOMORE) STOP
      RED(INDEX+1) = RED(INDEX) + DELTA
      INDEX = INDEX + 1
      GO TO 414
 6667 CONTINUE
      RETURN
      END
```

```
$IBFTC APIVOT
       SUBROUTINE GPIVOT  (N,A)
      DIMENSION A(41,42)
C
C     GAUSSIAN ELIMINATION WITH PIVOTING
C
      N1 = N+ 1
    4 DO 8 I =1,N
      I1 = I + 1
      IF ( I - N ) 40,45,45
   40 Q = ABS(A(I,I))
      MAX = 0
      DO 42 J = I1,N
      P = ABS(A(J,I))
      IF ( Q - P ) 41,42,42
   41 Q = P
      MAX = J
   42 CONTINUE
      IF (MAX) 45,45,43
   43 DO 44 K =1,N1
      B = A(I,K)
       A(I,K) =A(MAX,K)
   44 A(MAX,K) = B
   45 Z = A(I,I)
      DO 5 J = I1,N1
    5 A(I,J) = A(I,J)/Z
      IF ( I - N)6,8,6
    6 DO 7 K = I1,N
      DO 7 J =I1,N1
    7 A(K,J) = A(K,J) - A(K,I)*A(I,J)
    8 CONTINUE
      N2 = N - 1
      DO 9 K = 1,N2
      I = N - K
      I1 = I + 1
      DO 9 J = I1,N
    9 A(I,N1) = A(I,N1) - A(I,J)*A(J,N1)
      RETURN
      END
```

```
$IBFTC AGRAPH
      SUBROUTINE GLYPHO(ATOM,RED,TITLE,RATIO,FTITLE)
      DIMENSION X(60),Y(60),RED(20),ATOM(60,3,20),NUM(10),SPEC(60)
     1,X1(20),Y1(20),Y2(20),Y3(20),TITLE(60),RATIO(20),A1(2),FTITLE(4)
      READ(5,117) A1(1)
  117 FORMAT(6A10)
      READ(5,1117) DIG,DDIG,DDDIG
 1117 FORMAT(6A10)
      READ(5,1118) NGLYPH
 1118 FORMAT(I2)
      CALL START
      CALL PLOT(1.0,1.0,-3)
      DO 9083 NSPEC = 1,NGLYPH
      A1(2) = TITLE(NSPEC)
      DO 9084 I = 1,10
 9084 NUM(I) = 11
      NTAG = NSPEC/4
      ITERO = NSPEC-(NTAG*4)
      DO 9082 KT = 1,3
      DO 9081 I = 1,11
      JEMMY = I + (11*(KT-1))
      Y(JEMMY) = ATOM(NSPEC,KT,I)
 9081 X(JEMMY) = RATIO(I)
 9082 CONTINUE
      CALL SCALE(X,5.0,33,1)
      CALL SCALE(Y,5.0,33,1)
      DO 9150 J = 1,11
      K = J+11
      L = J+22
      X1(J) = X(J)
      Y1(J) = Y(J)
      Y2(J) = Y(K)
 9150 Y3(J) = Y(L)
      X1(12) = X(34)
      X1(13) = X(35)
      Y1(12) = Y(34)
      Y1(13) = Y(35)
      Y2(12) = Y(34)
      Y2(13) = Y(35)
      Y3(12) = Y(34)
      Y3(13) = Y(35)
      XN1 = ((X1(11)-X1(12))/X1(13)) + 0.1
      YN1 = ((Y1(11)-Y1(12))/Y1(13))
      YN2 = ((Y2(11)-Y2(12))/Y2(13))
      YN3 = ((Y3(11)-Y3(12))/Y3(13))
      CALL AXIS(0.0,0.0,FTITLE,-40,5.0,0.0,X(34),X(35))
      CALL AXIS(0.0,0.0,A1,20,5.0,90.0,Y(34),Y(35))
      CALL LINE(X1,Y1,11,1,1)
      CALL LINE(X1,Y2,11,1,2)
      CALL LINE(X1,Y3,11,1,3)
      CALL SYMBOL(XN1,YN1,0.1,DIG,0.0,10)
      CALL SYMBOL(XN1,YN2,0.1,DDIG,0.0,10)
      CALL SYMBOL(XN1,YN3,0.1,DDDIG,0.0,10)
      IF(ITERO.EQ.0) CALL PLOT(8.0,-21.0,-3)
      IF(ITERO.NE.0) CALL PLOT(0.0,7.0,-3)
 9083 CONTINUE
      IF(ITERO.EQ.0) CALL PLOT(-8.0,0.0,-3)
      CALL ENPLOT(9.0)
      RETURN
      END
```